Some other Pergamon titles of interest

HODGSON
Growth Points in Nuclear Physics Volume 1
(Nuclear Forces and Nuclear Reactions)

BOWLER
Nuclear Physics

BRINK
Nuclear Forces

CHOPPIN & RYDBERG
Nuclear Chemistry

GIBSON
The Physics of Nuclear Reactions

IRVINE
Nuclear Structure Theory

LODHI
Superheavy Elements

McCARTHY
Nuclear Reactions

SITENKO & TARTAKOVSKII
Lectures on the Theory of the Nucleus

SOLOVIEV
Theory of Complex Nuclei

THEWLIS
Concise Dictionary of Physics and Related Subjects
2nd Edition

Growth Points in Nuclear Physics

by

P. E. HODGSON
University of Oxford

VOLUME 2

PERGAMON PRESS
OXFORD · NEW YORK · TORONTO · SYDNEY · PARIS · FRANKFURT

UK	Pergamon Press Ltd., Headington Hill Hall, Oxford OX3 0BW, England
USA	Pergamon Press Inc., Maxwell House, Fairview Park, Elmsford, New York 10523, USA
CANADA	Pergamon of Canada, Suite 104, 150 Consumers Road, Willowdale, Ontario M2J 1P9, Canada
AUSTRALIA	Pergamon Press (Aust.) Pty. Ltd., P.O. Box 544, Potts Point, NSW 2011, Australia
FRANCE	Pergamon Press SARL, 24 rue des Ecoles, 75240 Paris, Cedex 05, France
FEDERAL REPUBLIC OF GERMANY	Pergamon Press GmbH, 6242 Kronberg-Taunus, Pferdstrasse 1, Federal Republic of Germany

Copyright © 1980 P. E. Hodgson

All Rights Reserved. No part of this publication may be reproduced, stored in a retrieval system or transmitted in any form or by any means: electronic, electrostatic, magnetic tape, mechanical, photocopying, recording or otherwise, without permission in writing from the publishers

First edition 1980

British Library Cataloguing in Publication Data
Hodgson, Peter Edward
Growth points in nuclear physics. -
Vol. 2
1. Nuclear physics
I. Title
539.7 QC776 79–40075
ISBN 0–08–023082–2

Printed and bound in Great Britain by
William Clowes (Beccles) Limited, Beccles and London

Preface

Science is continually growing, and this growth takes place in many different ways. There is the slow accretion of increasingly accurate measurements of the properties of materials and the behaviour of different phenomena. There are the discoveries of new particles, new materials and new processes. There are the new ideas that bring order and unity to particular areas of knowledge. Finally there are the grand generalizations, the insights of a Newton or an Einstein, that give us a new way of looking at whole continents of knowledge, bringing to them an order that endures for centuries.

These great generalizations capture the imagination and figure most prominently in the history of science. But most scientific work is of a less spectacular kind. Small but significant advances are taking place all the time although, like the slow growth of a tree, they are not obvious to the distant observer.

These advances are reported in scientific journals, and the more important appear first of all in those devoted to the rapid publication of short papers. In the field of nuclear physics the journals most frequently used for this purpose are *Physical Review Letters* and *Physics Letters*. Later on, when the work is complete, more detailed and comprehensive accounts are published in journals like the *Physical Review* and *Nuclear Physics*. Years later the work that has stood the test of time and has been confirmed by subsequent studies is collected together in review articles, monographs and finally textbooks.

The reader who relies on textbooks is thus always several years out of date. Even more important, if he is interested in the process of scientific discovery, he will completely miss all the tentative hypotheses, the false starts, the gradual winnowing of the wheat from

the chaff, that is the very lifeblood of scientific research. The essential purpose of this series of volumes is to provide rapid up-to-date summaries of the latest work in the main growth areas of nuclear physics to supplement the regular textbooks. The rapidity of publication implies that the winnowing process is not yet complete, so accounts of work that is later discredited or radically modified are inevitably included. This has the advantage of providing a unique insight into the growth of science.

The main text of these volumes consists of short summaries of new discoveries and ideas that are being published in *Nature* and the *New Scientist*, with introductory notes and references for further reading. The individual articles are grouped together around certain themes, which stand out as the main growth areas at the present time. Here there is a new experimental technique that enables a series of measurements to be made to far higher precision, revealing a wealth of new phenomena with intriguing regularities and anomalies. There we find a new theoretical insight that brings order to an hitherto tangled area. Then there will be a flurry of activity as groups of scientists in many laboratories push the new technique to the limit or explore all the implications of the new idea. Sometimes the new idea is confirmed and is incorporated into the accepted body of knowledge. In other cases later work fails to confirm the first reports and the idea is forgotten.

Even the apparent failures are not without value. The very process of refuting them often leads to the development of new techniques or more obliquely to more ideas. This process of testing and sifting is going on all the time, and many examples will be found in these volumes. If we were to rely only on textbooks most of this month-to-month drama would be lost.

These volumes are devoted to nuclear physics, understood as including nuclear structure and nuclear reactions, but not elementary particle physics. Not all the growth points in this area could be covered even in many volumes, and the choice of subjects naturally reflects the interests of the author. This particular volume is devoted to nuclear reactions, and is divided into three sections.

The first section is on nuclear forces and potentials, in particular the optical model potential that enables the elastic scattering of many

particles by nuclei to be calculated in a very simple manner. These potentials are needed to calculate nuclear reaction cross-sections, and comparison with experiment often yields important information on nuclear structure. The precise definition of the optical potential, the methods of calculating it from the nucleon–nucleon interaction, and the resolution of the ambiguities in the phenomenological analyses are continuing subjects of research. Also considered in this section are the three-body forces and the spin dependence of the nuclear potential.

Nuclear reaction mechanisms are considered in the next section. Reactions can take place in many ways, either directly or through the compound nucleus or by some intermediate process, and it is by no means obvious which is dominant in a particular experimental situation. When we know the mechanism, we can calculate the cross-section and use the reaction as a tool in nuclear structure research. It is thus particularly interesting to find reactions that are sensitive to particular features of nuclear structure. Higher order processes involving two or more stages are also being studied not only for their intrinsic interest but also because of the effect they can have on the total cross-section. New types of reaction also form a prominent growth area, as they can make accessible new types of nuclear states and also new nuclei far from the stability line.

The third and final section is devoted to heavy ion reactions, one of the most prominent growth areas of contemporary nuclear physics. This area has been opened up by the development of particle accelerators capable of giving nuclei enough energy to surmount each other's electrostatic repulsive Coulomb barriers, and of detectors able to measure the mass and charge and energy of the particles emitted from such interactions. A whole new realm of nuclear phenomena is thus opened up for study, and it is made particularly interesting because the semi-classical nature of many of the reactions of heavy ions makes them easy to visualize physically. It has proved possible to study the transient formation of nuclear molecules when two nuclei interact rather weakly, and the more complicated processes that occur when the energy is raised. Heavy ion reactions are particularly sensitive to some features of nuclear structure, and thus constitute a powerful tool in nuclear structure research. Most of the reactions

familiar from work with nucleons, deuterons and alpha-particles have also been studied with heavy ions, and most of them show new features of special interest. At very high energies, when two nuclei collide with enough energy to shatter them both into many fragments, a whole new area of research is being explored. The classical theories of non-equilibrium statistical thermodynamics are being used to understand the overall features of the interactions. There are speculations about the formation of nuclear shock waves, and many attempts to establish their presence experimentally. This is still a very new growth area, with many surprises in store.

All the articles have been sent to the scientists responsible for the original research for their comments and corrections, and much new material obtained in this way has been included in this volume. Apart from the correction of a few errors, the elimination of a few paragraphs to avoid undue repetition and the restoration of a few figures omitted in the first publication, the published articles have been left in their original form.

I am grateful to all those scientists whose original research is summarized here, and particularly those who have responded to my request for additional information. The invitation to write the articles in *Nature* came from Dr Alun Jones, and in the *New Scientist* from Dr Robert Walgate, and it was the Editor of *Nature*, Dr David Davies, who suggested that they might be collected together in one volume. I thank all these, together with the Macmillan Press and I.P.C. Magazines for permission to reproduce the articles from *Nature* and the *New Scientist* respectively.

Nuclear Physics Laboratory P. E. H.
Oxford
1979

CHAPTER 1

Nuclear Forces and Potentials

1.1 What Is the Nuclear Optical Potential?
(*Nature* **249**, 412, 1974)

The interaction of a nucleon of moderate energy with a nucleus is an exceedingly complicated process. Very many reactions can occur and they depend on the energy levels of the compound and residual nuclei. The conservation of particle flux links all the reaction channels together, so that any abnormal behaviour in one channel, a resonance or threshold for example, produces corresponding changes in all the others. It might well be thought that each interaction would have to be treated as a special case and that the detailed structure of each nucleus would have to be taken into account before the cross sections could be calculated.

One-body potential

In spite of this somewhat pessimistic expectation, the striking regularities in the neutron total and reaction cross sections as a function of energy and from nucleus to nucleus suggested that they could be described by a one-body potential varying smoothly with energy and nuclear size (Feshbach, Porter and Weisskopf, 1954). The success of this description led to the model being extended to nucleon elastic scattering and the range of other nuclear interactions.

Subsequently it was realized that this success was partly due to the relatively poor energy resolution of the early measurements. Later improvements in experimental techniques showed that the cross sections of reactions passing through the compound nucleus do

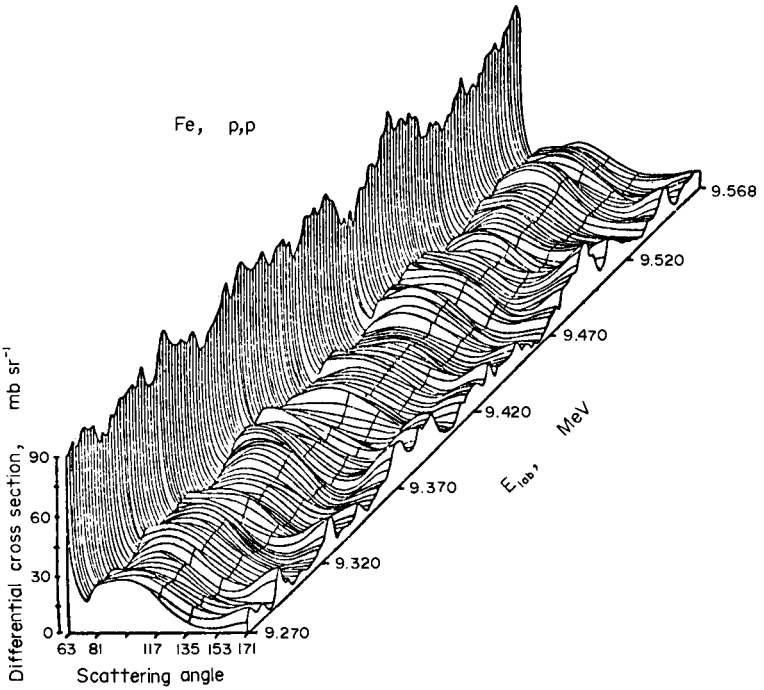

Fig. 1. Differential cross section for the elastic scattering of protons by ^{56}Fe, showing strong fluctuations with energy due to the part of the reaction passing through the compound nucleus (P. von Brentano *et al.*, 1965).

fluctuate as the incident energy varies (von Brentano *et al.*, 1964) but if the energy spread of the incident beam is greater than the mean width of the fluctuations an averaged cross section is obtained that generally varies quite smoothly with energy. Detailed analysis showed that this averaged cross section is the sum of compound nucleus and direct reaction components; the former may be calculated using the theory of Hauser and Feshbach (1952) and subtracted from the measured cross sections. As the energy increases the contribution of the compound nucleus processes falls rapidly and soon becomes negligible.

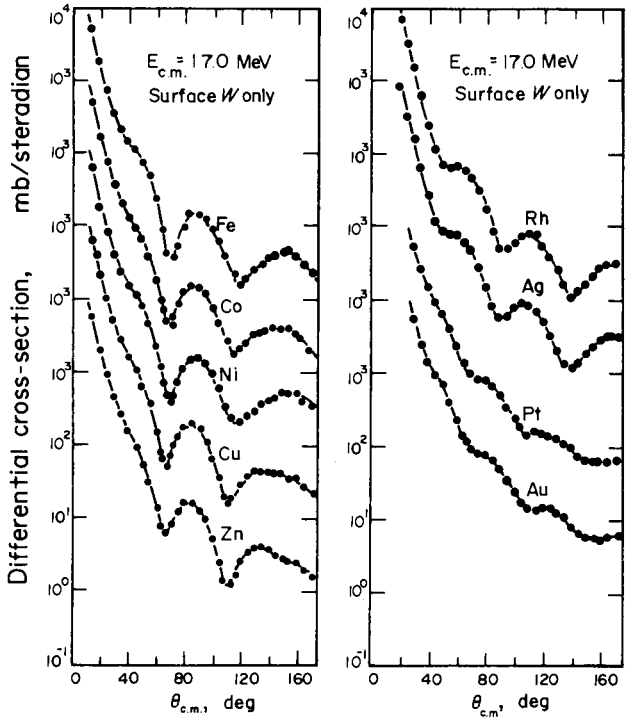

Fig. 2. Differential cross sections for the elastic scattering of 17 MeV protons compared with optical model calculations in which all the parameters of the potential were varied to optimize the fit in each case (Perey, 1963).

In precision analyses it is necessary to remove the compound nucleus contribution to the data by a preliminary Hauser–Feshbach calculation or preferably to confine the analysis to energies for which the compound nucleus contribution is negligible. For most nuclei, energies of about 15 MeV or more are adequate for this purpose. The direct cross section is then analysed by a simple optical potential.

Many such analyses were made and soon it was possible to specify potentials defined by rather few parameters that give strikingly good overall fits to a wide range of neutron and proton elastic scattering and reaction data (Perey, 1963; Perey and Buck, 1962). One of the most

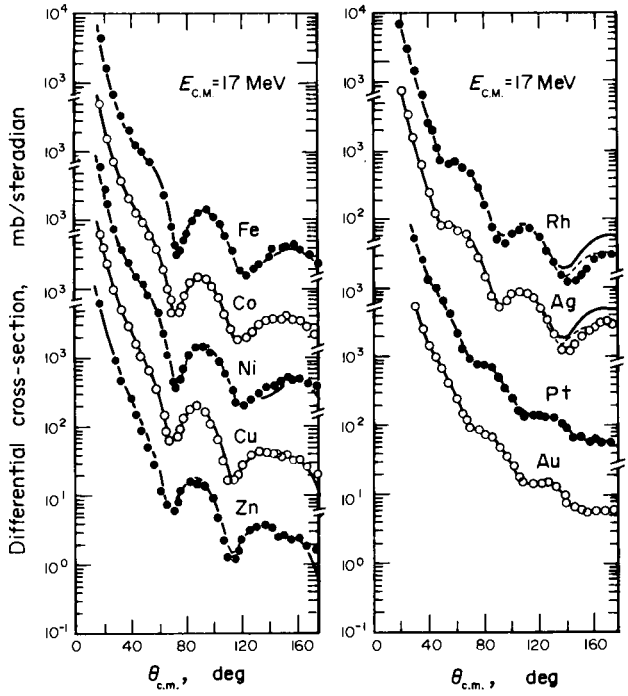

Fig. 3. Differential cross sections for the elastic scattering of 17 MeV protons compared with optical model calculations with the overall optical parameters given in the text (Perey, 1963).

successful of these potentials was obtained by Perey from an analysis of elastic scattering of protons of 9–22 MeV by a range of medium and heavy nuclei. He used a potential of the form

$$V(r) = U_0 f(r_w a_u) + ia_D W_D (d/dr)[f(r_D, a_D)] + (\hbar/m_\pi c)^2 U_s (1/r)(d/dr)[f(r_s, a_s)]\mathbf{L}.\sigma$$

where

$$f(r_i, a_i) \equiv [1 + \exp\{(r - r_i A^{1/3})/a_i\}]^{-1}$$

In the first analyses, the parameters of this potential were adjusted to optimize the fit to each set of data for scattering from a particular

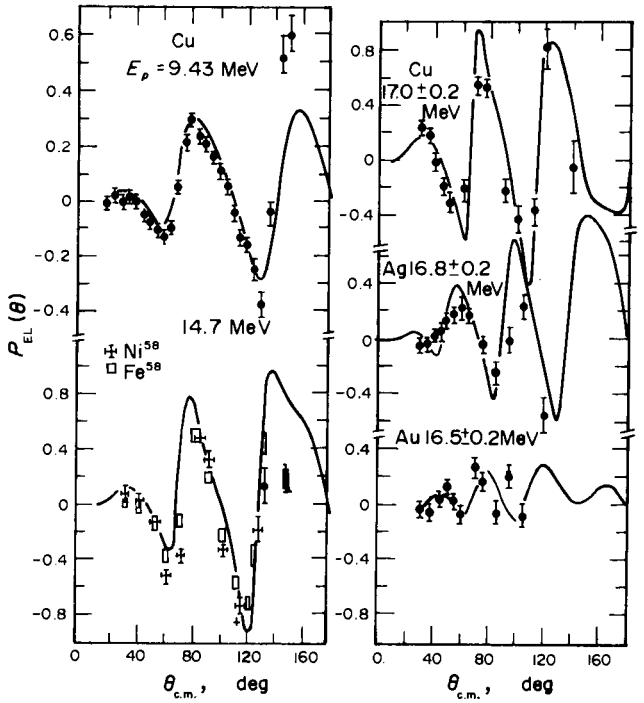

Fig. 4. Polarizations of elastically-scattered protons compared with optical model calculations (Perey, 1963).

nucleus at a particular energy. The most accurate data were the differential cross sections, supplemented by less accurate polarizations and reaction cross sections (Fig. 2).

The optimum parameters for different nuclei at different energies were found to be very similar, so the data were reanalysed fixing the form factor parameters to the values

$$r_u = 1.25; \quad r_D = 1.25; \quad r_s = 1.25$$
$$a_u = 0.65; \quad a_D = 0.47; \quad a_s = 0.65$$

The quality of the fits was still very high, though naturally not quite as good as previously (Figs. 3 and 4).

The depth of the real potential was found to vary systematically with energy and with the numbers of neutrons and protons in the nucleus, and the variation could be well represented by

$$U = 53.3 - 0.55E + 27a + 0.4Z/A^{1/3}$$

where $a = (N - Z)/A$.

The optimum imaginary potential was not so well determined, but a good average value is

$$W_D = 12A^{1/3}$$

The polarizations were best fitted with

$$U_s = 7.5 \quad (E < 17); \; U_s = 8.5 \quad (E > 17)$$

The fits obtained with this overall potential are very little worse than those obtained when several parameters were adjusted in each case.

The striking success of these analyses led to the hope that it would be possible to find an overall or global potential for all nuclei and one has tended to forget that the individual structure of each nucleus must affect the interaction to some extent. This raises difficulties concerning the concept of the optical potential, in particular whether it should give a good overall fit to many sets of data or whether it should be adjusted to fit each set of data as accurately as possible.

Optical potentials of the first type are the same for all nuclei, with perhaps a smooth and easily parameterized dependence on the incident energy and on Z and A. To achieve this one has inevitably to make some sacrifice in the quality of the fits to the data.

Optical potentials of the second type have parameters that are unique to each nucleus at each energy, so that accuracy has been purchased at the expense of loss of generality.

Both types of potentials have their advantages and disadvantages. In some interactions there are quite substantial deviations from the behaviour given by the overall potential, whereas potentials fitted accurately to particular sets of data are sometimes recognizably non-physical. These anomalies have a physical basis, so that one might

hope that detailed studies with both types of potential could teach us more about the physical process taking place.

It is important to see what can be done to eliminate the disadvantages of these potentials while preserving their good points. The first step is to identify the physical processes responsible for the deviation from 'normality' and make a physical model that allows them to be calculated explicitly. If this can be done within the framework of the optical model, then the process and its effect on the cross section can be represented by an extra term in the optical potential. In this way, for example, the polarizations of the elastically scattered nucleons were included in the model by the addition of the spin–orbit term to the potential and the dependence on the asymmetry parameter by the term proportional to $(N-Z)/A$.

At one stage it was hoped that all new physical effects and deviations from the simpler potential could be brought within the general optical potential by the addition of a series of small terms, giving a potential expressible as a simple analytical function of A and E and capable of fitting the elastic scattering data to high accuracy.

Unfortunately in recent years several deviations from normality have been found that can be understood physically but which cannot be treated in this way. These are of two types; the first can still be treated within the optical model formalism whereas the second requires more sophisticated theoretical treatment.

An example of the first is the exceptionally low neutron reaction cross sections found for magic nuclei at low energies, especially for ^{208}Pb (Perey and Buck, 1962). These are much less than those calculated from the highly successful Perey–Buck potential and can easily be understood as a consequence of the low level density at small excitation energies of such nuclei. The effect can be treated phenomenologically by allowing the absorbing part of the optical potential to depend on the shell structure but the absorbing potential cannot conveniently be expressed as an analytical function of Z and A. This phenomenon only occurs in the limited energy region and is not of general importance (Fig. 5).

The effects in the second category may be calculated by appropriate physical models but it is not possible to represent them by an easily-parameterized additional term in the optical potential. It is of

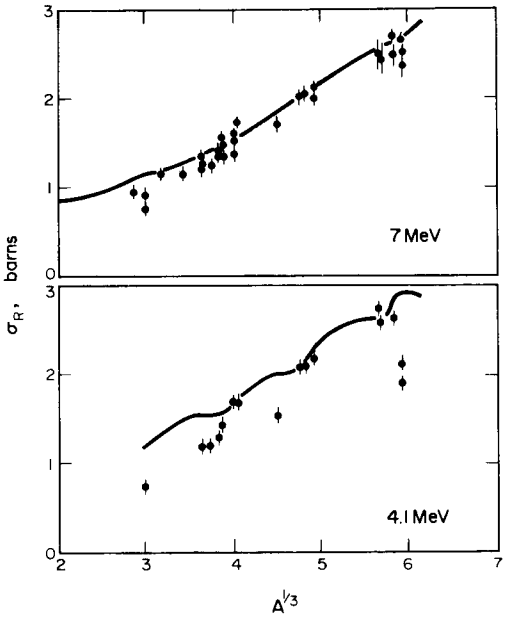

Fig. 5. Reaction cross sections for the interaction of 4.1 and 7 MeV neutrons with a range of nuclei compared with the values calculated from the non-local potential of Perey and Buck (1962). The smaller cross sections for magic nuclei are particularly noticeable at 4.1 MeV in the region of the doubly magic ^{208}Pb ($A^{1/3} = 5.92$).

course often possible to fit the data through the region of the anomaly with a particular optical potential, so that one can formally define the potential responsible for the effect as the difference between the general optical potential and the particular potential, but this is often highly singular and not conveniently parameterizable.

The extent to which this occurs implies a breakdown of the simple optical model, so that one is now faced with the alternatives of either using an ill-behaved effective potential in the framework of the simple optical model or of continuing a general optical potential in a more sophisticated formal framework. The second alternative is clearly the more desirable, even from the purely phenomenological point of view,

as it often unifies a range of phenomena in a simple way, whereas the effective potentials are much more difficult to handle.

This may be illustrated by the analysis of elastic scattering from strongly deformed nuclei. These have low lying collective states that are readily excited by inelastic scattering and the cross sections are so large that the elastic scattering cross section is significantly affected.

The inelastic cross sections vary in magnitude with β, but hardly at all in shape, and the elastic cross section departs more and more from its unperturbed value as β increases. If the elastic cross section is

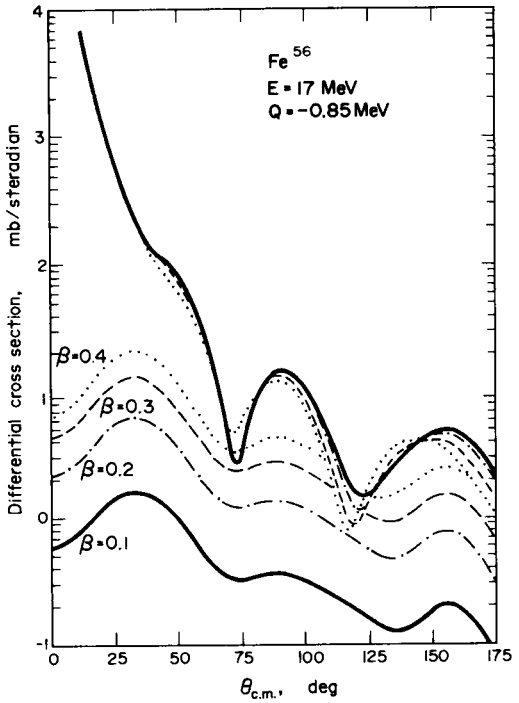

Fig. 6. Differential cross sections for the elastic and inelastic scattering of 17 MeV protons by ^{56}Fe calculated with the coupled-channels formalism for several different values of the deformation parameter β (Perey, 1963).

analysed for several deformed nuclei, the parameters of the resulting potential vary from nucleus to nucleus depending on the strength of the coupling to the collective states.

In particular, the imaginary potential is found to increase with increasing deformation. A coupled-channels analysis can, however, fit the elastic cross section with the same optical potential for each nucleus provided each has its characteristic deformation parameter. This was first shown by Perey (1964) in an analysis of the elastic scattering of protons of 17 MeV by some heavy spherical and deformed nuclei (Fig. 6).

Another example is provided by the scattering of α particles of 50 MeV by the even isotopes of samarium (Glendenning, Hendrie and Jarvis, 1968). The elastic scattering changes qualitatively from one isotope to the next; the diffraction oscillations become less and the envelope of the maxima steeper as the mass (and the nuclear deformation) increases. Simple optical model analyses of these data give quite different potentials, but the cross sections are all well fitted by the same optical potential when the coupling to the collective states is taken into account and each nucleus is characterized by its deformation parameter. The deviations from simple normality can thus be brought within the scope of the general optical model, although the deformation parameter cannot be expressed as an analytical function of Z and A (Fig. 7).

Further evidence for the reduction of the absorbing potential in the region of closed shells is provided by measurements of the s- and p-wave strength functions. These show characteristic maxima and minima as a function of A and the overall behaviour is quite well given by the optical model with standard potentials. Closer examination shows that although the maxima are quite accurately fitted, the experimental values are much less than the calculated ones in the regions of the minima. A coupled-channels analysis by Newstead showed that this can be obtained by reducing the imaginary potential in a way that varies from nucleus to nucleus. Since the imaginary potential corresponds to absorption it might be expected to be correlated with the number of three-quasiparticle states that can be formed in the initial stages of the nuclear excitation. Newstead estimated the numbers of such states in various nuclei and found that

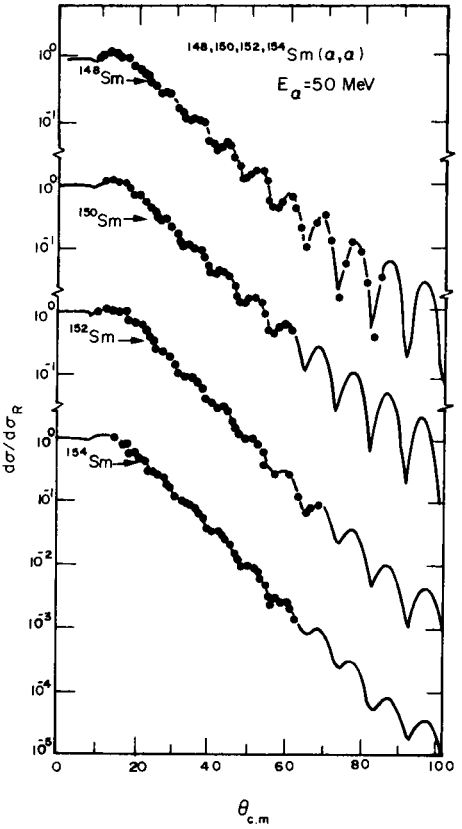

Fig. 7. Differential cross sections for the elastic scattering of 50 MeV alpha particles by the even samarium isotopes compared with coupled-channel calculations using the *same* optical potential but different deformation parameters for each isotope (Glendenning, Hendrie and Jarvis, 1968).

they correlate very well with the imaginary potentials W obtained by requiring a fit to the s-wave strength function data. Thus once again the deviations from normality can be explained by a physical model

TABLE 1

Correlation between estimated number of 3 quasi-particle states near neutron separation energy and absorptive potential in 3 S region.

Target	W, MeV	N (3QP), MeV^{-1}
^{54}Cr	0.44	3
^{52}Cr	0.8	7
^{50}Cr	1.12	15
^{40}Ca	1.5	13
^{49}Ti	3.0	55
^{45}Sc	6.0	105
^{59}Co	13.0	205

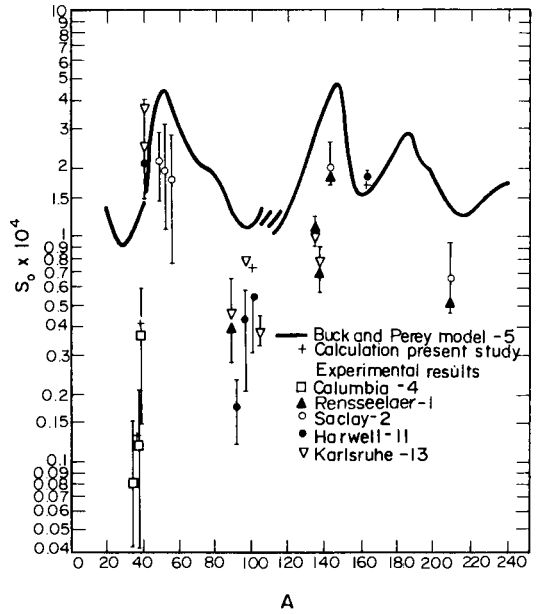

Fig. 8. S-wave strength function as a function of A compared with standard optical model calculations of Perey and Buck (solid line). The tendency of the experimental data to fall below the line, especially in the region of the strength function minima, is given by the coupled-channels calculations of Newstead (+) (1972).

but not in a way that can easily be parameterized in terms of A and Z.

Another effect that can easily be treated by the coupled-channels (Fig. 8) formalism is the marked resonances that occur when low energy nucleons are scattered by some light nuclei (Mikoshiba, Terasawa and Tanifugi, 1971). Some of these are single-particle resonances in the optical potential; others can be understood as core-excitation resonances. The coupled-channels formalism with a simple model of the nuclear excitation gives a good overall account of these resonances. The data also show higher order resonances that could presumably be treated by including the coupling to more complicated configurations.

The scattering from light nuclei at higher energies frequently shows deviations from normality and in some cases this is due to higher order processes. In the case of medium-energy proton scattering by ^{12}C and ^{16}O the core-polarization exchange mechanism with intermediate excitation of a giant resonance is responsible for the marked peaks in the backward cross section for inelastic scattering to non-normal parity states that cannot be accounted for by the simple optical model (von Geramb, 1972, 1973). This effect reflects back on the elastic channel and so should be taken into account explicitly at those energies where giant resonances are important.

As a final example, the (p, n) quasielastic reaction to the isobaric and analogue state has significant contributions from the two-step (p, d, n) intermediate particle transfer process (Rickertsen and Kunz, 1973). If it is analysed with a simple optical potential the fits are not strikingly good and the parameter of the isospin term which is responsible for the transition varies erratically from nucleus to nucleus. If the two-step process is included explicitly, making use of the properties of the known intermediate states, then the fits are significantly improved and the isospin potential is essentially the same for all nuclei. Thus once again by treating explicitly the process responsible for the deviations it is possible to recover a general optical potential.

The polarizations of the elastically scattered particles are much more sensitive to the interaction potentials than are the differential cross sections, as they depend on the differences of scattering amplitudes. This sensitivity is to a large extent offset by the lower

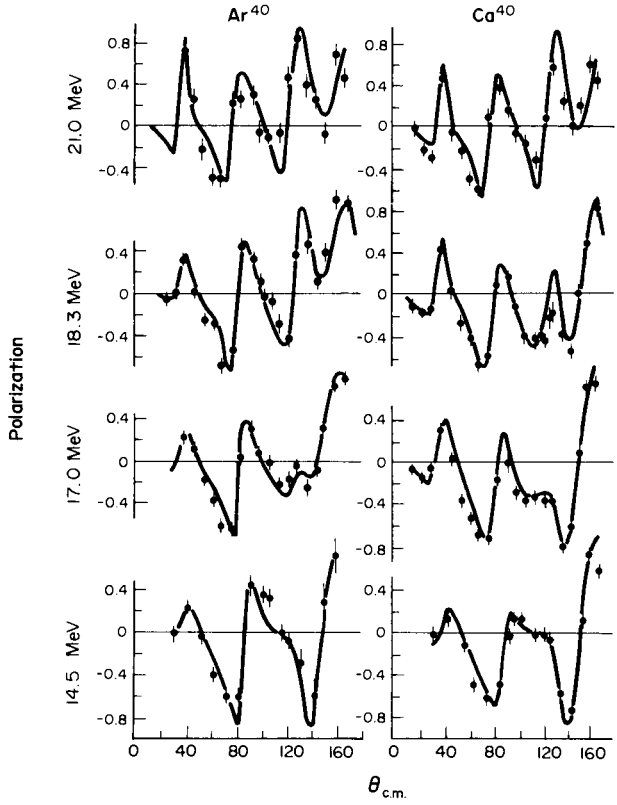

Fig. 9. Polarizations of protons elastically scattered by ^{40}Ar and ^{40}Ca compared with optical model calculations in which all the parameters of the potential were varied to optimize the fit (Boschitz, 1966).

accuracy of the polarization data, but nevertheless careful analyses of polarizations have shown anomalies that are not yet understood.

An example of this is provided by the work of Boschitz (1966), who analysed a series of differential cross sections and polarizations. He was able to obtain good overall fits to the polarization data but the optimum values of the parameters of the spin–orbit term in the optical

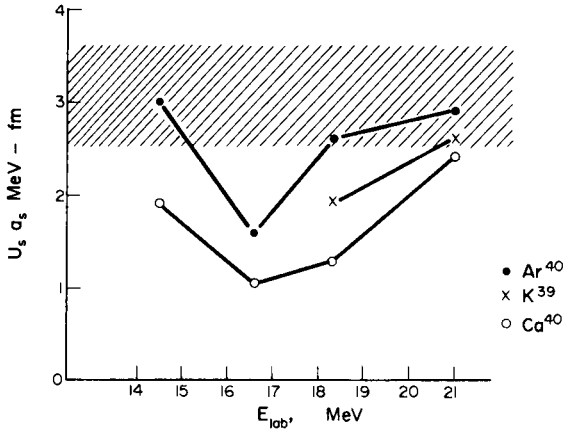

Fig. 10. The effective strengths $U_s\ a_s$ of the spin–orbit potentials obtained in the analyses shown in Fig. 9 plotted as a function of energy (Boschitz, 1966).

potential showed marked variations from one nucleus to another and as a function of proton energy. So far there is no convincing explanation of this behaviour (Figs. 9 and 10).

From these examples it will be seen that the processes that must be considered explicitly are of several types. The polarization and the dependence on the nuclear asymmetry can easily be incorporated in the optical model. The others require quite sophisticated calculations before the effects due to the general optical potential and the special process can be disentangled. The calculations with both processes included give directly the elastic cross section and there is no effective optical model potential as an intermediate stage. It is thus not possible to think of a general optical potential in which the effects of coupling to excited states, two-step reactions, core-polarization exchange processes and so on are included by appropriate analytical terms in a general expression of the optical potential. In this sense the optical potential ceases to be a concept able to give a detailed physical account of all the

data; it has been superseded in some regions by more sophisticated calculations that give an accurate account of the data that cannot be obtained in any other way.

One has thus arrived at a third concept of the optical potential as one that includes as many effects as possible in the parameterization of its parameters as functions of Z and A but which has to be used in a more sophisticated formalism if certain other effects are to be treated adequately. Thus some of the simplicity of the model has been lost, but further insight into more complicated phenomena has been attained.

References

Feshbach H., Porter C. E. and Weisskopf V. F., *Phys. Rev.* **96,** 448, 1954.
von Brentano P., *Jahresbericht, Max Planck Institut für Kernphysik,* p. 11, Heidelberg, 1965.
Hauser W. and Feshbach H., *Phys. Rev.* **87,** 366, 1952.
Perey F. G., *Phys. Rev.* **131,** 745, 1963.
Perey F. G. and Buck B., *Nucl. Phys.* **32,** 353, 1962.
Perey F. G., *Nuclear Spectroscopy With Direct Reactions,* Ed. F. E. Throw, ANL-6848, p. 114, 1964.
Glendenning N. K., Hendrie D. L. and Jarvis O. N., *Phys. Lett.* **26B,** 131, 1968.
Newstead C. M., European Conference on Intermediate Reactions, Plitvice, 1972.
Mikoshiba O., Terasawa T. and Tanifugi M., *Nucl. Phys.* **A168,** 417, 1971.
von Geramb H., *Nucl. Phys.* **A199,** 545, 1973; *Nuovo Cim. Lett.* **5,** 333, 1972.
Rickertsen L. D. and Kunz P. D., *Phys. Lett.* **47B,** IL1973.
Boschitz E. T., *Phys. Rev. Lett.* **17,** 97, 1966.

1.2 The Theory of the Nuclear Optical Potential (*Nature* **253,** 163, 1975)

One of the most basic interactions in nuclear physics is that between a nucleon and a nucleus. If we know this interaction we can calculate the cross section for elastic scattering and also the distortions of the nucleon waves by the nucleus which are essential for a thorough understanding of the reactions that can take place.

This interaction is really the sum of all the individual interactions between the incident nucleon and the nucleons of the target nucleus, modified by the correlation effects due to their proximity. As it is

extremely complicated, many studies have been made to see how accurate it is to replace it by a simple one-body potential that takes no explicit account of the structure of the target nucleus. This potential has a radial shape very similar to that of the nucleus itself and has a real part and an imaginary part of which the former may be thought of as refracting the incident nucleons and the latter as absorbing them: the absorption takes account of all inelastic scattering and reaction processes that remove flux from the elastic channel. The one-body potential is called the optical potential because of the similarity between the scattering and absorption of nucleons by nuclei and the scattering and absorption of light by a refracting and absorbing medium: the former can be described by a complex potential and the latter by a complex refractive index.

This simple idea has proved astonishingly successful and it is now possible to account for the elastic scattering cross sections for many nuclei at many energies by suitably choosing the parameters of the potentials. It has been developed by the addition of a spin–orbit term, which allows the polarization of the scattered nucleons to be calculated as well. The same potentials have been extensively used to generate the distorted waves needed in nuclear reaction calculations.

One of the main difficulties with these optical potentials is that they are frequently ambiguous; that is, it is possible to find several different potentials that give equally good fits to the experimental data. These ambiguities are much reduced as the precision of the data is improved, but some of them still remain.

Thus the purely phenomenological approach to the determination of the parameters of the optical potential, in which its parameters are systematically adjusted to optimize the fit to the experimental data, is inadequate. It needs to be supplemented by a more basic calculation of the potential from the constituent nucleon–nucleon interactions. Although this is very difficult and complicated, and many approximations have to be made in order to make the computations tractable, it is nevertheless able to give valuable information on the optical potential that substantially reduces the objectionable ambiguities.

The simplest of these calculations gives the real part of the optical potential as the folding of the nucleon–nucleon interaction $v(|\mathbf{r}-\mathbf{r}'|)$ with the nuclear density $\rho(\mathbf{r}')$ where $\mathbf{r}$ is the vector to the incident

nucleon and $\mathbf{r}'$ that to a nucleon in the target:

$$U(r) = \int v(\mathbf{r}-\mathbf{r}')\rho(\mathbf{r}')d\mathbf{r}'$$

Many calculations using this approach, following the work of Greenlees, Pyle and Tang (1968), have proved very successful.

The imaginary part of the potential is more difficult to calculate because in principle one should take account of all possible reaction processes, but some progress has been made by considering its strength as simply given by

$$W = \tfrac{1}{2}\hbar v\rho\bar{\sigma}$$

where v is the velocity of the nucleon, ρ the nuclear density and $\bar{\sigma}$ the mean collision cross section. This relation follows from the semi-classical theory of the optical potential.

The success of these calculations has stimulated many more detailed theories of the optical potential. Among these some very successful calculations have recently been completed by Jeukenne, Lejeune and Mahaux of the University of Liège (1974). In this work, the calculations were first of all made for infinite nuclear matter, and then the results were applied to finite nuclei using the local energy approximation. This means that we solve the problem for infinite nuclear matter as a function of its density, and then apply the results to nuclei using their known density distributions. Thus the potential at a point of density ρ is assumed to be that given by calculations of the properties of infinite nuclear matter of density ρ. This approximation is justifiable if the nuclear density changes slowly over distances of the order of the mean free path of nucleons in nuclei, which is certainly true in the nuclear interior but is more questionable in the nuclear surface. The reason for making the first calculations in infinite nuclear matter is because there the nucleon wavefunctions are plane waves, which naturally simplifies the calculations.

The nuclear matter calculations were made by solving the Bethe–Goldstone equation, which describes the interaction of two nucleons inside the nucleus. To do this calculation we need to know the interaction between two nucleons in free space, and this is known quite well from many phenomenological analyses of the scattering of protons by protons and by neutrons at many energies. Of several forms

now available the Reid potential was chosen as it has already been successfully used in a wide range of nuclear matter calculations. Inside the nucleus the nucleon–nucleon scattering is modified by the presence of the other nucleons and in particular many interactions are forbidden by the Pauli exclusion principle as they proceed to states that are already occupied. This effect, incidentally, ensures that the mean free path of nucleons in nuclear matter is long enough for the shell model to be a valid description.

The solution of the Bethe–Goldstone equation and the extraction of the optical potential requires lengthy calculations, and some of the results are shown in the figures. Fig. 11 shows the strength of the real

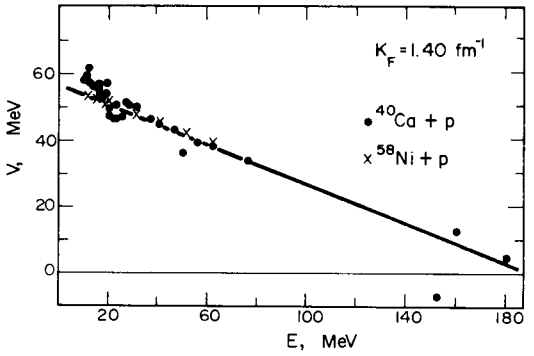

Fig. 11. Calculated strength of the real part of the optical potential as a function of incident nucleon energy compared with phenomenological potentials obtained from the cross sections for the elastic scattering of protons by ^{40}Ca and ^{58}Ni.

part of the potential as a function of energy calculated for a Fermi momentum in nuclear matter of 1.40 fm^{-1} and taking account of the various terms in the mathematical expression for the potential. It is compared with phenomenological potentials obtained by analysing the elastic scattering of protons by ^{40}Ca and by ^{58}Ni. Up to about 100 MeV the radial dependence of the real potentials obtained in these calculations is very similar to the Saxon–Woods form

$$f(r) = [1 + \exp\{(r - R)/a\}]^{-1}$$

used in most phenomenological analyses, but that at higher energies

shows a pronounced surface peaking. Already some phenomenological indications favouring such a form have been found, and it will be important to take this into account in future analyses of the data.

The calculated energy variation of the strength of the imaginary part of the optical potential is compared with some phenomenological determinations in Fig. 12. Its radial dependence changes from a

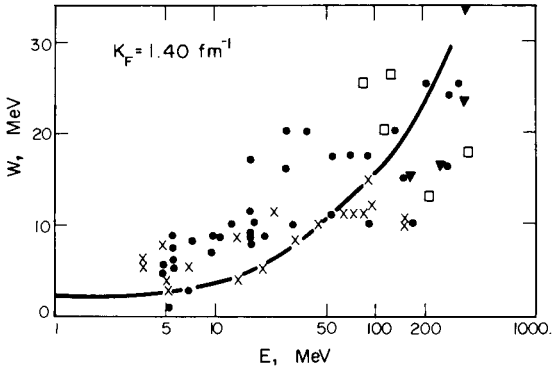

Fig. 12. Calculated strength of the imaginary part of the optical potential as a function of incident nucleon energy compared with a number of phenomenological values.

predominantly surface-peaked form at the lower energies to a predominantly volume form at higher energies, and this is just the same behaviour as the phenomenological imaginary potentials. In phenomenological analyses there is much ambiguity between the amounts of volume and surface components, so that it is difficult to determine them individually. It will be a great advantage to have available some reliable theoretical guidance for the relative contributions of volume and surface absorption.

This work is in process of extension by taking into account some of the higher order terms in the solution of the Bethe–Goldstone equation, which should give improved optical potentials. Already the results obtained are most encouraging, in that they reproduce many of the features of the optical potentials already known from phenomenological analyses. As confidence in the reliability of such calculations grows, they will play an increasingly important part in

guiding optical model analyses of elastic scattering cross sections. They should provide the essential behaviour of the form factors, leaving only the strength to be improved over the calculated values by optimization of the fit to the experimental data. This should provide more reliable potentials that will improve the accuracy of the information on nuclear structure obtained from analyses of nuclear reactions.

References

G. W. Greenlees, G. J. Pyle and Y. C. Tang, *Phys. Rev.* **171**, 1115, 1968.
J.-P. Jeukenne, A. Lejeune and C. Mahaux, *Phys. Rev.* **C10**, 1391, 1974.

1.3 New Calculation of the Nuclear Optical Potential (*Nature* **269**, 756, 1977)

The differential cross section and polarization for the elastic scattering of nucleons by nuclei can be very well described by a complex potential: the real part refracts the incident waves and the imaginary part absorbs them, just as a light wave is refracted and absorbed by a medium of complex refractive index. The absorbing potential takes account in a global way of all the reactions that remove flux from the elastic channel.

Unfortunately the potential describing the scattering is not unique: it is frequently possible to find several different potentials that fit the same data. This is unsatisfactory because these potentials give different wavefunctions, and unless we know which is correct it cannot be safely used to calculate the cross sections of non-elastic processes such as inelastic scattering and nucleon transfer reactions.

In principle the ambiguities between the potentials can be resolved by calculating the potential from more fundamental data, in particular from the nucleon–nucleon interaction, together with the structure of the target nucleus. In practice, however, this is difficult due to the many-body nature of the problem.

Over the past few years there have been many attempts to calculate the optical model potential. These differ in the choice of approximations made to simplify the calculations and they give results in fair agreement with the experimental data. Particularly encouraging work

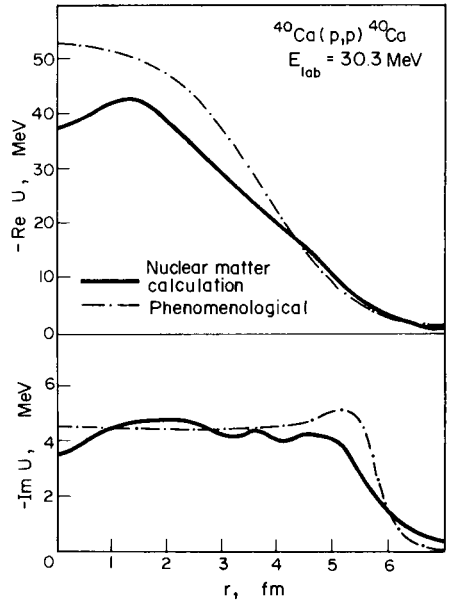

Fig. 13. Real and imaginary parts of the optical potential for protons on ^{40}Ca calculated from the nucleon–nucleon interaction compared with the corresponding phenomenological potentials.

has been carried out by Jeukenne, Lejeune and Mahaux of the University of Liège, who have been able to account for the volume integrals of the optical potentials (§ 1.2).

A new approach to this problem has been made by Brieva and Rook of the University of Oxford, and some preliminary results were reported at the Conference on Nuclear Structure at Tokyo in September 1977. They start from the Hamada–Johnston potential that gives an accurate fit to the nucleon–nucleon scattering data, and then solve the Bethe–Goldstone equation for the motion of nucleons in infinite nuclear matter subject to this potential. This gives a quantity called an averaged t-matrix that is used to obtain the optical potential by folding with the nuclear density distribution, using

$$V(r) = \int \rho(r')\, v(|r-r'|)\, \mathrm{d}r'$$

with addition of exchange terms.

In this calculation the approximations were carefully chosen to facilitate the calculation without too much loss in accuracy. It differs from most previous work in giving both the real and imaginary parts of the optical potential, and allows the radially-dependent *t*-matrix to be non-local and energy-dependent. The spin–orbit potential is also calculated and is found to be very similar to the phenomenological spin–orbit potential.

The optical potential they calculated for ^{40}Ca is shown in Fig. 13 and compared with the phenomenological potential that gives the best fit to the differential scattering and polarization data. It is particularly notable that the calculated real potential does not have the same radial shape as the phenomenological Saxon–Woods form. This indicates that this very frequently-used analytical form of the potential may not

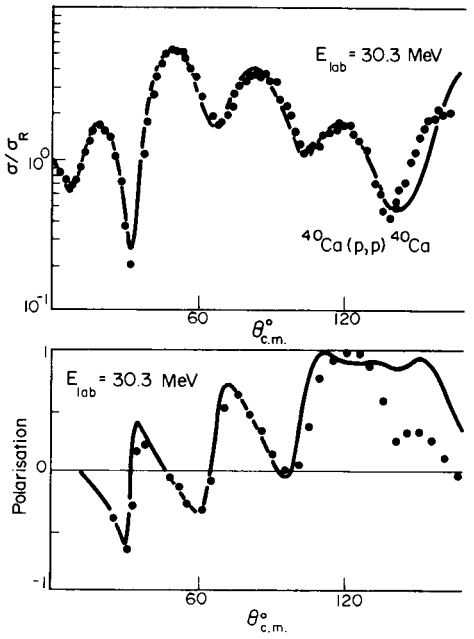

Fig. 14. Differential cross section and polarization for the elastic scattering of 30.3 MeV protons by ^{40}Ca compared with optical model calculations using the calculated potential.

always be adequate. The calculated imaginary potential shows considerable structure, partly due to the form of the nuclear density distribution and partly due to the self-consistency requirement imposed on the potential. The differential cross section and polarization calculated from these potentials are shown in Fig. 14. The agreement is strikingly good, indicating that it is now possible to calculate optical model potentials that give fits to the data that are comparable in quality to those found with phenomenological potentials with many adjustable parameters. In some respect they are even superior as they can give features of the cross sections that cannot be explained by phenomenological potentials.

This work is very promising, and needs to be extended and applied to a range of nuclei to enable its validity to be explored. It should also prove possible to extend the method to the calculation of the optical potentials appropriate to composite particles such as deuterons and alpha particles, and perhaps also to heavy ions. The availability of optical potentials that can be reliably calculated from fundamental data instead of being obtained by phenomenological analyses of elastic scattering data will be of the greatest value in nuclear structure studies.

References

F. A. Brieva and J. R. Rook, Proceedings of the International Conference on Nuclear Structure, *J. Phys. Soc. Japan* **44** (Supplement) 539, 1978; *Nucl. Phys.* **A291,** 299, 317, 1977; **A297,** 206, 1978.

J.-P. Jeukenne, A. Lejeune and C. Mahaux, *Phys. Rev.* **C10,** 1391, 1974.

1.4 Ambiguities in Helion Optical Potentials (*Nature Physical Science* **240,** 1, 1972 and *Nature* **255,** 579, 1975)

During the last few years there has been much interest in the determination of the best optical potentials to describe the elastic scattering of helions and alpha-particles by nuclei. It is found that several potentials of different depths will fit equally well the differential cross section for a range of forward angles but that, if data are available beyond a certain critical angle depending on the target nucleus and the incident energy, then only one potential will fit these data, and the ambiguity is thereby resolved. In this way it has been

shown in a series of analyses that the potential with the volume integral per nucleon of the real part about 330 MeV fm^3 is to be preferred over that having a volume integral of 440 MeV fm^3.

At the same time as this work on potential ambiguities there have been many studies of two-step contributions to nuclear reactions. It is impossible to understand many nuclear reactions by supposing that they can go only by a direct process from the initial to the final state. In addition, there are contributions from two-step processes that go by way of an intermediate state of the target nucleus, the residual nucleus, or of another nucleus formed from the target by a nucleon transfer process. If these are included in the calculation a good fit into the data can be obtained.

These two lines of work have recently been brought together by Shepard, Kunz and Kraushaar of the University of Colorado (1975). They have pointed out that two-step processes probably contribute to elastic scattering as well as to reactions, and go on to study what effect this has on the optimum optical potential.

They consider the elastic scattering of 83.5-MeV helions by ^{58}Ni, and make an optical model analysis of the differential cross section, which is available from 8° to 113°. This range includes sufficient high-angle data to resolve the ambiguities between the different potentials that all fit the forward angle data and they found that a satisfactory fit is obtained only with the shallow potential with volume integral 330 MeV fm^3. The deeper potential does not fit the data at all well at the higher angles. The result is in line with many previous analyses preferring the shallower of the two potentials.

Further calculations were then made with the inclusion of coupling to the alpha-particle channel by the process (h, a) (a, h) in which the incident helion picks up a neutron and then gives it back to the target nucleus before being emitted into the elastic channel. This two-step process can go by way of several states in ^{57}Ni, and the total amplitude was calculated using the coupled-channels formalism taking into account three intermediate states of ^{57}Ni.

These two-step amplitudes were then added to the direct optical model amplitudes, and the analysis of the elastic scattering data repeated. An acceptable fit was now obtained with the deep potential, contrary to the previous result.

This result shows that the explicit inclusion of two-step processes in the analysis of elastic helion scattering has a marked effect on the optical potential, even altering the choice of physical potential. This situation forces us to consider carefully what we mean by the optical potential (§ 1.1). Is it the potential that gives the best fit to a particular cross section or to a range of cross sections for many nuclei, or is it the potential that best fits the data when allowance is made for particular features of the nuclei concerned or after certain second-order processes have been removed?

It is quite arbitrary to say that one of these potentials is more physical than the others, but it is important to remember the conditions under which it was obtained and then how well it fits other data, particularly the cross sections of nucleon transfer reactions. The analyses of such data give different results depending on the inclusion of two-step and other higher order processes. It is indeed already found that the deeper potentials give a better description of some two-nucleon transfer reactions than the shallower ones, indicating that it might be preferable to include two-step processes explicitly when obtaining optical model potentials by analysing differential elastic scattering cross sections. The important thing is to ensure overall consistency, avoiding the danger of implicitly taking account of some processes more than once, and as far as possible fitting both elastic scattering and reaction data with the same potentials. There is clearly much more work to be done along these lines to find the best way of analysing the data.

References

C. J. Marchese, N. M. Clarke and R. J. Griffiths, *Phys. Rev. Lett.* **29**, 660, 1972.
J. R. Shepard, P. D. Kunz and J. J. Kraushaar, *Phys. Lett.* **56B**, 135, 1975.

1.5 Ambiguities in Alpha-particle Optical Potentials (*Nature Physical Science* **239**, 66, 1972; *Nature* **244**, 390, 1972; *Nature* **240**, 324, 1972)

Many analyses have shown that the cross-sections for the elastic scattering of nucleons, deuterons and other few-nucleon systems by

nuclei may usually be fitted by a complex optical potential (arising from the optical, or 'cloudy crystal ball', model of the nucleus) specified by its depth, radius and surface diffuseness parameters. In some cases it is found that almost equally good fits are obtained with a series of real potential depth such as 50, 100, 150 . . . MeV. Each increment of depth suffices, for each partial wave, to bring into the nuclear interior one additional half-wave of the corresponding wave function so that the asymptotic wave function, and hence the cross-section, remains unaltered. The equivalence of the potentials is exact for a particular partial wave, and it is found in practice that all the partial waves keep in step sufficiently for the ambiguity to remain.

Each of the equivalent potentials reproduces the elastic scattering but gives a different wave function in the nuclear interior, and this is important when such wave functions are used to calculate the

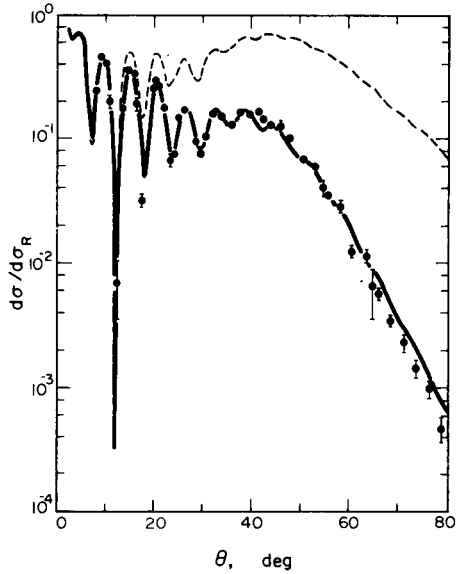

Fig. 15. Differential cross-section for the elastic scattering of 139 MeV alpha particles by ^{58}Ni, showing the diffraction region and the semi-classical region. The calculated value of the critical angle is 63°, rather greater than the point where the fall-off becomes exponential. ——, Optical model; ---, semi-classical (no absorption).

cross-sections of non-elastic processes, such as inelastic scattering and nucleon transfer reactions.

In the case of nucleon scattering this ambiguity is easily resolved, for the real part of the optical potential is essentially that of the shell model of the nucleus, and studies of nuclear bound states require a depth of about 50 MeV. Deuterons are so loosely bound that their optical potentials may be calculated approximately as the sum of the corresponding neutron and proton potentials averaged over the internal wave function of the deuteron. This gives about 100 MeV for the real part of the deuteron optical potential. This method of calculating the optical potential becomes progressively more uncertain for the heavier composite particles such as helions, tritons and alpha particles, and it is for these that the problem of the ambiguities in the potentials becomes acute.

It has recently been found that for higher energies the discrete ambiguities disappear, leaving only one potential to represent the interaction, and D. A. Goldberg and S. M. Smith (1972) noticed that the corresponding cross-sections, when plotted as a ratio to the Rutherford cross-section, show an almost exponential fall-off with scattering angle at angles greater than those showing the characteristic diffraction scattering. This behaviour can be interpreted semiclassically, and provides a definite prescription, as a function of nuclear size, for the energy at which the discrete ambiguities disappear.

The underlying physics of this can be understood by first considering the purely classical scattering by a centre of force, for which there is a definite relation between the impact parameter and the scattering angle, and hence a maximum scattering angle. This critical angle θ_c may be less than 180° or it may be greater, in which case the incident particle may orbit several times round the scattering centre before escaping, like a golfball running round the lip of the hole. As the incident energy increases θ_c falls and when it is less than 180° this spiral scattering (as it is called) can no longer occur. In cases where the maximum scattering angle is less than 180°, scattering through greater angles is classically forbidden; it can, however, take place quantum mechanically and in this region the semi-classical theory in the form of the JWKB (Jeffreys–Wenzel–Kramers–Brillouin) approximation may be used. The lth partial wave is identified with the particle trajectory

with impact parameter $(l+\frac{1}{2})/k$, where k is the wave number, and the deflexion angle θ_l of the particle is twice the differential of the sum of the nuclear and coulomb phase shifts with respect to l. The JWKB approximation gives an explicit expression for θ_l in terms of the nuclear and coulomb potentials. The maximum value of θ_l for all l is then identified as the critical angle θ_c. In the semi-classical region the cross-section falls exponentially for angles between θ_c and 180°.

Goldberg and Smith have compared the optical model and the semi-classical cross-sections and, as shown here, they find that the latter reproduces the overall shape quite well, although it is substantially larger because absorption is neglected. An optical model calculation without absorption agrees very well with the semi-classical result.

They then made a series of optical model analyses of alpha particle elastic scattering using data extending over different angular ranges, and found that the discrete ambiguities persist as long as the data extend only to θ_c, but that as soon as data from higher angles are included the fits for all but one of the potentials become unacceptable and the ambiguity vanishes. Thus to eliminate the ambiguity it is essential for θ_c to be less than 180° and to have data for angles greater than θ_c.

These semi-classical calculations thus contribute to an understanding of why the ambiguities are found in some cases and not in others, as they provide a way of calculating the critical angle θ_c. As the energy rises, θ_c falls, and at a particular energy θ_c increases with A. Thus energies high enough to eliminate ambiguities in light nuclei may not be high enough to do so in heavier nuclei.

This work thus provides a way of calculating the incident energy necessary to eliminate the ambiguities in the optical potential, and this should facilitate the determination of physically-realistic potentials that can be used with confidence in reaction calculations and in comparisons with the corresponding microscopic calculations.

Further insight into this question has now been obtained by the quantum-mechanical analysis of Goldberg, Smith, Pugh, Roos and Wall (1973). They examine the behaviour of the phase shifts for each partial wave as the incident energy changes, and find that it changes in character above the critical energy E_c; at energies less than E_c the

ambiguities occur, but for higher energies they are extinguished.

To see how this comes about, recall that the differential cross-section may be expressed as a function of the phase shifts so that ambiguous potentials must give very nearly the same phase shifts for all the partial waves that contribute to the scattering. But a phase shift is an angle, so increasing or decreasing it by any integral multiple of π does not affect the cross-section. Thus if all the phase shifts below a critical value l_c of the orbital angular momentum increase by $n\pi$ the ambiguity can occur.

This can happen for helion and alpha-particle scattering, as shown in Fig. 16. The total effective potential $V(r)$ acting on the incident particle

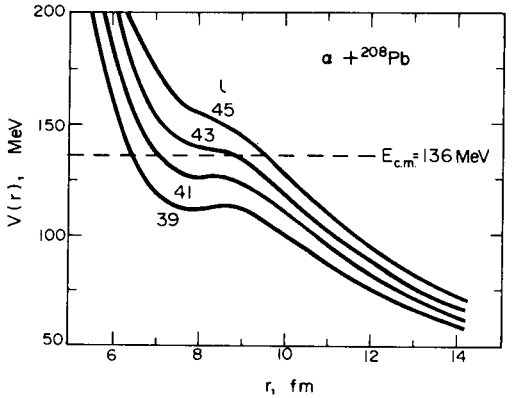

Fig. 16. Effective potentials for the elastic scattering of alpha particles by ^{208}Pb for values of l around 43.

of orbital angular momentum l is the sum of the nuclear potential, the electrostatic or Coulomb potential and the centrifugal potential $l(l+1)/r^2$ and this is shown as a function of r for several values of l for alpha particles on ^{208}Pb. These particles are strongly absorbed, so the scattering is essentially determined by the potential beyond the classical turning point defined by the condition that the incident energy equals $V(r)$. Now if the position of the turning point is regarded as a function of l at a fixed energy, it can be seen from Fig. 16 that it moves inwards suddenly at a particular value of l. This sudden movement of

the classical turning point allows the phase shift to increase by $n\pi$ and hence gives rise to potential ambiguities.

The connexion between this sudden movement and the ambiguities is shown in Fig. 17. Here several different potentials all giving

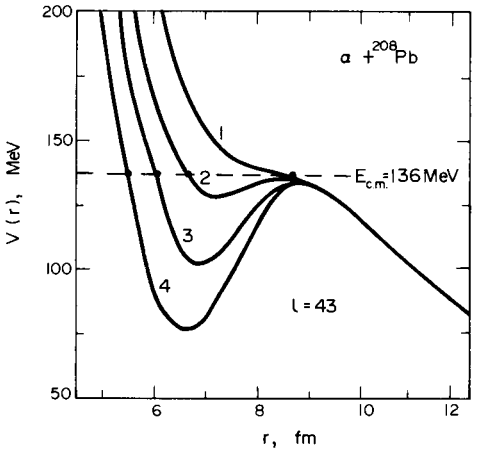

Fig. 17. Effective potentials for the elastic scattering of alpha particles by ^{208}Pb for $l = 43$ only. Each of these potentials gives the same scattering, showing that the phase shifts differ by $n\pi$.

essentially the same differential cross-section are plotted as a function of radial distance for the critical partial wave with $l = 43$. For each potential, the turning point moves in suddenly by amounts corresponding to phase shift increases of π, 2π and 3π. For energies less than E_c, the ambiguities occur for values of $l < l_c$, but at energies higher than E_c they do not arise, because there is no dip in the effective potential and hence no sudden inward movement of the turning point. It is thus possible to understand why the potentials show ambiguities at low energies but not at high energies, and to relate the critical energy to the form of the effective potential.

Another way of removing the so-called 'discrete ambiguities' involves the scattering of α particles from aligned nuclei. Elastic α particle scattering can be very well described using the optical model of the interaction. According to this model, the α particle moves in a

complex potential with radius and surface diffuseness similar to that of the nucleus itself, and with appropriate choice of parameters the differential cross-section can be fitted to high accuracy. Unfortunately, it is frequently found that there are several different sets of potentials which give equally good fits to the data ('discrete' ambiguities), and within each set it is often possible to make correlated variations of the parameters that preserve the fit ('continuous' ambiguities). Physically this is easily understood; elastic scattering depends only on the asymptotic form of the wavefunction and in addition the α particles interact so strongly with the nuclear field that those that are elastically scattered can only have passed through the surface region, so that all potentials giving the correct behaviour in this surface region give the same scattering.

These ambiguities lead to difficulties when the potentials are used to generate wavefunctions for use in reaction calculations, so many attempts have been made to resolve them. In the case of deuterons, the low binding energy makes it easy to calculate the deuteron-nucleus potential from the constituent neutron-nucleus and proton-nucleus optical potentials, but for the more tightly bound helions, tritons and α particles this cannot yet be done with sufficient accuracy. The discrete ambiguities tend to disappear at higher energies, and this can be understood physically as explained above.

Parks *et al.* (1972) have found another means of getting round the problem. Scattering from aligned nuclei is much more sensitive to the potential than the scattering from non-aligned nuclei—providing, of course, that the nucleus itself, and hence the potential, is deformed—and in their experiment, nuclei of the strongly-deformed ^{165}Ho were aligned by reducing the temperature to within a fraction of a degree of absolute zero. At these temperatures the forces within the metallic crystal align the nuclei, and this alignment is not destroyed by thermal motion.

The measurements were made by comparing the cross-section at 0.26 K, when the nuclei were aligned, with that at 1.75 K when they were not. Then the quantity

$$\frac{\Delta\sigma}{\sigma} \equiv \frac{\sigma(0.26\,\mathrm{K}) - \sigma(1.75\,\mathrm{K})}{\sigma(1.75\,\mathrm{K})} = \sum_{m>0} A_m \sigma_m(\theta)$$

gives a measure of the effects of the alignment on the scattering. This is shown in Fig. 18 for incident α particle energies from 20 to 24 MeV for scattering through 160°. It is also expressible as a sum over the cross-sections $\sigma_m(\theta)$ for scattering by the nucleus in a magnetic substate m. The coefficients A_m can be calculated from the temperature of the crystal, its structure and the parameters of the nuclear hyperfine Hamiltonian, and $\sigma_m(\theta)$ can be obtained from a coupled-channels calculation of the interaction. Thus $\Delta\sigma/\sigma$ can be calculated

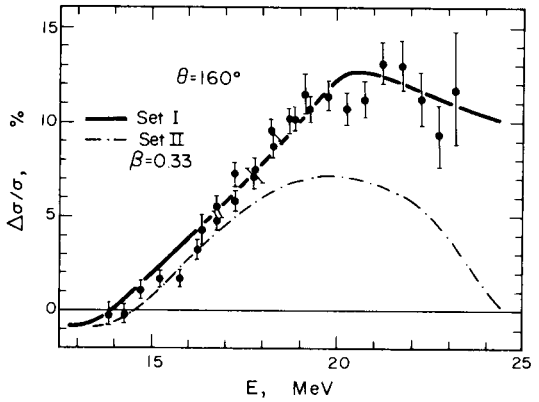

Fig. 18. $\Delta\sigma/\sigma$ as a function of incident α particle energy. The two curves are calculated from optical potentials that give equally good fits to the differential cross-sections.

from the optical potential, and results of two such calculations, using potentials found by Aponick *et al.* (1970) to give equally good fits to the differential cross-section, are also shown in Fig. 18.

It is clear that one is consistent with the data and the other is not, so that the discrete ambiguity is resolved. The best value of the nuclear deformation found by optimizing the fit to the data ($\beta = 0.320 \pm 0.020$) agrees well with the results found by analyses of Coulomb excitation ($\beta = 0.33$) and the photoneutron cross-sections ($\beta = 0.319 \pm 0.003$). The sign of β is determined because $\Delta\sigma/\sigma$ would have opposite sign for an oblate deformation.

Comment by Professor Goldberg

The critical angle θ_c is the rainbow angle studied classically by Ford and Wheeler (1959). In the case of scattering by light ions there are two rainbows corresponding to extreme positive and negative deflections; these are the Coulomb and the nuclear rainbows respectively. The original Ford–Wheeler work and much of the recent low-energy heavy-ion data are examples of the former whereas our own work refers to the latter.

It can easily be seen from a simple classical argument why measurements beyond the rainbow angle eliminate ambiguities in the potential. Thus given two potentials of similar shape the one with the greater depth should have the larger maximum deflection (rainbow) angle, and hence determining that angle should determine the potential. Classically, this is done by moving the detector to increasingly large angles until no more particles are observed, so that the rainbow angle is determined by making measurements beyond it. It is also interesting to note that the condition which precludes phase-shift equivalence is precisely that required to preclude spiral scattering, namely that the energy be greater than the highest angular momentum barrier.

References

K. W. Ford and J. A. Wheeler, *Ann. Phys.* (New York) **7**, 259, 1959.
D. A. Goldberg and S. M. Smith, *Phys. Rev. Lett.* **29**, 500, 1972.
D. A. Goldberg, S. M. Smith, H. G. Pugh, P. G. Roos and N. S. Wall, *Phys. Rev.* **C7**, 1938, 1973.
D. A. Goldberg, S. M. Smith and G. F. Burdzik, *Phys. Rev.* **C10**, 1362, 1974.
D. R. Parks, S. L. Tabor, B. B. Triplett, H. T. King, T. R. Fisher and B. A. Watson, *Phys. Rev. Lett.* **29**, 1264, 1972.

1.6 Helion Inelastic Scattering as a Nuclear Probe

(*Nature Physical Science* **238**, 113, 1972)

In recent years increasing attention has been given to the interaction of composite particles with nuclei, in particular to the elastic and inelastic scattering of deuterons, tritons, helions and alpha-particles.

These particles are strongly absorbed by the nucleus, and hence a study of their interactions provides information on the nuclear surface, whereas the more penetrating nucleons give more information on the interior.

The optical model has been developed to the stage where it can give accurate fits to the differential cross-sections for elastic and inelastic scattering and the polarizations can also be fitted by the addition of a spin-orbit term to the potential.

The theory of inelastic scattering requires a model of the nucleus in its ground and excited states, and as this interaction preferentially excites collective states the familiar rotational and vibrational models are the most appropriate. It is then possible to express the wave function describing the whole system in terms of the wave functions describing the motions of the elastically and inelastically scattered particles and of the nucleus in its ground and excited states. The Schroedinger equation for the total wave function then gives a series of coupled equations for the elastic and inelastic wave functions and these may be solved to give the required scattering cross-sections. The optical potentials can be obtained from the elastic scattering data and then comparison of the calculated and measured inelastic data gives the required nuclear structure information, usually the static or dynamic deformation parameters for the rotational or vibrational models respectively.

Analyses of this type have been made for many years, but recently G. R. Satchler (1972) pointed out that it would be particularly interesting to measure the elastic and inelastic scattering at energies similar to that of the Coulomb barrier, for the interference between nuclear and Coulomb excitation amplitudes is then very sensitive to the phase of the nuclear interaction. At low energies an incident particle feels only the repulsive Coulomb (electrostatic) potential, but as the energy increases to that of the Coulomb barrier it begins to feel the attractive nuclear potential, and these interfere destructively. If however, the nuclear potential is imaginary, this interference becomes constructive. Thus the cross-section in this region is very sensitive to the ratio of the real and imaginary parts of the optical potential.

Some measurements in this region have now been made by F. T. Baker and colleagues (1972) at Rutgers University, and some of their

results are shown in the figure for the inelastic scattering at 140° of helions exciting the 0.56 MeV 2^+ state of ^{114}Cd. The quantity plotted is the value of the ratio R/R_{PC} as a function of energy, where $R = d\sigma$ (inelastic)/$d\sigma$ (elastic) for the interaction studied and R_{PC} is the same quantity in the absence of nuclear forces. At low energies R/R_{PC} is unity as only the Coulomb field is encountered, but it rises steeply at energies above 12 MeV, when the incident particles penetrate to the nuclear field.

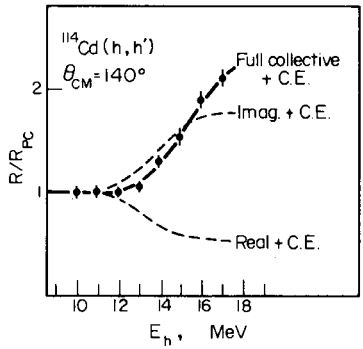

Fig. 19. Experimental results for the inelastic scattering at 140° of helions exciting the 0.56 MeV 2^+ state in ^{114}Cd.

The points show the experimental data and the curves give the values of the ratios to be expected if the potential is purely real, purely imaginary and complex in the proportions required to give the optimum fit to the experimental data. It is clear from this comparison that the interaction is almost wholly imaginary.

Some additional calculation showed that these curves are very sensitive to the shape of the imaginary part of the helion-nucleus potential in the nuclear surface, and so this comparison can be used to determine its shape at low energies.

References

F. T. Baker, T. H. Kruse, M. E. Williams, J. L. Matthews and W. Savin, *Phys. Lett.* **40B**, 355, 1972.

G. R. Satchler, *Phys. Lett.* **39B**, 492, 1972.

1.7 Nuclear Three-body Forces
(*Nature* **256,** 164, 1975)

One of the main aims of nuclear physics is to understand the structure of nuclei in terms of the interactions between the constituent nucleons. The nucleon–nucleon interaction may be studied by measuring the cross sections, polarizations and other characteristics of the scattering of free nucleons, in particular proton–proton and proton–neutron scattering. (It is not practicable to measure neutron–neutron scattering directly since suitable targets cannot be made.) Additional information is obtainable from studies of the only bound two-nucleon system, the deuteron. Very many studies of the nucleon–nucleon interaction have been made over the years in these ways, and the results can be represented by a phenomenological potential that depends on the distance between the two nucleons and on their spins. These potentials cannot be deduced from the experimental results; instead a trial form of the potential is postulated using forms suggested by meson theory and its parameters are adjusted to give the best fit to the data. The potential is thus not unique, and in fact several potentials have been found that give a good overall fit to the data on the interaction of two nucleons.

The next stage is to use this potential to calculate the properties of nuclei consisting of three or four nucleons, and to see how well the results agree with measurements on the nuclei themselves. There are several difficulties in carrying out this programme. First our knowledge of the nucleon–nucleon interaction is incomplete and subject to ambiguities. This is not too serious since it is possible to compare the results obtained by using different nucleon–nucleon interactions and if they are essentially the same it is reasonable to assume that the differences between the interactions are not important for the nuclear property under consideration.

Second, in a many-body system a nucleon–nucleon interaction takes place in the field of other nucleons, which can absorb momentum. A collision can then occur in which energy is not conserved by an amount ΔE, provided it takes place in a time Δt related to the energy uncertainty by $\Delta E \Delta t < h$. This is expressed by saying that nucleon–nucleon interactions inside the nucleus can take place 'off the energy

shell'. Nucleon–nucleon interactions in free space, on the other hand, must conserve energy and momentum exactly so that they are on the energy shell. A phenomenological nucleon–nucleon potential fitted to the two-nucleon data does not necessarily have the correct off-energy-shell behaviour, and so may not be correct for calculating interactions inside the nucleus when other nucleons are present.

Third, the purely mathematical difficulties involved in calculating the properties of a many-body system from a knowledge of the two-body interaction are so severe that only approximate results can be obtained for any but the simplest system or the simplest nuclear property. It is for this reason that the most important information is obtained from studies of the two bound three-nucleon systems, the helion and the triton. Here it is possible to obtain quite accurate results using a variational calculation or by the methods of Faddeev.

Finally, there is a difficulty in principle that would still remain even if we had a complete knowledge of the nucleon–nucleon interaction and could overcome the difficulties of calculating from it the properties of many-body systems. This is that there may be forces that only come into play in the presence of three or more nucleons. By definition we can never find out anything about these forces by studying the interactions of two nucleons. Indeed, assuming that we can overcome the other difficulties, we can obtain some indication of the importance of three-body forces by seeing how well we can calculate the properties of a three-nucleon system using only two-body forces. If there is a discrepancy, indicating the presence of three-body forces, a three-body force can be included in the interaction and the calculation repeated to see if this gives agreement with the data.

Such three-body forces can be chosen phenomenologically, but here the difficulty is that there are many possible forms, for example $V_3 f(r_{12}+r_{13}+r_{23})$ or $V_3 f(r_{12}r_{13}r_{12})$, where r_{12} is the distance between particles 1 and 2 and so on, and it is not clear what is the best form to take. An alternative approach is to try to calculate the three-body force from meson theory, and use this in calculations of nuclear structure.

In the last few years there have been several sophisticated calculations of the properties of the triton using the best phenomenological potentials fitted to the two-nucleon data, and it has been found that they all give a binding energy that is lower than the experimental value

by one or two MeV. Additional calculations show that the binding energy can be varied by as much as 3 MeV by altering the off-energy-shell behaviour, but if this is done so as to give the correct binding energy the charge distribution no longer agrees with that found from electron elastic scattering. On the other hand if the off-energy-shell behaviour is adjusted to give correct charge distribution the binding energy becomes unacceptably low. It is thus not possible to obtain a simultaneous fit to the binding energy and the charge distribution by varying the off-energy-shell behaviour.

These calculations therefore suggest that possibly the three-body forces contribute significantly to the structure of the triton, and recently Yang (1974) has made a detailed calculation from meson theory to investigate this. He took into account the emission and absorption of pions to lowest order as well as exchange of a ρ meson with a pion and the scattering of a nucleon into an N* excited state at 1,236 MeV. He then evaluated the contribution of the resulting three-body potential to the binding energy of the triton using a variational triton wave function and found that it gives an important contribution of 2.32 MeV to the binding energy. This is indeed more than enough to bind the triton, the excess being about 0.3 to 0.8 MeV, but it is likely that this is due to higher-order processes not taken into account by Yang.

These calculations suggest that the major part of the discrepancy in the calculated binding energy of the triton can be accounted for by taking three-body forces into account. Furthermore, the contribution of the three-body forces is appreciable, amounting to about a third of the total binding energy. This conclusion is highly unwelcome, since it suggests that the three-body forces, which are complicated and difficult to handle, are likely to be important in a wide range of nuclear structure calculations.

The current work on proton knockout reactions can also give information on the importance of three-body forces. Koltun and others have shown that if only two-body forces operate the total energy of the nucleus may be expressed as a sum of the nucleon removal and kinetic energies over all the occupied orbits. A recent analysis of experimental data for the (e,e'p) reaction on ^{12}C at 497 MeV (Vol. 1, §3.3); showed that for protons this sum rule gives -4.0 ± 0.5 MeV for

the mean binding energy per proton compared with the accurate value of −6.93 MeV obtained from the nuclear masses with Coulomb corrections. One possible explanation is that there are some fragments of the single-particle strength so far away from the main peak that they escape detection, so that the real centroid energy is appreciably different from the apparent centroid energy. Another explanation is that three-body forces, which were not taken into account in the derivation of the sum rule, are indeed important. A rough estimate however indicated that the contribution of the three-body forces is small, so it was concluded that the former explanation is the correct one. The results of Yang now make it likely that three-body forces must be taken into account in the derivation of the sum rule.

Another indication of the importance of three-body forces comes from the calculations of Blatt and McKellar (1974). They studied the contribution of three-body forces to the binding energy of nuclear matter, and found that it is enhanced if the nucleon–nucleon correlations are taken into account. In this calculation they used the correlation function derived from the Reid soft core potential, that has been obtained by systematically fitting a large body of data on nucleon–nucleon interactions. Their most surprising result is that the two-pion exchange three-body forces contribute as much as 6 MeV to the binding energy of nuclear matter. This result shows that the Reid potential overbinds nuclear matter when three-body forces are included. Since higher order three-body force terms and four-body force terms are likely to be negligible this indicates that the Reid potential needs to be modified to bring it into accord with all the data.

All these calculations indicate that it is not justified to neglect the contributions of three-body forces, and that they will now have to be taken into account in many nuclear reaction and nuclear structure calculations.

Some further calculations of the importance of three-body forces have recently been made by Faessler, Krewald and Wagner (1975). They investigated the effect of the limited ranges of energy and momenta that were measured in the (e,e'p) experiment. The sum rule applies to all energies and momenta for the ejected proton that are allowed by the conversation laws, whereas for instrumental reasons the energies were limited to less than 80 MeV and the momenta to less

than 300 MeV/c. Calculations can be done in the restricted region by using 'effective' interactions in place of the 'real' interactions appropriate to the whole region. Three ways of doing this were studied: (1) allowing the nucleon–nucleon interaction to depend on the density of other nucleons in their vicinity, (2) using the 'effective' three-body interaction that is equivalent to the density-dependent two-body interaction, and (3) taking account of the occupation probabilities of the single-particle orbits in what is known as the renormalized Brueckner Hartree–Fock theory.

In each case they used standard interactions obtained in other studies, and found that this accounted for essentially all the discrepancy in the sum rule, within the uncertainties of the calculation. This shows that the sum rule is satisfied within the region of energy and momenta that is studied experimentally so that there is no evidence from this region for the presence of 'real' three-body forces of the type studied by Yang.

What happens in the region of higher energies and momenta is still an open question. The short-range correlations are expected to affect momenta greater than 500 MeV/c, and a detailed calculation of this effect is highly desirable. A comparison of the results of such a calculation with the total sum rule should show whether the real three-body forces must be taken into account in the derivation of the sum rule. The results of Yang make this rather probable.

Comment by Professor B. H. J. McKellar

The correct result for our calculation of the contribution of the two-pion exchange three-body forces to the binding energy of nuclear matter is about -4 MeV. Grangé *et al.* (1976) have since pointed out that the introduction of an energy gap can reduce this figure; the second order term is reduced until it cancels the first order term, as shown in Table V of Coon *et al.* (1979). This latter paper indicates that the best estimate is about -2 MeV.

This leaves open the question of ρ-exchange contributions, and three pion contributions. We are considering these but have no results yet. Empirically it is found that ρ-exchange and form factor effects

seem to lead to the same results, so −2 MeV should still be a good estimate.

No good calculations have yet been made for the triton. All the previous calculations have ignored ρ-exchange terms and form factors. It seems likely that these could contribute a few tenths of an MeV, but a full calculation is needed and is being attempted by Coon.

References

D. W. E. Blatt and B. H. J. McKellar, *Phys. Lett.* **52B,** 10, 1974.
S. A. Coon, M. D. Scadron, P. C. McNamee, B. R. Barrett, D. W. E. Blatt and B. H. J. McKellar, *Nucl. Phys.* **A317,** 242, 1979.
A. Faessler, S. Krewald and G. J. Wagner, *Phys. Rev.* **C11,** 2069, 1975.
P. Grangé and M. Martzolff, *Lett. Nuovo Cim.* **16,** 156, 1976.
P. Grangé, M. Martzolff, Y. Nogami, D. W. L. Sprung and C. K. Ross, *Phys. Lett.* **60B,** 237, 1976.
B. H. J. McKellar and R. Rajaraman, Chapter in *Muons in Nuclei,* Ed. Sir Denys Wilkinson and Dr M. Rho (North-Holland).
S-N. Yang, *Phys. Rev.* **C10,** 2067, 1974.

1.8 Triton Potentials

(*Nature* **260,** 749, 1976)

There have been rather few studies of the interaction of tritons with nuclei, mainly because tritons are highly radio-active, with a half-life of about 12 years. Very stringent safety precautions have to be enforced, so work with tritons is usually done in Government laboratories. A series of measurements of the differential cross sections for the elastic scattering of tritons by nuclei was made some years ago at Aldermaston, and analysed to give triton optical model potentials. There were hardly any measurements of triton polarization and these were of low accuracy, so very little was known about the spin–orbit term in the triton optical potential.

Recently a polarized-triton source has been installed on the Los Alamos Scientific Laboratory Tandem Van de Graaff accelerator, and this has made possible new measurements of triton elastic scattering of a higher accuracy than ever before. The Los Alamos group have measured the differential cross sections and polarizations for tritons elastically scattered from several nuclei, and analysed the results with the optical model.

It is possible to calculate the triton optical potential by averaging the known nucleon–nucleus interaction over the three nucleons comprising the triton. This folding model, as it is called, has already been used successfully to calculate the optical potentials for deuterons, helions, and alpha particles, so it is important to test it for tritons as well.

The folding model gives for tritons an optical potential that is about three times as deep as the nucleon optical potential, has about the same radius and is slightly more diffuse in the surface region. The two neutrons in the triton are anti-aligned, so that the spin–orbit force between a triton and a nucleus is the same as that between a nucleon and a nucleus.

Now the spin–orbit force is written as $V_{so}(r)\mathbf{L}.\sigma$, where σ is the spin of the projectile and $\mathbf{L}$ the relative angular momentum betweem the projectile and the target. For the same incident velocity this angular momentum is three times greater for a triton than for a nucleon, so we

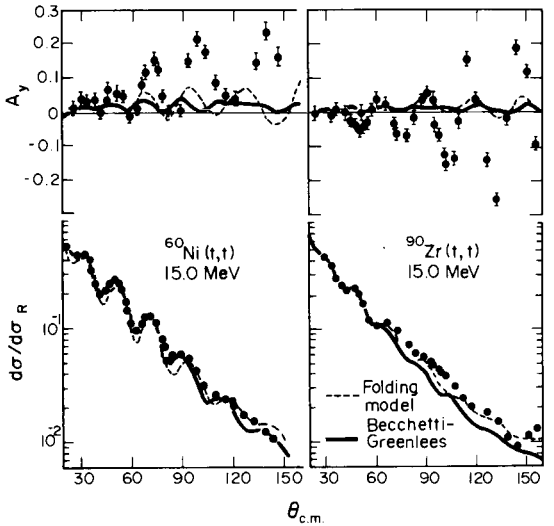

Fig. 20. Polarizations (top) and differential cross sections (bottom) for the elastic scattering of 15 MeV tritons by ^{60}Ni and ^{90}Zr compared with optical model calculations with a folding model potential (dashed lines) and with a Becchetti–Greenlees potential (full lines). Both potentials fit the differential cross sections quite well, but give polarizations that are far too small.

expect the spin–orbit potential depth to be one-third the nucleon value to leave the whole potential the same. Since the depth of the nucleon spin–orbit potential for nucleons is about 6 MeV we expect a value of about 2 MeV for the triton spin–orbit potential.

To test this prediction, the differential cross sections were first compared with calculations using a triton optical potential obtained by folding, and the parameters were slightly altered to optimize the fit. As shown in Fig. 20, this gives a good fit to the cross section. The polarizations calculated with a spin–orbit potential of 2.5 MeV are however far smaller than the measured values. Further calculations were made using optimum potentials obtained by Becchetti and Greenlees, with very similar results.

The parameters were then varied to try to fit the polarizations as well as the differential cross sections, and it was found necessary to alter the absorbing part of the potential as well as the spin–orbit potential itself. Potentials were found that fit the polarizations very well, but they have spin–orbit depths of 6 MeV, which is much greater than that given by the folding models.

The new data can therefore be successfully analysed by the optical model, but the strength of the spin–orbit potential is unexpectedly high, and poses a challenging theoretical problem.

Reference

R. A. Hardekopf, L. R. Veeser and P. W. Keaton, *Phys. Rev. Lett.* **35**, 1623, 1975.

1.9 Short-range Nuclear Forces (*Nature* **266**, 222, 1977)

Experiments on the photo–proton reaction on oxygen from 100 to 300 MeV by a joint MIT–Glasgow group have recently provided evidence that in this energy range the reaction proceeds through the $\Delta(1232)$ nucleon isobar as an intermediate state, and it is likely that this process is increasingly important at high energies.

The experiment was carried out by bombarding a beryllium target with a bremsstrahlung beam and measuring the spectrum of the emitted protons. The differential cross sections for the photo–proton

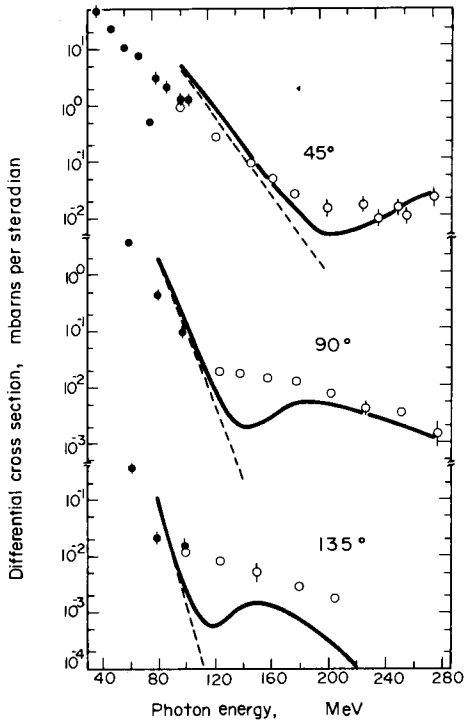

Fig. 21. Differential cross section for the $^{16}O(\gamma, p_0)^{15}N$ as a function of photon energy.

reactions on oxygen that leave the residual nucleus in its ground state are shown for several angles as a function of photon energy in Fig. 21.

It is simplest to suppose that the reaction proceeds by a single-step process in which the incident photon interacts with a single proton in the target nucleus and knocks it out. This is indicated diagrammatically in Fig. 22*a*, and gives the dashed curves in Fig. 21. It is clear that this theory, allowing for uncertainties in the calculations, is in qualitative accord with the data at low energies, but quite fails at higher energies. The calculations are rather rough, since harmonic oscillator wave functions were used, and the distortion of the wave function of the outgoing proton was neglected, but this does not affect the general conclusion.

The experimental cross sections at higher energies are much higher than those given by the one-step process. Such cross sections can be attributed phenomenologically to short-range correlations due to the repulsive core of the nucleon–nucleon interaction or a microscopic model can be made in terms of a two-step process. One such process, involving the Δ (1232) nucleon isobar excited in an intermediate state,

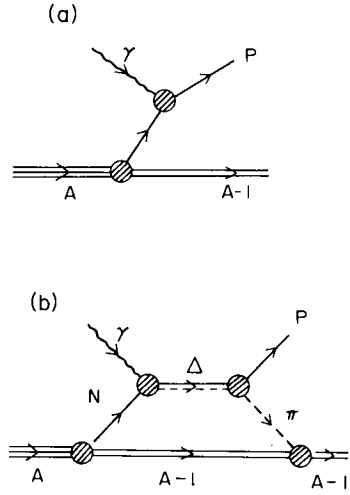

Fig. 22.

is indicated in Fig. 22*b*. Calculation with this process gives the full curves in the figure, when added to the results of the calculations of the one-step process already considered. Although there are differences in detail due to the approximations made in the calculation, it is clear that the overall trends are qualitatively given. This provides evidence that the Δ-process can make a major contribution to the photo–proton cross-section in the 100–300 MeV region, and thus gives further insight into the structure of the short-range nuclear forces.

Reference

J. L. Matthews, W. Bertozzi, M. J. Leitch, C. A. Peridier, B. L. Roberts, C. P. Sargent, W. Turchinetz, D. J. S. Findlay and R. O. Owens, *Phys. Rev. Lett.* **38**, 8, 1977.

1.10 Target-spin Effects in Elastic Scattering
(*Nature* **251**, 281, 1974)

Measurements of the elastic scattering of helions and alpha particles by nuclei have shown that the differential cross sections for odd nuclei oscillate less strongly with angle than the corresponding cross sections for neighbouring even nuclei. Since even nuclei have spin zero and odd nuclei have spins greater than zero it was at first suggested that this difference may be explained by a coupling between the relative orbital angular momentum **L** and the target spin **I** which can be represented by an **L.I** term in the optical potential. This term is similar to the $\mathbf{L}.\sigma$ spin-orbit term which is known to reduce the oscillations of differential cross sections. But this explanation of the difference was rendered unlikely by Satchler's calculations (1963) of the magnitude of the **L.I** target-spin term, which showed that it is far too weak to account for the observed differences in the cross sections.

It has recently been suggested by Satchler and Fulmer (1974) that another possible explanation may be found in the different shapes of neighbouring odd and even nuclei due to particle–core coupling. According to this model the odd nucleus is considered as a single particle (or hole) coupled to states of the core with spin **L**, where the core is the adjacent even nucleus. The coupling allows the valence particle to polarize the core and thus gives it a quadrupole moment, and the extra scattering from the quadrupole moment has the effect of smoothing the angular distribution of the scattering from odd nuclei.

To test this explanation, Fulmer measured the differential cross section for the elastic scattering of 49.9 MeV a particles by ^{59}Co ($I = 7/2$) and by ^{60}Ni ($I = 0$). As shown in Fig. 23, the ^{60}Ni cross section oscillates significantly more than the ^{59}Co cross section.

The theory of elastic scattering from odd and even nuclei taking into account the quadrupole moment scattering predicts that they are related by

$$\sigma_{\mathrm{EL}}(\mathrm{odd}) \approx \sigma_{\mathrm{EL}}(\mathrm{even}) + \sum_{L} K_L \sigma_{\mathrm{INEL}}\,(\mathrm{even};\, 0^+ \rightarrow L^+),$$

where K_L is a coefficient that can be found from the measured 2^L-pole moments of the ground state of the odd nucleus and the measured

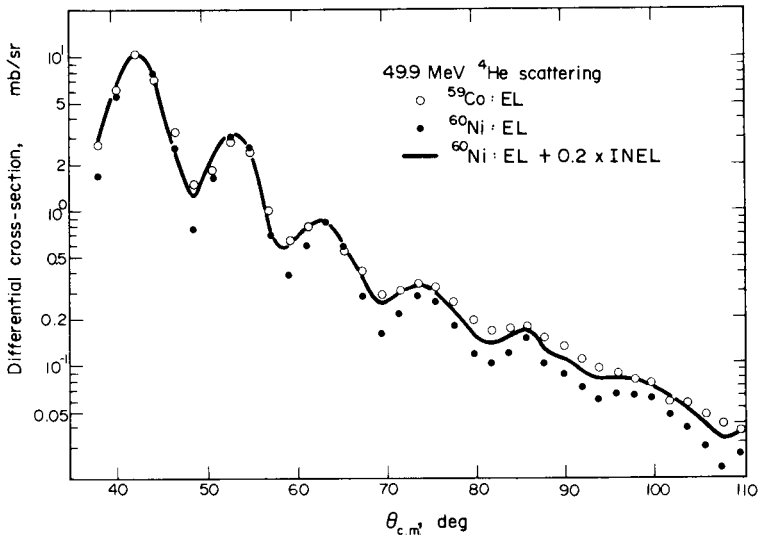

Fig. 23. Differential cross sections for the elastic scattering of 49.9 MeV α particles by ^{59}Co and by ^{60}Ni showing the difference in the oscillatory structure. The full line is the cross section for ^{59}Co calculated as described in the text from the cross section for ^{60}Ni plus auxiliary data, and agrees well with the ^{59}Co measurements.

strength of the electromagnetic excitation of the corresponding state in even nucleus. The inelastic cross section $\sigma_{\text{INEL}}(\text{even}; 0^+ \rightarrow L^+)$ for the excitation of an L^+ state in the even nucleus is also known experimentally. It is thus possible to calculate the elastic scattering from an odd nucleus from measurable properties of the neighbouring even nucleus in a direct way using a simple model.

The ^{59}Co cross section was found in this way from the ^{60}Ni cross section and the appropriate inelastic scattering and electromagnetic transition data, and the results are shown by the full line in the figure. This agrees very well with the measured results for ^{59}Co, indicating that quadrupole moment scattering is indeed responsible for at least the major part of the difference between the scattering from ^{59}Co and ^{60}Ni.

Further calculations showed that the same model is also able to account for the observed differences between the elastic scattering of

60 MeV helions by ^{59}Co and ^{60}Ni. It is likely that it could account for other odd–even differences that have been observed in elastic scattering, except for nuclei with $I = \frac{1}{2}$, for which quadrupole moment scattering is zero. Examples of this occur for ^{89}Y and ^{207}Pb, and such nuclei are therefore suitable for the study of target-spin effects.

This work sheds further light on the character of the optical potential. It would presumably be possible to fit the observed difference between the elastic scattering from odd and even nuclei by including an **L.I** term in the potential and arbitrarily adjusting its strength. This strength would, however, vary from nucleus to nucleus depending on the deformation and would be much greater than the value calculated from the microscopic theory of the optical potential. This is clearly unsatisfactory, and a much better way of analysing the data is provided by the present work, which shows that a more detailed account of the physics of the interaction enables the data to be understood in a systematic way without arbitrary parameters.

References

G. R. Satchler, *Nucl. Phys.* **45,** 197, 1963.
G. R. Satchler and C. B. Fulmer, *Phys. Lett.* **50B,** 309, 1974.

1.11 Spin-spin Forces in Nuclei
(*New Scientist* **73,** 272, 1977)

Recent calculations have thrown serious doubt on the interpretation of experiments that were previously thought to provide evidence for the presence of spin-spin forces in nuclei.

Over the years there have been many experiments designed to study the strong forces between a nucleon (a single proton or neutron) and a nucleus. Naturally they depend on the distance between the two particles; and some features of their interaction, particularly the extent to which an initially unpolarized beam is polarized when it is scattered by a nucleus, can be explained by postulating a spin-orbit force that depends on the spin of the nucleon and its own angular momentum around the nucleus.

In addition many people have tried to find out whether the forces

depend on the spin of the nucleus as well as on the spin of the nucleon, and in particular on their mutual interaction. These are the postulated spin-spin forces.

Unfortunately it is extremely difficult to study this experimentally. To get a significant result it is necessary to have a polarized beam of nucleons colliding with a polarized target. It is fairly easy to make a polarized beam of nucleons—and this is usually the way we study the spin-orbit forces—but it is very difficult to polarize the target. Even the best techniques will only work for a very few substances, including cobalt-59.

It is not possible to polarize the spins and to carry out the scattering experiment with a thin target, but only with a thick one, and this means that we have to use neutrons and not protons so that they do not lose much of their energy by ionization. So our experimental difficulties force us to use neutrons on cobalt or some similar material.

Some of these experiments have been taken to indicate that for neutrons less than about 1 MeV the strength of the spin-spin force is about -2.5 MeV, with a strong energy variation. This was difficult to understand, as the best theoretical estimates indicate a strength of about 0.35 MeV for the spin-spin force, with no strong dependence on the energy of the incoming neutron.

The experimental values of the strength of the spin-spin force required using the 'optical model' of the nucleus with a spin-spin force included. In this calculation it was tacitly assumed that all the scattering took place by a direct process—one that takes place in a time comparable to the time it takes the incident neutron to cross the target nucleus.

Now it is also possible for the reaction to take place by the capture of the neutron by the target nucleus and its subsequent emission, after a longer time interval, with its full energy. This is called a 'compound nucleus' reaction. It was assumed that such reactions only gave unpolarized neutrons and so if they occurred they could at worst dilute the observed effects and hence reduce the estimate of the strength of the spin-spin force.

Now the new work by Thompson has shown by a careful analysis of the compound nucleus reaction that because of the spin dependence of the nuclear level densities it is possible for such slow processes to make

a large negative contribution to the observed effective strength of the spin-spin force. It thus seems that most of the effects observed so far are attributable to compound nucleus reactions and not to spin-spin forces at all. Certainly even if they are present it will be very difficult to detect their effects in the presence of the effect of the compound nucleus reactions.

Comment

Since the publication of Thompson's work, Heeringa *et al.* (1977) have studied the spin-spin interaction by scattering 8 to 31 MeV polarized neutrons by aligned ^{59}Co. They conclude that compound nucleus processes should be negligible in this energy range, but still find it difficult to extract an accurate value of the spin-spin potential. Their best estimate is about four times the theoretical value of Satchler (1971, 1972), and of the opposite sign, so the situation is still unclear.

References

W. Heeringa, H. Postma, H. Dobiasch, R. Fischer, H. O. Klages, R. Maschuur and B. Zeitritz, *Phys. Rev.* **C16,** 1389, 1977.
G. R. Satchler, *Phys. Lett.* **34B**, 37, 1971; *Particles and Nuclei*, **1,** 397, 1972.
W. J. Thompson, *Phys. Lett.* **65B,** 309, 1976.

1.12 Nuclear Glue Probed with Gamma Rays
(*New Scientist* **72,** 213, 1976)

All nucleons are surrounded by a cloud of mesons, and this is why mesons are emitted when nucleons collide at very high energies. One of the best ways of probing the mesonic fields of nuclei is by measurements of photomeson production. In this process, an energetic gamma ray interacts with a nucleon and liberates a meson, or more precisely a pion, for it is these mesons that are most plentifully found around nucleons.

Several theories of photomeson production have been developed, and these enable the probability of the reaction taking place, and the angular distribution of the emitted pions, to be calculated. This depends on the details of the interaction between the photon and the

nucleon, so various hypotheses are made and the results compared with the experimental data.

Unfortunately, photomeson production is not easy to study experimentally in a precise way. In most cases very many different reactions take place together and this complicates the theoretical interpretation and makes it difficult to draw definite conclusions. What is wanted is a way of studying just one reaction at a time.

This has recently been done by a group at MIT and Boston University (Bernstein *et al.*, 1976). They realized that photomeson production on carbon can lead to the ground state of nitrogen 14, and this can be identified by its 11 msec beta-radioactivity with an end point at 16.3 MeV. This makes it possible to study just the $^{12}C(\gamma,\bar{\pi})^{12}N$ reaction on its own without interference from any of the other reactions that are taking place at the same time. This reaction also has the advantage that the negative pion is attracted by the nuclear field and so interacts more strongly with it than a positive pion, so that the cross-section of the reaction is more sensitive to the smaller terms in the interaction.

The experiment was carried out by irradiating a tantalum–aluminium target with electrons from the MIT Linear Accelerator. These electrons are deflected by the nuclear fields of the target nuclei and produce a beam of high energy photons that hit the carbon target. The beta rays from the decay of the ^{12}N nuclei produced in the photomeson production reaction are deflected away from the target and are counted by plastic scintillation counters. Coincidences between four counters were required to reduce the background due to delayed neutron capture gamma rays, and separate experiments were made to evaluate the proportions of electrons from other processes so that they could be subtracted from the total number of counts. The layout of the experimental apparatus is shown schematically in Fig. 24.

In the experiment, the yield of pions was measured as the energy of the gamma rays was increased, and the results were compared with calculations based on various possible assumed interactions between the photon and the nucleon. Since this takes place through the mesonic field, this tells us about the field itself.

The most important part of the interaction is represented by a term that is proportional to $\sigma.\varepsilon$ where σ is the nucleon spin operator and ε is

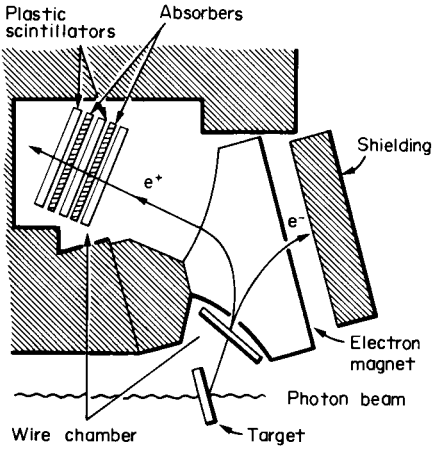

Fig. 24. Layout of the experimental apparatus for the measurement of the total photomeson cross-section in the reaction $^{12}C(\gamma,\bar{\pi})^{12}N$.

the photon polarization vector. It was found that the experimental cross-section rises far more rapidly with energy than is predicted by this term alone. When other terms, depending on the pion momentum, were also included in the calculation the agreement was improved, but even then the experimental cross-section rises rather more rapidly than predicted by the theory.

This new method of measuring accurately the cross-section of a particular photomeson production reaction to a particular final state is thus a powerful way of probing the nuclear mesonic field. It is likely that more such measurements will be made, and that the comparison of the results with the theories will lead to more detailed understanding of the mesonic field.

Reference

A. M. Bernstein, N. Paras, W. Turchinetz, B. Chasan and E. C. Booth, *Phys. Rev. Lett.* **37**, 819, 1976.

CHAPTER 2

Nuclear Reaction Mechanisms

2.1 Nuclear Reaction Times
(Nature **245,** 240, 1973)

It is usual to divide nuclear reactions into two stages: the first is the direct interaction of the incident particle with the target nucleus, and this takes place in the time it takes for the particle to cross the nucleus, usually about 10^{-22} s. After the direct stage, the remaining nucleus is in an excited state in which the energy is shared statistically among all its nucleons. Many interactions can take place among them, and eventually it happens that a nucleon or group of nucleons near the nuclear surface receives enough energy for it to escape, and this continues until the remaining nucleus is left in its ground state. This process is the decay of the compound nucleus, and takes a much longer time, of the order of 10^{-13} to 10^{-18} s.

The theories of the direct and compound stages of the nuclear interaction are now quite well understood, and it is possible to calculate the angular and energy distributions of the particles emitted in each stage, and to compare their sum with the experimental observations.

The time delay between the two processes naturally raises the question whether they can be observed individually, but because the most refined electronics cannot resolve times shorter than about 10^{-9} s, it is quite impracticable to do it directly. A very ingenious way of doing this indirectly has, however, been developed recently, and Professor G. M. Temmer and his colleagues at Rutgers University and Bell Laboratories reported at a recent conference that they have used it to resolve the direct and compound contributions to the elastic

scattering of protons by germanium-72.

The method depends on using a crystal as a target so that the nuclei are in a regular spatial array. If a nucleus in a regular crystal emits a particle along the direction of one of the crystal axes, it will collide with the next nucleus and be scattered. Thus particles emitted in these directions are blocked and cannot escape from the crystal. If, however, the emitting nucleus moves from its original position, a particle emitted along the crystal axis will travel between the lines of nuclei and so escape. A struck nucleus recoils and the distance it travels before emission depends on the time between the initial impact and the decay; this is different for a direct and a compound process. In a direct process the target nucleus does not have time to move, but in a compound nucleus process it may move sufficiently far from its equilibrium

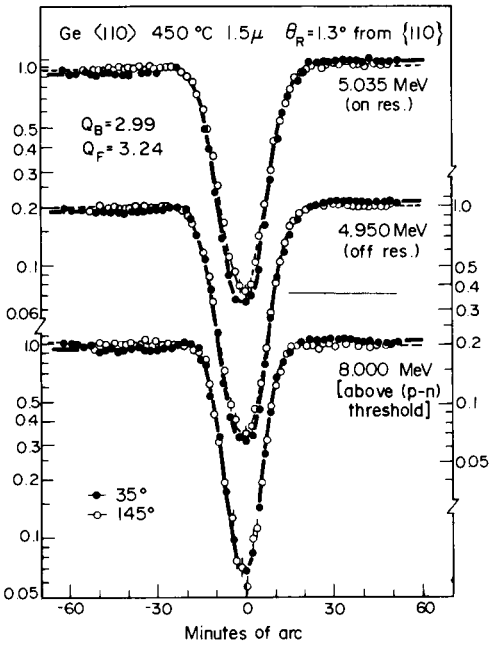

Fig. 25.

position to increase the chance of escape of a particle emitted along a crystal axis.

Fig. 25 shows the intensities of particle emission as the detector moves across the line of the crystal axis, and the dip due to blocking is clearly seen. This was done for emission angles of 35° and 145°, and a small difference between them can be seen. The direct process contributes proportionately more at the forward angle of 35° than at the backward angle of 145°, and the amount of this difference allows the mean lifetime of the compound nucleus to be determined; the result is found to be about 1.4×10^{-16} s. The three sets of measurements illustrated refer to energies on and off the isobaric resonance at 5 MeV and at an energy above the (p,n) threshold. At this last mentioned energy so many reaction channels are available for the decay of the compound nucleus that the compound elastic process is negligible. Thus the direct reaction dominates at both angles, so the transmission curves are the same.

This very ingenious measurement makes possible a series of refined tests of nuclear reaction theories in an entirely new way and marks a notable advance in nuclear physics techniques.

Comment by Professor G. M. Temmer

In the four years following this report, we have extended our measurements to very thin nickel crystals (7000Å thick); because of the very high neutron threshold in ^{58}Ni (9.5 MeV) one is able to reach higher excitation regions of the compound nucleus ^{59}Cu where fine-structure levels begin to overlap. An excitation curve on a thin evaporated target shows a very complicated fluctuating structure. We were able to determine the compound-elastic fraction of the scattering cross section at 145 degrees, as well as to determine its mean life. We found that the mean level width corresponding to this lifetime was about 50 eV, at least two orders of magnitude less than the width inferred from conventional Ericson fluctuation analysis. We believe that the fluctuations are in fact caused by the overlap of analogue states in ^{59}Cu whose density is already quite high because of the energetics in this particular nucleus. A width of about 10 keV for analogue states in this region is quite reasonable.

We also addressed the question as to whether, in a fluctuating cross section situation, the lifetime would turn out to be the same on the average whether the measurement is carried out in a region of large or small cross section; we did in fact find a significant difference, yielding a 30 per cent shorter lifetime near a peak compared to the lifetime near a valley in the cross section. This can only be explained in terms of some enhancing intermediate structure.

References

E. P. Kanter, D. Kollewe, K. Komaki, I. Leuca, G. M. Temmer and W. M. Gibson, *Nucl. Phys.* **A299**, 230, 1978.

G. M. Temmer, E. P. Kanter, Y. Hashimoto, K. R. Alver, I. Leuca and W. M. Gibson, *Proceedings of the International Conference on Nuclear Physics*, Munich, 27 August to 1 September 1973 (North-Holland/American Elsevier) I, 512; *Phys. Rev. Lett.* **35**, 1326, 1975.

2.2 Measurement of Short Nuclear Lifetimes

(New Scientist **71**, 284, 1976)

Nuclei that are given some extra energy soon lose it by emitting particles and gamma rays. This takes place so quickly that it is very difficult to measure: times around 10^{-18} seconds are typical of nuclear lifetimes. Even the fastest electronics cannot measure times much smaller than 10^{-9} seconds, so an entirely new method has to be devised to measure nuclear lifetimes.

One very ingenious method of doing this is called the blocking technique. It depends on the fact that particles emitted from nuclei within a crystal cannot get out in the directions corresponding to travelling along one of the crystal planes. Thus in Fig. 26 (first figure) no particles can get out in the direction A: there are just too many other particles in the way. The radiation is blocked.

If, however, a nucleus steps out of line, it can easily send a particle in this direction. It goes between the rows of nuclei, as shown in Fig. 26 (second figure).

Now when a nucleus is excited to a higher energy state, for example by being struck by another particle, it recoils, and thus can move out

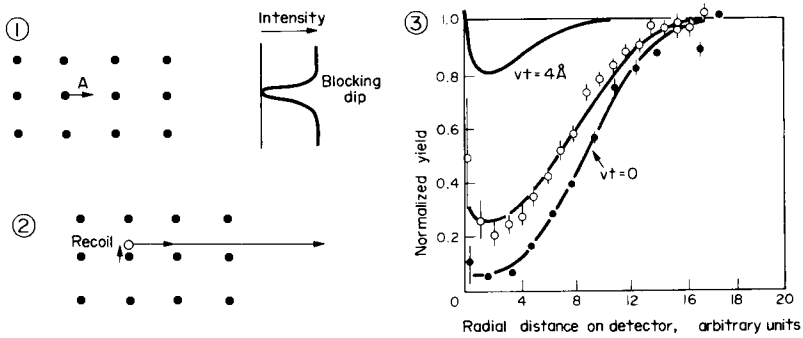

Fig. 26.

of line. If its lifetime is very short it does not move appreciably before the radiation is emitted and the radiation is blocked. But if the lifetime is long enough for it to move out of line, the radiation can escape from the crystal. Since we can calculate the energy of the recoiling nucleus from the details of the initial interaction, we know its velocity, and hence how far it can go in a given time. The degree of blocking is thus directly related to the nuclear lifetime, and can be used to measure it with some precision.

In practice, a position-sensitive detector enables the dip around the blocked direction to be measured. A broad and deep dip corresponds to a very short lifetime and a narrow and shallow dip to a longer lifetime. Some typical blocking curves are shown in Fig. 26 (third figure). Detailed calculations have to be made to take account of the various directions of nuclear recoil, but when this is done we obtain a relation between the depth and width of the blocking dip and the nuclear lifetime.

This method has recently been used to study the decay of the compound nucleus formed by the bombardment of tungsten with 90 MeV oxygen ions. The tungsten target was in the form of thin crystals, and the intensity of particles emitted in various directions was measured. Since the compound nucleus undergoes fission, the particles are fission fragments. The curve obtained for the blocking dip is shown in Fig. 26 (third figure).

In this figure, the lower curve is the one that would be obtained from immediate decay (zero lifetime), and the full circles are experimental

measurements of such a process. The upper curve corresponds to a product of recoil velocity and lifetime of 4 angstroms. The experimentally observed points for the oxygen–tungsten process (open circles) fall between these two curves, and cannot be fitted by a blocking curve corresponding to any one nuclear lifetime. Calculations showed that it could be explained as the superposition of two curves of different lifetimes, and this tells us how the compound nucleus decays. There are two possibilities corresponding to the two lifetimes: firstly the nucleus can undergo fission directly with a characteristic lifetime of less than 10^{-18} seconds, and alternatively it can evaporate a few neutrons and then undergo fission. Since the fission after evaporation is slow, it has little effect on the corresponding lifetime and its characteristic period is about 10^{-16} seconds.

Combining the results of these two processes accounts for the measured blocking curve, and shows that the immediate fission accounts for about 80 per cent of the decays and the evaporation followed by fission for the remaining 20 per cent.

References

J. U. Andersen, E. Laegsgaard, K. O. Nielsen, W. M. Gibson, J. S. Forester, I. V. Mitchell and D. Ward, *Phys. Rev. Lett.* **36**, 1539, 1976.

2.3 Wigner Cusps in Nuclear Reactions
(*Nature* **259**, 364, 1976)

When a proton is incident on a nucleus, many different reactions can take place. It may be elastically or inelastically scattered, it may be captured to form a compound nucleus which subsequently emits neutrons, protons or other particles, it may undergo (p,n) charge exchange, it may pick up a neutron to form a deuteron, it may knock out an alpha particle and so on. The relative probabilities of these processes depend on how easily the particles can get in and out of the nucleus (barrier penetration factors) and on the structure of the nucleus. The penetration factors depend on energy, and as the energy of the incident particle increases more and more reactions become possible.

At low energies the compound nucleus processes dominate, and

then the cross section for all the non-elastic reactions depends on the penetration factor for the incoming particle, and this increases smoothly with energy.

As this energy increases this cross section has to be shared out among more and more of the reaction processes. The situation is rather like steadily increasing the flow of water into a closed tank, and at the same time making more and more holes of different sizes in the side of the tank. If we then concentrate our attention on the water coming out of one particular hole, we still see that at first it increases because of the increasing flow of liquid into the tank, and then decreases because more and more of the water is flowing out of all the other holes.

If we look very carefully, we may notice another effect: the flow of water out of our one hole falls slightly just after another hole has been made. This is because at any one time the total flow out must be the same as the total flow in, since the tank is closed and water is incompressible.

A very similar effect in nuclear reactions was predicted by Wigner in 1968. Each reaction process has a threshold energy: if the incident particle is below this energy the reaction cannot take place, but as soon as it is exceeded the cross section increases rapidly from zero. (This is the counterpart to punching another hole in the tank.) But since the total flux is constant, this must produce a small reduction in the cross section for all the other processes, and Wigner calculated the shape of the resulting cusps in the cross section as a function of incident energy.

It is interesting to try to observe these cusps as they would provide a delicate test of nuclear reaction theory, but they are not easy to see. Usually there are so many hundreds or thousands of reactions taking place at the same time that the opening of another reaction channel, as it is called, does not make any perceptible difference.

The best conditions for observing Wigner cusps occur in the reactions of light nuclei, for in this case the level density is smaller and hence there are fewer channels. The effects of opening another channel are then more prominent, and indeed several cusps have been observed in light nucleus reactions, associated with the crossing of thresholds in neutron-induced reactions.

It is also interesting to look for Wigner cusps in proton reactions on heavier nuclei, and a remarkable example has recently been found in

the $^{64}Ni(p,\gamma)^{65}Cu$ reaction by Mann and his colleagues at the California Institute of Technology (1975).

This reaction was chosen because even though it is on quite a heavy nucleus it provides especially favourable conditions for the observation of a Wigner cusp. These are that the new channel opens quickly, absorbing an appreciable fraction of the total flux, and that there are very few channels open already to share the resulting decrease in flux. These conditions are very well satisfied for the (p,γ) channel on ^{64}Ni at the opening of the neutron threshold. The lowest excited states of ^{64}Ni are at relatively high energies and this, together with the low energy of the neutron threshold (opening of the (p,n) channel), reduces the contribution of the inelastic scattering and compound elastic processes to the total reaction cross section. A possible competing reaction, alpha particle emission, is strongly inhibited by the Coulomb barrier, so that the total reaction cross section below the (p,n) threshold is mainly composed of the (p,γ) channels. Another favourable feature is the high density of low-lying states in ^{64}Cu, the final nucleus in the (p,n) reaction, which ensures that the total (p,n) cross section increases very rapidly, producing a strong depletion in the (p,γ) cross section.

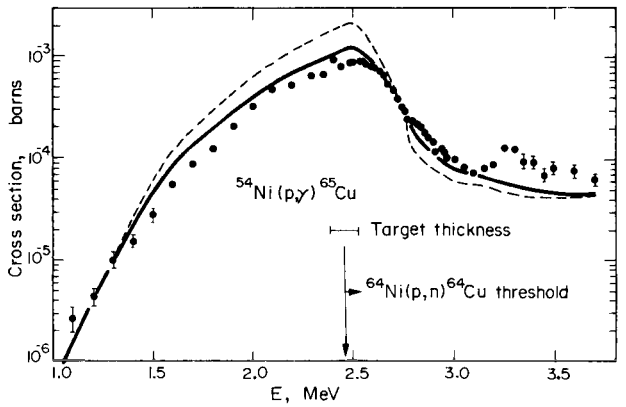

Fig. 27. Excitation function for the $^{64}Ni(p,\gamma)^{65}Cu$ reaction showing the Wigner cusps due to the crossing of the neutron threshold at 2.46 MeV. The curves show the results of Hauser–Feshbach statistical model calculations with (full) and without (dashed) the width fluctuation correction.

The measurements of the (p,γ) cross section were made from 1.1 to 3.7 MeV in 100 keV steps, and the yields for the reaction to the first three excited states of ^{65}Cu were summed to give the results shown in the figure. It is notable that the cross section increases steadily from 1 to 2.5 MeV and then drops dramatically by a factor of 10 over the next 0.5 MeV as a result of the crossing of the (p,n) thresholds. In this case the Wigner cusp is not a tiny perturbation but a major feature of the cross section. Many neutron thresholds are passed above 2.5 MeV and these all contribute to the drop in the (p,γ) cross section.

A small resonance is visible in the (p,γ) cross section at about 3.27 MeV. This is attributed to the state in ^{65}Cu that is the analogue of the first excited state of ^{65}Ni.

At such low energies the reaction is dominated by the compound nucleus process; the incident proton is captured by the ^{64}Ni nucleus to form a compound nucleus ^{65}Cu and after a long time on the nuclear scale it emits one or more gamma rays until it returns to the ground state. The cross sections for such processes can be calculated by the Hauser–Feshbach statistical theory, using barrier penetration factors calculated from the appropriate optical model potentials. Since the number of open channels is small, this reaction is a severe test of the theory.

The results of Hauser–Feshbach calculations are shown by the dashed curve in Fig. 27 and are in qualitative agreement with the measurements. If account is also taken of the correlations between the partial widths in the entrance and exit channels by including the width fluctuation correction the improved results shown by the full line are obtained.

This comparison shows that the Hauser–Feshbach theory is well able to account for the Wigner cusps, and that it is important to include the width fluctuation correction.

Comment by Professor W. A. Fowler

The Kellogg Laboratory has continued its work on cusps and that found in ^{54}Cr(p,γ)^{55}Mn is discussed by Zyskind *et al.* (1978). Measurements have been made for several other reactions and will be published shortly.

Because the term 'Wigner cusps' has been applied to the threshold effects observed when single isolated resonances are involved, our use of the term was incorrect. Meyerhof (1962, 1963) has pointed out that we are observing 'energy-averaged Wigner cusps'. We now use the term 'cusps' or 'competition cusps'. A mathematician might even quarrel with this since a mathematical cusp requires the two tangents to be parallel at the discontinuity.

We have made extensive comparisons of our experimental results with Hauser–Fishbach theories with an adjustable isospin mixing parameter. We have concluded that complete mixing yields satisfactory results if width fluctuation corrections are included and if empirical neutron strength functions are employed.

References

F. M. Mann, R. A. Dayras and Z. E. Switkowski, *Phys. Lett.* **58B**, 420, 1975.
W. E. Meyerhof, *Phys. Rev.* **128**, 2312, 1962; **129**, 692, 1963.
E. P. Wigner, *Phys. Rev.* **73**, 1002, 1968.
J. L Zyskind, J. M. Davidson, M. T. Esat, M. H. Sapiro and R. H. Spear, *Nucl. Phys.* **A301**, 179, 1978.

2.4 Direct or Semi-direct?

(*Nature Physical Science* **232**, 178, 1971)

Recent measurements of the spectra of the gamma rays emitted when 9.2, 11.2 and 13.2 MeV neutrons are captured by ^{208}Pb have enabled Bergqvist and his collaborators at Los Alamos to confirm the semi-direct (or collective) capture theory of photonuclear reactions (1971).

The theories of photonuclear capture have developed over the years as data of higher precision have demanded more sophisticated models. The simplest model is the familiar compound nucleus theory which assumes that the incident neutron is captured to form an excited compound nucleus that persists for a long time (on the nuclear scale) before decaying to its ground state by cascade emission of gamma rays. According to this model, the energy brought in by the incident nucleon is shared and reshared among all the nucleons of the compound nucleus so that statistical equilibrium is established. The model

predicts that the gamma rays are emitted symmetrically in the forward and backward directions with respect to the incident particle, and use of the statistical theory of nuclear level densities also allows their energy distribution to be calculated.

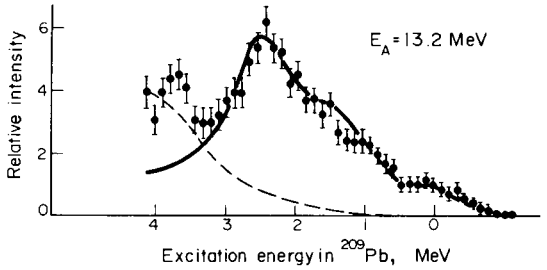

Fig. 28. Spectrum of gamma rays from the reaction ^{208}Pb (n,γ) for 13.2 MeV neutrons; ---, prediction of the compound nucleus theory; —, prediction of the semi-direct capture theory.

This compound nucleus theory accounts very well for the spectra of particles emitted from some low energy nuclear reactions, and is also satisfactory for photonuclear reactions in the same energy region. As the energy increases beyond about 4 MeV, however, the measured cross-sections become progressively greater than those given by the compound nucleus theory and at 14 MeV, for example, the theory is low by one to two orders of magnitude for light nuclei and four to five orders of magnitude for heavy nuclei (Lane and Lynn, 1959).

Clearly another mechanism is operating at higher energies and several authors have proposed that the incident particle makes a direct radiative transition to the lower single-particle states of the compound system. Calculations by Daly, Rook and Hodgson (1964) showed that this model can account for the chief features of the measured cross-sections at higher energies, though the absolute magnitudes are still about an order of magnitude too low. Some additional process that enhances the cross-sections above their direct capture values must be taking place.

A possible mechanism for this enhancement was found by taking collective effects into account. This semi-direct model, as it is called, assumes that the incident particle is first captured into a lower single-particle orbit with simultaneous excitation of the giant dipole

resonance of the target. This intermediate state then decays with gamma emission, and the intensity of the gamma rays is enhanced by the collective nature of the excitation. Calculations by Clement, Lane and Rook (1965) showed that the enhancement is of the correct order of magnitude to give the measured cross-sections.

The measurements of Bergqvist *et al.* were designed to provide an accurate test of this theory. They chose the nucleus ^{208}Pb whose doubly magic nature ensured that good single-particle wavefunctions are available for the low-lying compound nuclear states. The neutrons were obtained from the t(p,n)h reaction with pulsed and bunched protons from the Los Alamos tandem Van de Graaff accelerator. A cylinder of pure ^{208}Pb formed the target and the emitted gamma rays were detected by a sodium iodide crystal. Measurements were made over the whole giant dipole resonance, and one of their gamma ray spectra is shown in Fig. 28, together with the results of calculations using the compound nucleus theory (dashed line) and the semi-direct capture theory (full line). The compound nucleus theory accounts very well for the low-energy gamma rays, indicating that the last stages of the de-excitation of the compound nucleus proceed by a statistical process; but it is quite unable to account for the gamma rays of higher energy that are emitted in the initial stages of the capture process. The semi-direct theory succeeds very well, however, and describes some of the detailed structure of the experimental results.

The calculations of the semi-direct cross-section made use of the energies of the single-particle states of ^{209}Pb and the position and width of the giant dipole resonance obtained in previous investigations. As there are still some uncertainties remaining in the theory the curves were normalized to the data over the upper portions of the spectra. It is unfortunate that the authors do not give their normalizing factor so that the magnitude of the remaining discrepancy is unknown. In spite of this uncertainty about absolute cross-sections, these new experiments provide impressive evidence in support of the semi-direct theory of photonuclear capture. It will be necessary to perform further experiments and calculations to check that the absolute magnitudes agree, and it is also to be hoped that experiments on other nuclei will be undertaken so that the theory can be verified for a large number of nuclei. The more complicated phenomena associated with capture by

nuclei with several nucleons outside the closed shells are particularly good candidates for study, for there are already some anomalous effects that awaited a detailed explanation.

References

I. Bergqvist, D. Drake and D. K. McDaniels, *Phys. Rev. Lett.* **27**, 269, 1971.
I. Bergqvist, D. M. Drake and D. K. McDaniels, *Nucl. Phys.* **A191**, 641, 1972; **A231**, 29, 1974.
I. Bergqvist, B. Palsson, L. Nilsson, A. Lindholm, D. M. Drake, E. Arthur, D. K. McDaniels and P. Varghese, *Nucl. Phys.* **A295**, 256, 1978.
C. F. Clement, A. M. Lane and J. R. Rook, *Nucl. Phys.* **66**, 273, 1965.
P. J. Daly, J. R. Rook and P. E. Hodgson, *Nucl. Phys.* **56**, 331, 1964.
A. M. Lane and J. E. Lynn, *Nucl. Phys.* **11**, 646, 1959.
A. Likar, A. Lindholm, L. Nilsson, I. Bergqvist and B. Palsson, *Nucl. Phys.* **A298**, 217, 1978.
A. Lindholm, L. Nilsson, I. Bergqvist and B. Palsson, *Nucl. Phys.* **A279**, 445, 1977.

2.5 Accurate Spectroscopic Factors (*Nature* **249**, 695, 1974)

During the past ten years the one-nucleon transfer reactions have been developed into one of the most powerful tools for studying the single-particle aspects of nuclear structure. Among these the (d,p) reaction has been most widely used, but extensive studies have also been made using (d,n), (p,d), (d,t), (d,h) and many similar reactions that either add a proton or neutron to or remove one from the target nucleus.

As a typical example, consider the (d,p) reaction on ^{24}Mg. The incident deuteron interacts with the ^{24}Mg target and deposits a neutron in one of the unoccupied neutron states, and the remaining proton goes on alone. At lower energies this process can take place by absorption of the deuteron to form a compound nucleus followed a long time after by proton emission, but at higher energies the direct process that takes place in a time comparable with the time taken by the deuteron to cross the target nucleus predominates to such an extent that the compound nucleus process is negligible.

The differential cross section for this direct (d,p) reaction can be written as the product of two factors, one depending only on the

structure of the nuclei involved and the other only on the reaction mechanism:

$$[d\sigma/d\Omega] = S_{JL} F_{JL} (\theta,E)$$

All the dependence of the cross section on the angle of emission θ of the proton and on the incident deuteron energy E is contained in the reaction factor F_{JL} (θ,E), and this can be calculated by the distorted wave theory. These angular distributions are in general characteristic of the total quantum number J and orbital angular momentum quantum number L of the state entered by the captured neutron so that comparison between the observed angular distribution and those calculated for various J and L enable these quantum numbers to be determined, and these give the spins of the corresponding states of ^{25}Mg.

The spectroscopic factor S_{JL} is a measure of the single-particle strength of the neutron state and is given by the ratio of the measured cross-sections to the calculated value of the F_{JL} (θ,E).

The analysis is thus able to give the quantum numbers and the single-particle strengths of all the nuclear states of ^{25}Mg reached by the reaction. Numerous analyses of nuclear states in all stable nuclei have been made with this technique, and it is one of our main sources of information on nuclear structure. The main limitations to this method are, first, that it is not always possible to determine J and L and, second, that the uncertainties in the distorted wave theory make the spectroscopic factors uncertain to about 20%, even in the best circumstances.

A new method of analysing one-nucleon transfer reactions has now been proposed by C. F. Clement of Harwell (1973) and used to obtain more reliable J,L and more accurate spectroscopic factors. This method depends on the j-dependent sum rules that relate the spectroscopic factors of the reactions that remove a neutron (or proton) from a nucleus to the spectroscopic factors for the corresponding reaction that adds a neutron to the same nucleus. The j is the total angular momentum of the transferred nucleon. These sum rules provide a rigid set of equations that must be satisfied by the spins of the final states and by the spectroscopic factors of the corresponding transitions.

These sum rules must be distinguished from the more familiar J-dependent total sum rules that relate the spectroscopic factors to the total single-particle strengths of the states. The j-dependent sum rules provide additional constraints on the spectroscopic factors only if the spin of the ground state of the target nucleus is different from zero. All these sum rules were derived long ago by J. P. French, but it is only recently that they have been applied to nuclear structure analyses.

Clement and Perez (1973) have now applied this analysis to the reactions (d,t) and (d,p) that remove neutrons from or add them to the states of ^{45}Sc with spin 7/2. The sum rules give a set of eight equations connecting sixteen sums of spectroscopic factors for stripping and pick-up to states of different spin. The measured spectroscopic factors satisfied these equations to an accuracy of 4% in relative magnitude and 10% in absolute magnitude. Several additional spin assignments to states of the residual nuclei ^{46}Sc and ^{44}Sc were made by this analysis.

An important problem in all analyses of single-particle states is the fraction of the strength that is far removed from the main concentration. Clement and Perez find that it would be difficult to maintain their fits to the sum rules if more than 10% of the total is in the continuum. Thus nearly all the $f_{7/2}$ strength is concentrated in a limited energy region; this is an important conclusion for the basic single-particle model of nuclear structure and supports the validity of the distorted wave theory.

Subsequently Clement and Perez have applied the sum rule analysis to other nuclei and have still further reduced the uncertainties in the absolute spectroscopic factors. This is clearly a technique of great power that can provide valuable information on nuclear structure and stringent tests of the present techniques for obtaining it.

Comment by Dr C. F. Clement

Further experiments have shown that the spin assignments made to states of ^{44}Sc and ^{46}Sc on the basis of the sum rule analysis were almost entirely correct. Subsequent sum rule analyses have been made to transfer data on ^{35,37}Cl (Clement and Perez, 1974) and on ^{41,43}Ca, ^{49}Ti, and ^{51}V (Clement and Perez, 1977). Statistical analyses of the pickup data on ^{51}V have shown that experiments with different light ions

((p,d), (d,t), and (h,α)) and at different energies ((d,h) at 30, 50, and 80 MeV) give relative magnitudes of spectroscopic factors to an accuracy of better than 5%, which is consistent with values obtained with the best sum rule fits. Sum rule analyses give absolute magnitudes of spectroscopic factors to an accuracy of about 10% and the resulting $f_{7/2}$ occupancies for ^{41,43}Ca, ^{45}Sc, ^{49}Ti, and ^{51}V agree with simple shell-model expectations to the same level of accuracy.

Altogether it appears that transfer experiments and standard distorted wave predictions of $F_{JL}(\theta,E)$ can be analysed to give spectroscopic factors to a much higher accuracy than the figure of ±30% considered possible a few years ago. This accuracy enables much more quantitative statements to be made about the validity of nuclear models. In particular the basic validity of the shell model for the $f_{7/2}$ shell has been established for several nuclei.

References

C. F. Clement, *Nucl. Phys.* **A213,** 469, 493, 1973.
C. F. Clement and S. M. Perez, *Nucl. Phys.* **A213,** 510, 1973; *J. Phys.* **A7,** 1464, 1974; *Nucl. Phys.* **A284,** 469, 1977.
J. P. French, *Phys. Lett.* **13,** 249, 1964; **15,** 327, 1965.

2.6 Nuclear Spectroscopy
(Nature **253,** 501, 1975)

Studies of nucleon transfer reactions have long been established as one of the most powerful nuclear spectroscopic techniques. The angular distribution is characteristic of the angular momentum transfer L and the magnitude of the cross section is a measure of its single-particle strength. If the target nucleus has spin zero and the transferred particle is initially in a state of zero orbital angular momentum the spin of the final state is simply given by the vectorial sum of the relative orbital and spin angular momenta in the transfer process. For a (d,p) reaction, for example, $\mathbf{J} = \mathbf{L} + \frac{1}{2}$ giving $J = L \pm \frac{1}{2}$. Thus a $L = 2$ transfer can go to $J = 3/2$ or to a $J = 5/2$ state. The ambiguity can often be resolved from the known systematic behaviour of single-particle states but in other cases it remains a difficulty. Measurement of the polarization of the outgoing proton together with distorted wave calculations or a

simple comparison with the proton polarizations in reactions leaving the residual nucleus in states of known spin resolves the ambiguity, but is time consuming.

It has however proved possible in some cases to resolve the ambiguity by examination of certain features of the differential cross sections and it is found that they are characteristic of $J = L + \frac{1}{2}$ or $J = L - \frac{1}{2}$ final states. Such features are sometimes difficult to reproduce by distorted wave calculations but nevertheless can be used as empirical guides provided that they can be calibrated by studies of transitions to states of known spin.

These J-dependent effects, as they are called, are sufficiently distinctive to be used with confidence only for particular reactions in restricted energy ranges, so it is always valuable to find new circumstances or new reactions that display them prominently. Two recent papers have provided evidence of this type.

In the first paper, Kong-a-Siou and Chien of Michigan State University (1974) measured the angular distributions of several $L = 3$ transitions in the (p,d) reaction on ^{61}Ni and ^{62}Ni at 40 MeV and found a very stable J dependence over a range of intensities and excitation

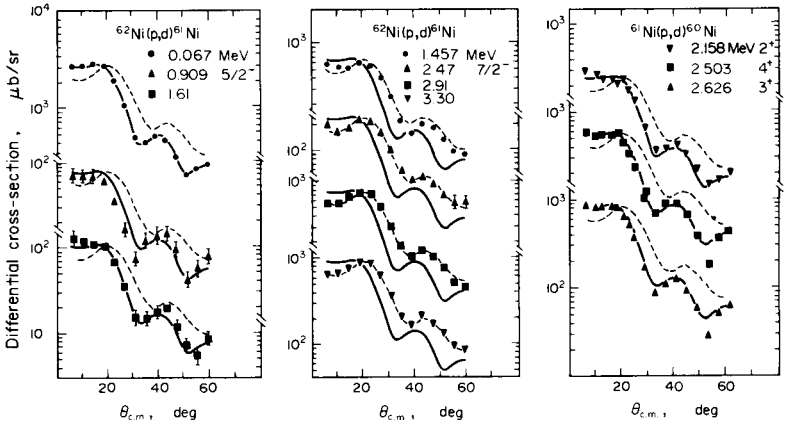

Fig. 29. Differential cross sections for the ^{61}Ni(p,d)^{60}Ni and ^{62}Ni(p,d)^{61}Ni reactions. The solid and dashed lines are smooth curves through the experimental data points of the known $f_{5/2}$ and $f_{7/2}$ transfers to the states at 0.067 and 3.30 MeV in ^{16}Ni. All the cross sections follow closely one curve or the other.

energies. Some of their results are shown in Fig. 29, and it is clear that the angular distributions fall sharply into two classes, one characteristic of $J = L - \frac{1}{2} = 5/2$ and the other of $J = L + \frac{1}{2} = 7/2$, and that in each case the data fall quite definitely on one or the other. The data for ^{62}Ni(p,d)^{61}Ni thus allow the spins of the states of ^{61}Ni to be determined.

The result for ^{61}Ni(p,d)^{60}Ni to states of known spins 2^+, 4^+ and 3^+ respectively show angular distributions characteristic in each case of quite pure $J = 5/2$ transfer. For the 4^+ state, only $L = 3$ transfer is allowed by the conservation of angular momentum and of parity, but for the 2^+ and 3^+ states both $L = 1$ and $L = 3$ transfers can complete. The data show that only $L = 3$ is present and this can indeed be understood by shell-model calculations.

In the second paper, Kemper *et al.*, of Florida State University (1974), report a study of the relatively unfamiliar (^{7}Li, ^{6}He) reaction that shows marked J-dependent effects for reactions to d and f states. For this reaction the transferred proton comes from the $p_{3/2}$ orbit in ^{7}Li so that the vector equation for the angular momenta is $\mathbf{3/2 + L = J}$, where **L** is the orbital angular momentum of the transferred proton and J the spin of the final state. If for example $J = 3/2$, the l can be 0, 1,

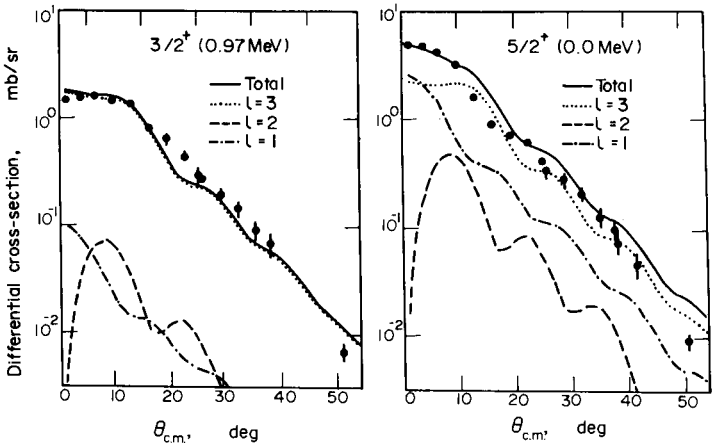

Fig. 30. Differential cross sections for the ^{29}Mg(^{7}Li,^{6}He)^{25}Al reaction to $d_{3/2}$ and $d_{5/2}$ states in ^{25}Al. The curves are distorted wave calculations and show the difference between the relative contributions from $l = 1, 2$ and 3 transfer in the two cases.

2 or 3. If the final state has orbital angular momentum **L**, then J can be $L \pm \frac{1}{2}$ and the possible values of l are $l = L$ or $L \pm 1$. The relative proportions of these that contribute are given by the Racah coefficient W $(L,J,\ 1,3/2;\ \frac{1}{2}l)$ and it turns out that the components $l = L$ and $l = L - 1$ are much more important for the states with $J = L + \frac{1}{2}$ than for those with $J = L - \frac{1}{2}$.

This is shown clearly in Fig. 30 by the angular distribution for the ^{24}Mg(^{7}Li, ^{6}He)^{25}Al reactions at 34 MeV to $d_{3/2}$ and $d_{5/2}$ states of ^{25}Al. The curves show separately the distorted wave calculations of the contributions to the two cross sections, and it is found that the reaction to the $J = 3/2$ state $(J = L - \frac{1}{2})$ is nearly all $l = 3$ with very small contributions from $l = 1$ and 2, whereas for the reaction to the $J = 5/2$ state the $l = 1$ and 2 components are relatively much more important. Since the contributions of different l have markedly different angular distributions this gives a difference between the cross sections for the réactions to the $J = 3/2$ and $J = 5/2$ states, and this can be used to distinguish between them.

Reactions like this are only just beginning to be studied in detail, and it is likely that other types of J dependence will be found and that they will prove powerful tools in nuclear spectroscopy.

References

K. W. Kemper, R. L. White, L. A. Charlton, G. D. Gunn and G. E. Moore, *Phys. Lett.* **52B,** 179, 1974.
D. H. Kong-a-Siou and W. S. Chien, *Phys. Lett.* **52B,** 175, 1974.

2.7 *J*-dependence in Nuclear Reactions (*Nature* **250,** 464, 1974)

The general character of the differential cross sections of direct one-nucleon transfer reactions is dominated by the orbital angular momentum L of the transferred particle. Except at low energies when the angular distributions are backward-peaked and similar for all L values, the angular distributions are peaked at an angle in the forward hemisphere that increases with the value of L. In most cases a comparison between the experimental data and distorted wave calculations enables the value of L to be determined.

Since the transferred nucleon also has a spin of $\frac{1}{2}$, the total transferred angular momentum J is the vector sum of L and $\frac{1}{2}$, and since these can be added or subtracted, $J = L \pm \frac{1}{2}$. If the target nucleus has zero spin, this J is just the spin of the final state of the residual nucleus.

The angular distributions of reactions of the same L but different J are usually very similar, but in some cases small but systematic differences have been found. These are called the J-dependent effects, and have proved quite useful in assigning spins to nuclear states simply by the shape of the angular distribution, without any detailed calculations.

These J-dependent effects depend on the transferred orbital angular momentum L and on the incident energy, and are more marked in some cases than in others, so it is clearly important to understand how they arise, both for their intrinsic interest and in order to enhance their utility in nuclear spectroscopy.

The most marked J-dependent effects are found for $L = 1$ transitions, and Robson has shown that these can be accounted for very well by distorted wave calculations with a spin-orbit interaction in the incoming and out-going channels, provided the optical potentials are chosen to fit both the differential cross section and the polarization of the corresponding elastic scattering.

For $L = 2$ and 3 the J-dependent effects cannot be accounted for in this way and several attempts have been made to develop the distorted wave theory, in particular by including the deuteron D-state. This is a complicated calculation, and some of the results show J-dependent effects that are similar to those observed. The difficulty of the calculations has however deterred an extensive study, so most of the J-dependent effects remain unexplained.

Quite recently a new explanation of J-dependent effects has been proposed: they are attributed to the contributions of two-step processes to the reaction amplitude. The importance of two-step processes is now widely known, especially when the nuclei are deformed and when the direct one-step transition is forbidden or inhibited by some selection rule. A substantial proportion of the reaction can proceed by the incident particle first exciting the target nucleus to a low-lying collective state by inelastic scattering, followed by the particle transfer to the final state. Similarly, the particle transfer can take place first to

the ground or to an excited state of the residual nucleus, which can then be excited to the final state by an inelastic process as the outgoing particle leaves. All possible processes of this type combine to give the observed cross section.

In recent years the formalism for calculating such processes has been extensively developed, and many studies have shown the importance of including two-step processes. It has now been applied by Hoffmann, Udagawa, Coker, McIntyre and Mahlab (1974) to study the J-dependent effects in the reaction ^{30}Si(d,p)^{31}Si at 10 MeV to the 2.32 MeV ($3/2^+$) and 2.79 MeV ($5/2^+$) states of the residual nucleus. As Fig. 31 shows, the cross sections of these two reactions differ markedly in the forward direction, although they are both $L = 1$ and very similar in energy. The short-dashed curves are standard DWBA calculation, which gives very similar angular distributions for the two reactions, and does not account at all for the difference between them. The calculation including the two-step process via the $1/2^+$ state of ^{31}Si at 0.75 MeV gives the full curves, which are in excellent accord with the data in the forward direction. The small differences in the backward hemisphere are probably attributable to compound nucleus contributions. A final calculation including those two-step processes through the lowest 2^+ state of ^{30}Si gave the long-dashed curves which do not agree with the data, which is expected since the excited states of the two states of ^{31}Si have a small parentage in terms of the 2^+ state in ^{30}Si, so that this process does not contribute significantly to the reaction.

Inclusion of the two-step contribution to this reaction is thus able to give a very good account of all the J-dependence of the cross sections to $3/2^+$ and $5/2^+$ states of ^{31}Si. Other effects, such as those caused by the deuteron D-state, may contribute, but in this case at least they are small.

Further calculations by Coker, Udagawa and Hoffmann have shown that the two-step process is also able to account for the $L = 2$ J-dependent effects in the ^{28}Si(d,p)^{29}Si reaction at 10, 13 and 18 MeV to several final states.

This work shows that two-step processes via low-lying collective excitations account for some of the J-dependent effects in one nucleon transfer reactions in deformed nuclei. The J-dependent effects,

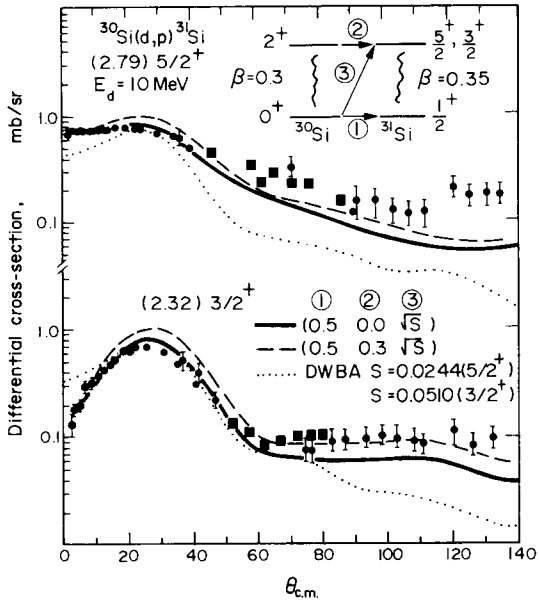

Fig. 31. Differential cross sections for the one-nucleon transfer reaction ^{30}Si(d,p)^{31}Si at 10 MeV to the 2.32 MeV 3/2$^+$ and 2.79 5/2$^+$ states of ^{31}Si compared with distorted wave calculations. The short-dashed curves are the simple one-step calculation and the full curves show the effect of including the two-step process (1). The long-dash curves show the effect of including the coupling (2) between the excited states, which does not contribute significantly. The figures in the brackets are the spectroscopic factors for the various transitions.

however, are also found for nuclei to which this explanation cannot apply. It is therefore necessary to carry out a series of analyses for a range of nuclei and incident energies for different L-values with consistent parameters for the distorting potentials. This will make it possible to establish in a systematic way the contribution of two-step processes to J-dependent effects in nuclear reactions.

References

W. R. Coker, T. Udagawa and G. W. Hoffmann, *Phys. Rev.* **C10,** 1792, 1974.
G. W. Hoffmann, T. Udagawa, W. R. Coker, J. McIntyre and M. Mahlab, *Phys. Lett.* **50B,** 249, 1974.

2.8 *j*-dependence in Nuclear Reactions
(*Nature* **256,** 615, 1975)

In a nuclear transfer reaction angular momentum is conserved vectorially, so that the spin of the final state of the residual nucleus $\mathbf{J_R} = \mathbf{J_T} + \mathbf{j}$, where J_T is the spin of the ground state of the initial (or target) nucleus and j the angular momentum of the transferred nucleon. This j is itself composed of its orbital and spin angular momenta, $\mathbf{j} = \mathbf{l} + \frac{1}{2}$. The angular distribution of the outgoing particle, for example that of a proton in a (d,p) reaction, is usually characteristic of the orbital angular momentum transfer l, and thus l can be determined. Since J_T is known, this suffices to set limits on J_R and to determine it in some special cases.

For example, if $J_T = 0$, $\mathbf{J_R} = \mathbf{j} = \mathbf{l} + \frac{1}{2}$, so that $J_R = l \pm \frac{1}{2}$. So if $l = 2$, the final state is $d_{3/2}$ or $d_{5/2}$. This ambiguity may be resolved either by rather difficult measurements of the polarization of the outgoing particle, or by careful examination of some special features of the differential cross sections (§§ 2.6, 2.7).

The situation is more complicated if J_T is greater than zero, for then several values of j may be possible in reactions to states of the same J_R. Thus if $J_T = \frac{1}{2}$, $J_R = 1$, and $l = 1$, then j can be $\frac{1}{2}$ or 3/2. It is an interesting problem to determine j, for if this can be done we can learn more about the reaction and also use such reactions to determine J_R in cases where it is not known. Furthermore, j has to be known in order to apply the j-dependent sum rules to determine nuclear spectroscopic factors (§ 2.5).

Some years ago Kocher and Haeberli (1969) showed that the vector analysing power in one-nucleon transfer reactions is sensitive to the value of j and thus provides a good way of determining it. They obtained the vector analysing power from the left–right asymmetry of the protons emitted from a reaction initiated by a polarized beam of particles. The $j = \frac{1}{2}^-$ reactions ^{52}Cr(d,p)^{53}Cr ($Q = 5.17$ MeV) and ^{54}Fe(d,p)^{55}Fe ($Q = 6.60$ MeV) at 10 MeV had vector analysing powers quite different from the $j = 3/2^-$ reactions ^{52}Cr(d,p)^{53}Cr ($Q = 5.73$ MeV) and ^{54}Fe(d,p)^{55}Fe ($Q = 7.01$ MeV) at 10 MeV. In the mixed-j reaction ^{53}Cr(d,p)^{54}Cr ($Q = 6.71$ MeV) at 10 MeV, both these values of j were possible, and the vector analysing power closely

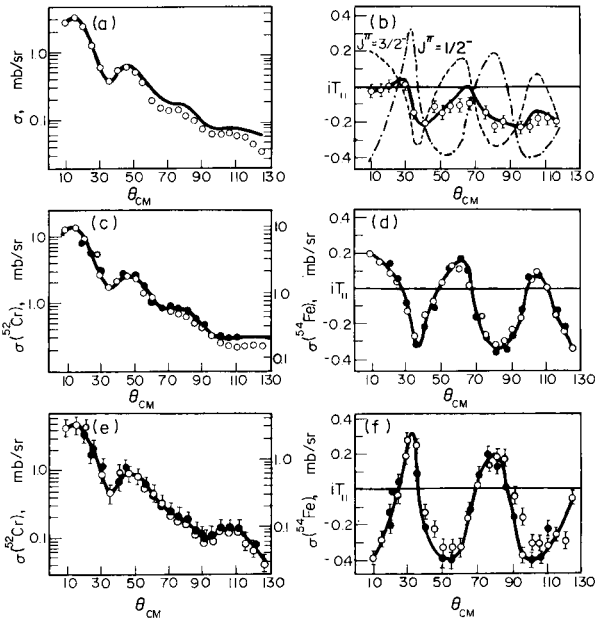

Fig. 32. (a), (b) Measured cross sections and vector analysing powers for the reaction ^{53}Cr(d,p)^{54}Cr* ($Q = 6.71$ MeV) at 10-MeV bombarding energy. The solid curves are fits to the data assuming a mixture of $j^\pi = \frac{3}{2}^-$ and $\frac{1}{2}^-$ reactions (see text). The dashed and dashed-dotted curves in (b) are the results for the pure $j^\pi = \frac{3}{2}^-$ and $\frac{1}{2}^-$ reactions given by the solid curves in (d) and (f), respectively. (c), (d) Measured cross sections and vector analysing powers for the $j^\pi = \frac{3}{2}^-$ reactions ^{52}Cr(d,p)^{53}Cr ($Q =$ 5.73 MeV), open circles; and ^{54}Fe(d,p)^{55}Fe ($Q = 7.01$ MeV), closed circles, at 10–MeV bombarding energy. The solid curves show the trend of the data for ^{54}Fe. (e), (f) Measured cross sections and vector analysing powers for the $j^\pi = \frac{1}{2}^-$ reactions ^{52}Cr(d,p)^{53}Cr* ($Q = 5.17$ MeV), open circles, and ^{54}Fe(d,p)^{55}Fe* ($Q = 6.60$ MeV), closed circles, at 10–MeV bombarding energy. The solid curves show the trend of the data for ^{54}Fe.

followed a curve obtained by adding together in definite proportions the vector analysing powers found in the other two reactions as shown in Fig. 32. This proportion gave the relative contributions of the $j = \frac{1}{2}$ and $j = 3/2$ components to the reaction. The technique of finding the mixing parameter in mixed-j transitions has the special advantage of being independent of detailed theoretical calculations, but is somewhat laborious to apply in practice.

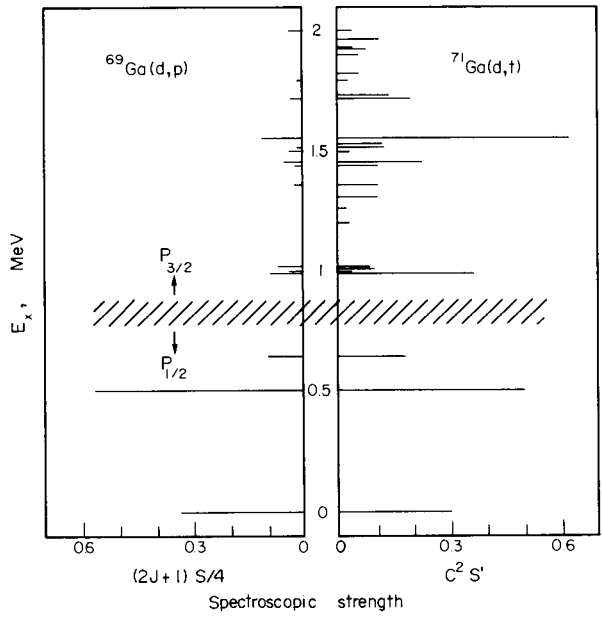

Fig. 33. Distribution of the $l = 1$ spectroscopic strengths in ^{69}Ga(d,p)^{70}Ga and ^{71}Ga(d,t)^{70}Ga showing the similarity of amplitudes below 1 MeV excitation energy and the excess amplitude for the ^{71}Ga reaction above 1 MeV (Dohan and Summers-Gill, 1975).

A new method of finding the j value has recently been proposed by Dohan and Summers-Gill (1975), and applied to the ^{69}Ga(d,p)^{70}Ga and ^{71}Ga(d,t)^{70}Ga reactions to the same state of ^{70}Ga. It depends on the fact that, on the simple shell model, the $2p_{1/2}$ neutron state is empty in ^{69}Ga, half-full (containing one neutron) in ^{70}Ga and full in ^{71}Ga. Thus the (d,p) and (d,t) reactions on ^{69}Ga and ^{71}Ga respectively go equally well, and thus have very similar spectroscopic factors. The $2p_{3/2}$ state, on the other hand, is full for all these nuclei, so the (d,p) reaction on ^{69}Ga is forbidden, as there is no room for another neutron, while the (d,t) reaction on ^{71}Ga takes place easily as there are plenty of $2p_{3/2}$ neutrons to be removed. This picture is expected to be somewhat blurred as the simple shell model is not followed exactly, but

nevertheless we expect to find very similar amplitudes for $2p_{1/2}$ transfer and very different amplitudes for $2p_{3/2}$ transfer in the two reactions.

In practice these expectations are remarkably well fulfilled. The transitions to the lower states up to about 1 MeV have almost the same amplitudes for the two types of reaction while those above 1 MeV have very small amplitudes for the (d,p) reaction and large amplitudes for the (d,t) reaction as shown in Fig. 33. Thus we can with some confidence assign the first group to $2p_{1/2}$ transfer and the second group to $2p_{3/2}$ transfer. This is a very simple and direct way of determining the j value of the transferred particle, and is applicable to reactions where the subshell corresponding to one j value is filling more rapidly than the other. It will be interesting to see how far it can be extended.

In heavy ion reactions the situation is more complicated since the transferred particle can have an angular momentum greater than zero in the projectile. Thus the neutron in the deuteron has $l = 0$, whereas the proton in ^{7}Li that is transferred by the (^{7}Li,^{5}He) reaction has $l = 1$, $j = 3/2$ as it comes from a $p_{3/2}$ orbit in ^{7}Li (§ 2.6).

References

D. A. Dohan and R. G. Summers-Gill, *Nucl. Phys.* **A241**, 61, 1975.
D. C. Kocher and W. Haeberli, *Phys. Rev. Lett.* **23**, 315, 1969.

2.9 Neutron Pickup at High Energies
(*Nature* **259**, 450, 1976)

There have been many studies of nucleon transfer reactions at low energies (5 to 50 MeV) and these have given much information on the single particle states of nuclei (see for example, §§ 2.5–2.8 and Vol. 1, Chapter 3). Very few analyses have been made at higher energies, partly because it is then difficult to resolve the final states and partly because it is thought unlikely that such studies could give any information that could not be obtained from the technically much easier studies at lower energies.

In 1974 a group working at the Saturne synchrotron (Baker *et al.*,

1974) published the results of their measurements of the $^{12}C(p,d)^{11}C$ neutron pickup reaction at 700 MeV. These data were remarkable because the energy resolution was sufficient to resolve several states of ^{11}C, and thus provided the only stripping or pickup data available above 200 MeV.

The group made a preliminary analysis of their data using the distorted wave formalism, with the zero-range approximation for the neutron-proton force. At high energies, however, the momentum transfers are large, and this invalidates the approximation. They also ignored the D-state component of the deuteron wave function, although this is expected to contribute strongly at high energies. In spite of this, they found that the overall shape of the differential cross section is given quite well by their calculation, as shown in Fig. 34, but the absolute magnitude is wrong by a factor of two.

In the past few years computer programs using a finite range neutron-proton force have been developed, mainly to analyse heavy ion reactions. Rost and Shepard (1975) have now used one of these programs to analyse the $^{12}C(p,d)^{11}C$ data, and have also included the effect of the D-state of the deuteron.

As shown in the figure, they found that the theory then gives a cross-section in good agreement with the experimental data, both in absolute magnitude and in overall shape. As expected, the contribution of the D-state is dominant, so the previous agreement in shape must be largely fortuitous. It is thus very important for reactions of deuterons at high energies to use an accurate deuteron wavefunction, and the results can themselves provide information about that wave-function.

This conclusion is reinforced by studies of the contribution of the S-state component of the deuteron wavefunction. Rost and Shepard used an S-state waveform calculated from the Reid soft-core potential, that has been obtained by fitting a large body of nucleon-nucleon and deuteron data. Calculations with the Hulthèn wavefunction, a simple analytical function widely used at low energies, gave cross-sections completely in disagreement with the experimental data.

This work shows the value of repeating familiar analyses at substantially higher energies, whenever it is practicable to do so.

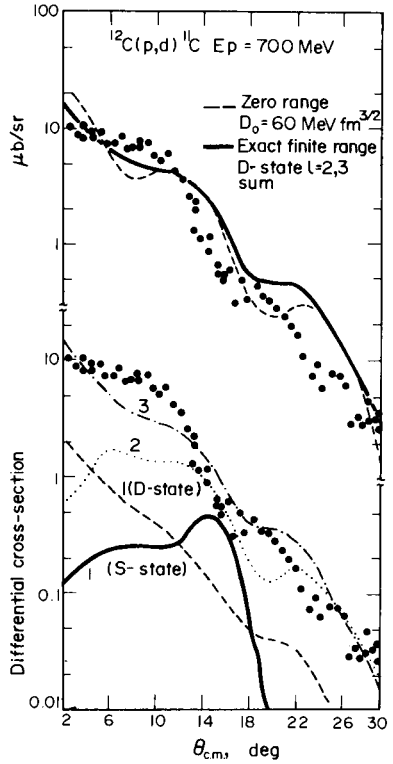

Fig. 34. Differential cross section for the $^{12}C(p,d)^{11}C$ reaction at 700 MeV compared in the top section with zero-range and exact finite-range distorted wave calculations. The zero-range curve has been arbitrarily divided by two to fit the data. The lower section shows the individual cross-sections for the S-state $L = 1$ and the D-state $L = 1,2,3$ contributions.

Comment

Subsequently, Rost *et al.* (1978) made exact finite-range calculations of the $^4He(p,d)^3He$ reaction at 700 MeV, but were unable to fit the experimental data. Until this failure is understood, the application of this theory to light nuclei must remain uncertain.

References

S. D. Baker, R. Bertini, R. Beurtey, F. Brochard, G. Bruge, H. Catz, A. Chaumeaux, C. Cvijanovich, J. M. Durand, J. C. Faivre, J. M. Fontaine, D. Garreta, F. Hibou, D. Legrand, J. C. Lugol, J. Saudinos, J. Thirion and E. Rost, *Phys. Lett.* **52B**, 57, 1974.
E. Rost and J. R. Shepard, *Phys. Lett.* **59B**, 413, 1975.
E. Rost, J. R. Shepard and D. A. Sparrow, *Phys. Rev.* **C17**, 1513, 1978.

2.10 Multinucleon Transfer Reactions
(*Nature* **267**, 107, 1977)

Multinucleon transfer reactions are now used extensively to study nuclear structure, and recently a group at Los Alamos has found remarkable similarities between the spectra of states excited in the same final nucleus by the (^{6}Li,d) reaction on the one hand and by the (t,p) and (h,n) reactions on the other.

The group measured the (^{6}Li,d) reaction on ^{54}Fe, ^{56}Fe, and ^{58}Fe for excitation energies up to about 4 MeV in the final nuclei, using a lithium beam of 34 MeV. About 20 states are known in this region of excitation for these nuclei, and it was found that only a few of them are excited by this reaction, and with few exceptions these are just the states also excited by (t,p) reactions going to the same final nuclei.

The exceptions are the 0^+ states at about 3.5 MeV in each of the final nuclei that are excited by (^{6}Li,d) but not by (t,p). These are very probably the states strongly excited by the (h,n) reaction, and interpreted as two-particle two-hole pairing vibration states in the $Z = 28$ proton closed shell.

The group therefore concludes that the (^{6}Li,d) reaction is sensitive to the same neutron and proton pairing correlations that govern the corresponding two-nucleon transfer reactions. This conclusion supports recent work on the alpha-particle spectroscopic factors, in which the four-particle amplitude is factored into coupled two-nucleon structure factors. The similarity between the (^{6}Li,d) and (t,p) reactions is then explained as the transfer of the proton pair to the ground state and the neutron pair to the ground and excited states as in the (t,p) reactions. The similarity between the (^{6}Li,d) and (h,n) reactions is explained in the same way.

This work suggests further experiments on the two- and four-particle transfer reactions to determine the spectroscopic factors and to relate

them to the details of nuclear structure. It also shows that the (^{6}Li,d) reaction can be used to study two-particle excitations that cannot be studied directly by two-particle transfer reactions because the requisite target nucleus is unstable. Such studies should also shed further light on the alpha-particle spectroscopic factors that are important for the study of alpha-clustering in nuclei.

Reference

N. Stein, J. W. Sunier and C. W. Woods, *Phys. Rev. Lett.* **38**, 587, 1977.

2.11 Two-step Nuclear Reactions (*Nature* **247**, 179, 1974)

There has recently developed a growing awareness of the importance of multistep processes in nuclear reactions. These are of two types: reactions involving pre-excitation of the target nucleus or post-excitation of the residual nucleus by inelastic scattering and reactions involving sequential transfer. If the direct process is inhibited in any way, the multistep processes can account for a significant fraction of the measured cross section, so that any conclusions concerning the structure of the participating nuclei based on the assumption that only the direct one-step process contributes may be gravely in error. Among the many possible multistep processes the two-step ones are the easiest to calculate, and detailed theories have now been programmed for electronic computation.

A relatively simple example of the importance of including two-step processes is provided by the (p,n) reaction to the isobaric analogue state of the target nucleus. This final state has essentially the same structure as the ground state of the target apart from a reversed isospin vector for one of the target nucleons: a neutron is replaced by a proton in the same shell-model state. On a simple view the reaction thus proceeds entirely by the isospin term in the nucleon-nucleus optical potential. The total wave function is thus expressible as a sum of the wave-function in the elastic channel and that in the (p,n) or quasi-elastic channel. Use of the Schrödinger equation with an isospin-dependent potential that can cause transitions from the elastic to the

quasi-elastic channel gives a pair of coupled differential equations (called the Lane equations) for the two wave functions. These can be solved to give the observable cross sections in terms of the parameters of the potentials used. It is then possible by comparing calculations with the experimental data to obtain the best values of the parameters of the potential, in particular of the isospin term. Such analyses have been moderately successful in that with suitable choice of parameters it is possible to fit the data fairly well, and to obtain an estimate of the isospin potential.

These analyses assume that the reaction is a direct one-step process from the incident to the final state. It is, however, possible that the reaction can take place in two or more stages, and this can be investigated using a microscopic model of the interaction in which the contributions of all nucleons outside closed shells are explicitly included.

This model has recently been used by Rickertsen and Kunz (1973) to study the contribution to the quasi-elastic cross section due to successive particle transfer: instead of direct (p,n), there is a (p,d) pickup followed by (d,n) stripping, leading to the same final state as before. The formalism for this process is much more complicated than for the one-step process, but it has been worked out to give a set of coupled differential equations that can be solved on a computer.

In these microscopic interactions the essential parameters are those of the effective nucleon-nucleon interaction, expressed as a sum of central and isospin terms, together with those of the potentials describing the distortion of the incident and outgoing waves and the shell model used for the initial and final nuclei.

Rickertsen and Kunz have made a series of analyses of (p,n) quasi-elastic cross sections using both the one-step process on its own and then the one-step with the addition of the two-step. It was found, as shown in Fig. 35, that the one-step alone is not always very successful, even if the absolute magnitude is adjusted by altering the strength of the isospin term but that with the addition of the two-step process the agreement is very satisfactory. It is notable that the one-step contribution on its own gives a cross section greater than that observed, so there is considerable destructive interference when the two-step process is included as well.

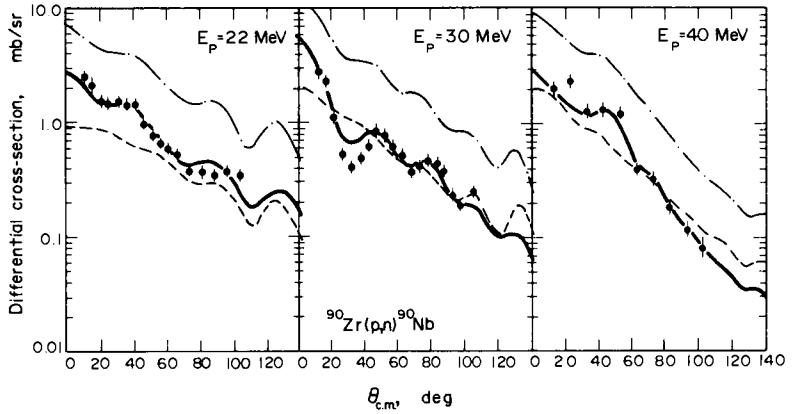

Fig. 35. Differential cross sections for the (p,n) reactions to the isobaric analogue states compared with calculations with the one-step process only (—·—), the two-step process only (– – –) and the one-step and two-step processes combined (——).

It is also found that the strength of the isospin term in the effective nucleon-nucleon interaction varies over a wide range from about 15 MeV to 33 MeV if the data are analysed with the one-step process alone, whereas if the two-step process is included the values of the strength cluster much more closely around a mean value of about 29 MeV. The contributions of the two-step process differ from nucleus to nucleus depending on their individual shell structure and they are such as to account for the data, when combined with the one-step process, with parameter values having a more uniform behaviour from nucleus to nucleus.

Thus both the angular distributions and the absolute magnitudes of the (p,n) quasi-elastic cross sections are much better accounted for by the inclusion of the two-step process. It is physically very plausible and gives a more coherent account of the experimental data. The contribution of a two-step process involving pre- or post-excitation of the target or residual nucleus by inelastic scattering was also calculated and found to be quite small.

The possibility of such two-step contributions to nuclear reactions must therefore be carefully considered, and a full calculation made if one is to obtain a detailed and accurate account of the data.

References

H. Amakawa, A. Mori and K. Yazaki, *Phys. Lett.* **76B,** 157, 1978.
L. A. Charlton and P. D. Kunz, *Phys. Lett.* **72B,** 7, 1977.
P. D. Kunz and E. Rost, *Phys. Lett.* **47B,** 136, 1973.
P. D. Kunz and L. A. Charlton, *Phys. Lett.* **61B,** 1, 1976.
L. D. Rickertsen and P. D. Kunz, *Phys. Lett.* **47B,** 11, 1973.

2.12 Deuteron–gamma Angular Correlations (*Nature* **256,** 695, 1973)

When deuterons are inelastically scattered by nuclei they leave the target nucleus in an excited state, which usually decays by gamma emission. The angular correlation between the inelastically scattered deuteron and the subsequent de-excitation gamma ray can provide important information about the mechanism of the reaction.

An illustration of this has recently been provided by the work of Scheib, Hofmann and Vogler (1975) on the inelastic scattering of 10 MeV deuterons by ^{24}Mg. The angular correlation was measured for gamma rays emitted in the reaction plane, and in this case the correlation function is given by

$$W(\varphi_\gamma) = A + B \sin^2(\varphi_\gamma - \varphi_1) + C \sin^2 2(\varphi_\gamma - \varphi_2)$$

where φ_γ is the angle between the beam direction and the angle of emission of the gamma ray, and A, B, C, φ_1 and φ_2 are constants whose values are obtained by fitting the experimental data. The constants A, B, and C are related to products of the reaction substate amplitudes, which may be calculated from a detailed theory of the reaction. This makes the correlation function much more sensitive to the details of the reaction than is the differential cross section, which is given by the sum of the absolute squares of all the reaction amplitudes. The sensitivity allows the correlation function to tell us more about the details of the reaction mechanism than we could learn from the differential cross section alone.

This is strikingly shown by the ^{24}Mg results. Fig. 36 shows the differential cross section compared with calculations using two different models of the reaction. The upper curves show the results of distorted wave calculations with three different sets of distorting potentials and assuming that the reaction takes place in a single step

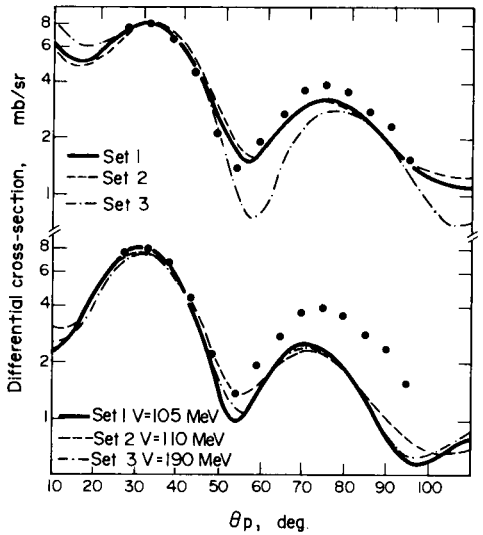

Fig. 36. Differential cross-section for the inelastic scattering of 10 MeV deuterons by ^{24}Mg with excitation of the lowest 2^+ state compared with distorted wave calculations with three sets of distorting potentials using the one-step theory (upper curves) and the two-step theory (lower curves). V is the depth of the real part of the distorting potential.

from the ground state to the 2^+ excited state. The lower curves show similar calculations for the two-step theory. Some additional calculations showed that the effect of also coupling to the 4^+ state is very small. All the calculations used the symmetric rotator model including spin-orbit interactions.

When comparing such theories with the experimental data we look for a good fit to the main forward peak, which is given by both theories and all potentials, together with a qualitative agreement with the rest of the cross section. The angle and width of the second peak are given quite well but its magnitude is somewhat under-estimated by all calculations, rather more so by the theory including the two-step process than by the one-step theory. All these fits are acceptable, but do not distinguish between the two reaction mechanisms.

When we examine the deuteron–gamma correlation data the comparison is quite different. Figures 37 and 38 show the results for

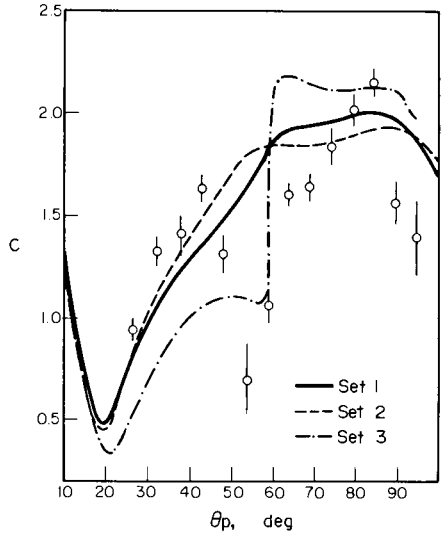

Fig. 37. The deuteron–gamma angular correlation parameter C compared with distorted wave calculations with three sets of distorting potentials using the one-step theory.

the parameter C in the above expression for $W(\varphi_\gamma)$ compared with the results of the six calculations already mentioned. Fig. 37 shows that the three calculated curves for the direct theory differ markedly, showing the greater sensitivity of the correlation function, and none fits the data, even qualitatively. Figure 38 shows that two of the calculations for the two-step theory are in good qualitative agreement with the data, and in particular give the deep minimum found around 55°. These two potentials are quite similar, and correspond to the deuteron potentials known to be physically realistic by calculations based on the nucleon-nucleus potential and using the folding model. The third potential is physically unrealistic and also fails to give a good fit to the angular correlation data.

It is of course well known from many other studies that two-step processes must be taken into account in a detailed treatment of inelastic scattering, and this is confirmed by the correlation analysis. What is new is the striking way that it definitely excludes the one-step process as a sufficient explanation, and this shows that the correlation

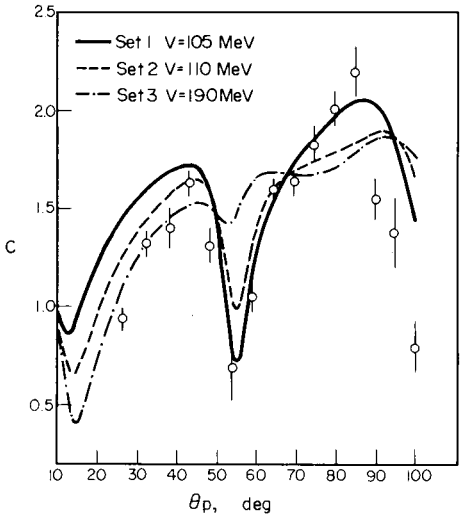

Fig. 38. The deuteron–gamma angular correlation parameter C compared with distorted wave calculations with three sets of distorting potentials using the two-step theory.

analysis could be a powerful way of determining the reaction mechanism in cases where it is not already known.

Comment

Following this work Professor Scheib and his colleagues (1977) have measured the vector analysing power of the reaction $^{24}Mg(d,d_1)$ to look for similar effects in the polarization. They also made some correlation measurements on ^{30}Si and ^{26}Mg, and found in the case of ^{30}Si that the correlations are similar to those for ^{24}Mg, and multistep processes are necessary to describe the correlation amplitude C. In the case of ^{26}Mg, however, the one-step process calculated by the distorted wave theory is sufficient to describe the correlation data.

Reference

U. Scheib, A. Hofmann and F. Vogler, *Phys. Rev. Lett.* **34,** 1586, 1975; *Lett. Nuovo Cimento* **18,** 301, 1977.

2.13 Parity Determination with Polarized Deuterons (*Nature* **258,** 288, 1975)

A new technique for determining the parity of nuclear states has been developed recently by Kuehner *et al.* (1975) at McMaster University, Hamilton, Ontario. The method depends on the properties of the coupling between the orbital and spin angular momentum vectors in the initial and final states. In certain conditions the yield of particles from a reaction at 0° (or 180°) on an even-even target is zero for states of natural parity $(-)^J$, so a single measurement determines the parity if the spin J of the state is known.

The conditions for this to hold are that the magnetic quantum numbers m are zero in the initial and final states. Since these are the z-components of angular momenta (taking the beam direction as the axis of quantization) this may be ensured by using a polarized incident beam with $m = 0$ and detecting the products of the reaction along the beam axis, that is at 0° or 180°. Nucleons have $m = \pm\frac{1}{2}$, and so cannot be used, but deuterons having spin one can be in the $m = 0$ or ± 1 states, and it is possible to polarize the beams.

Although this method is simple in principle, it is not simple to carry out in practice. It is difficult to produce polarized beams, and existing techniques cannot yet give 100% polarization. It is therefore necessary to compare the results of measurements with unpolarized and partially polarized beams. It is also difficult to make measurements very near to 0° but a subsidiary study showed that in practice the intensities of the forbidden reactions are very low below 2°, and so measurements made at this angle are sufficiently good.

Kuehner *et al.* applied this technique to the reaction $^{12}C(d, \alpha)^{10}B$, and some of their results are shown in Fig. 39. The upper spectrum was obtained with an unpolarized beam and the lower with a partially polarized beam. It is immediately evident that the relative intensities are different, and the actual ratios are also displayed. The intensities of the states with parity $(-)^J$ are most strongly reduced, though not to zero, because of the residual $m = \pm 1$ components in the partially polarized beam. A subsidiary calculation shows that these states should be reduced by the ratio indicated by the dashed line in the figure.

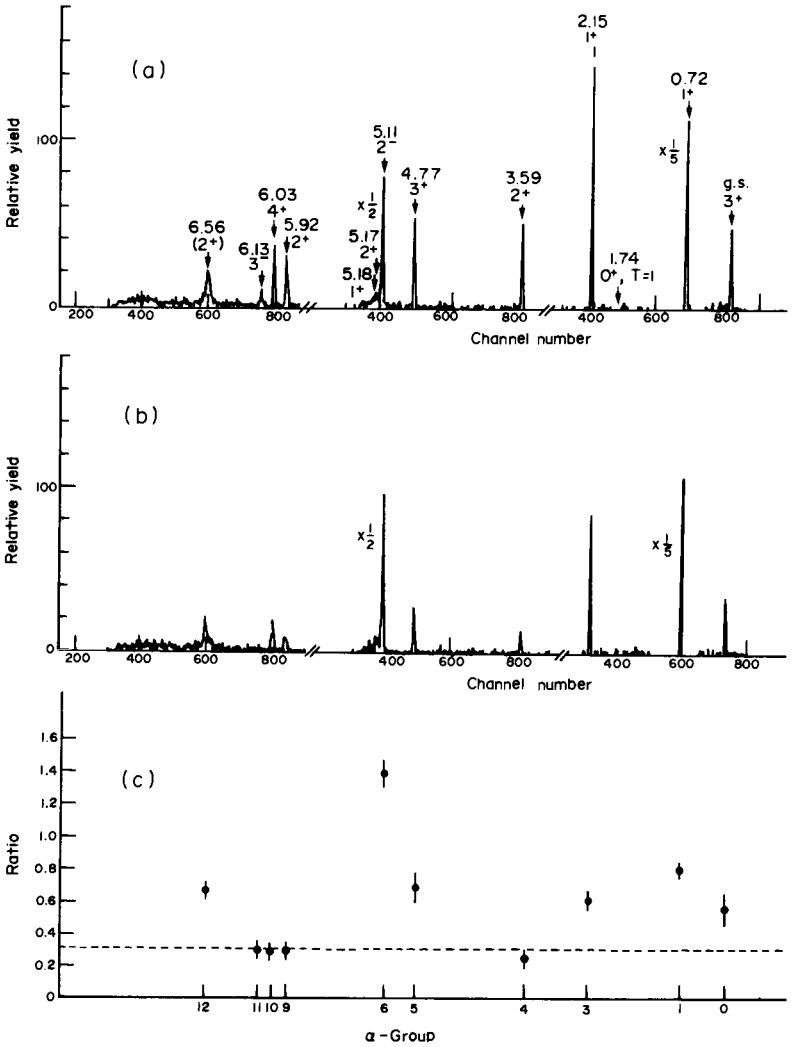

Fig. 39. Spectra of alpha-particles from the reaction $^{12}C(d,\alpha)^{10}B$ at 2° to the incident beam for an unpolarized (*a*) and for a partially polarized beam (*b*). Also shown (*c*) is the ratio of the intensities for the two cases; this has the value shown by the dashed line for states with parity $(-)^J$ and a higher value for states with parity $(-)^{J+1}$.

These ratios therefore give immediately the parity of the final state of ^{10}B: those with ratios on the dashed line have parity $(-)^J$ and those with ratios above the line have parity $(-)^{J+1}$. Since the spins are usually known, this gives the required parities. There may be some cases where the parity is known and the spin from other measurements must have either of two consecutive values; in this case the method determines the spin.

An example of this latter situation is provided by the state of ^{10}B at 6.56 MeV. Previous measurements had indicated 2^+, though 3^+ was also a possibility. The measurements of Kuehner *et al.* show that the spin must be odd, and thus the assignment 3^+ is confirmed.

This new technique should prove a powerful way of determining the parities or spins of nuclear states. If both the spin and the parity are known, it can be also used to determine the tensor polarization of a beam of spin-one particles; this could be particularly useful for projectiles like ^{6}Li for which the usual double-scattering method is difficult.

References

J. A. Kuehner, P. W. Green, G. D. Jones and D. T. Petty, *Phys. Rev. Lett.* **35,** 423, 1975.
J. A. Kuehner, J. Szücs, P. Ikossi, A. M. McDonald and D. T. Petty, *Phys. Lett.* **66B,** 32, 1977.

2.14 Resonance Transfer Reactions
(*Nature* **246,** 14, 1973)

When an ion collides with an atom, the probability of electron transfer depends on the time they spend near each other (the collision time) and on the transfer time itself. If these times are similar, the transfer of one electron is most likely. If the collision time is twice the transfer time the electron can be transferred from the atom to the ion and back again, and so on. Since the collision time is inversely proportional to the relative velocity of the two atoms, the probability that an electron will be transferred from the atom to the ion attains peak values at a series of energies corresponding to one, three, five . . . transfers of the electron. A simple analysis shows that the cross-section is of the form $\sigma(E) = A(E) + B(E)\cos^2(bE^{-\frac{1}{2}})$ where $A(E)$ and $B(E)$ depend on the

incident energy E and b is a constant. Measurements of electron transfer have been made by Ziemba and Everhart (1959) that confirm this formula with surprising accuracy.

The simple theory works very well for the transfer of electrons between atoms because the electron is very light compared with the atoms themselves. If the transferred particle is comparable in mass to the colliding particles much of the simplicity is lost because of the increasing importance of recoil effects.

Resonant transfer processes, as they are called, have been looked for in nuclear reactions, and in particular it has been conjectured that they might be observable in neutron-proton collisions as multiple pion exchange or in heavy ion reactions as nucleon or cluster exchange (Temmer, 1962). Some indications of the characteristic signature of resonant transfer, a cross-section following the formulae outlined here, have been found from time to time, but have not been substantiated by further work.

Recently a more convincing example of resonant transfer has been found in a study of Kelleter, Hrehuss and Mayer-Böricke (1973) of the scattering of alpha particles by ^{7}Li. The cross-section of this reaction shows a rather irregular dependence on energy, as might be expected for such nuclei, but if it is plotted relative to the energy-averaged cross-section an oscillatory behaviour is apparent, as shown in Fig. 40. In particular, it shows an increase of 'wavelength' with energy very similar to that given by the resonant transfer, with small deviations readily attributable to the neglect of recoil and other effects in the simple theory. Since ^{7}Li can be considered as formed by a triton bound to an α particle, this oscillatory component of the reaction may be interpreted as due to transfer of a triton between the incident α particle and the α particle in ^{7}Li.

This interpretation is strengthened by an estimate of the parameter b, which is approximately given by $E_{ex}t_{int}/\hbar$, where E_{ex} is the average exchange energy and t_{int} the interaction time. The values of b obtained in this way are in qualitative agreement with those found by fitting the resonant transfer formula to the measured cross-sections.

Further work needs to be done to develop a detailed theory of the process, taking into account the recoil effects and the presence of other reaction channels, and it would be useful if additional examples could

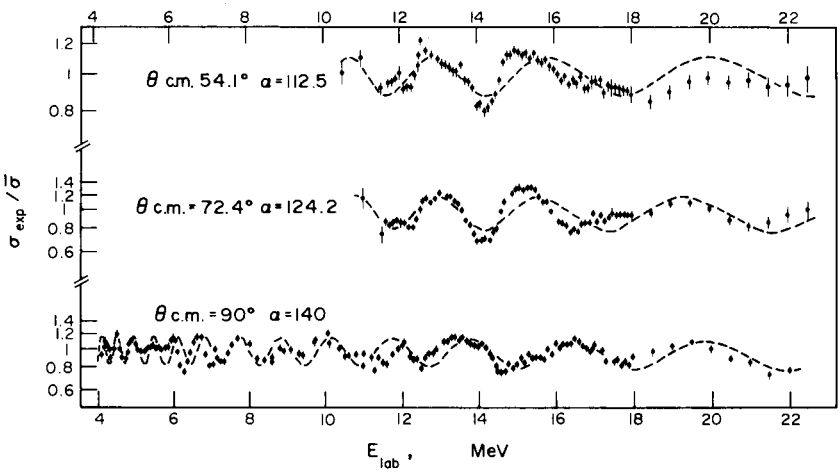

Fig. 40. Ratio of the cross-section for the elastic scattering of alpha particles by ^{7}Li to the energy-averaged cross-section as a function of energy showing oscillatory structure interpreted as due to a resonant transfer of a triton between the two α particles. The dashed curves show the variation expected from the simple theory of the resonant transfer process.

be found experimentally. It is likely that such studies of resonant transfer reactions will provide a useful opportunity to develop nuclear reaction theory.

References

H. Kelleter, G. Hrehuss and C. Mayer-Böricke, *Nucl. Phys.* **A210,** 502, 1973.
G. M. Temmer, *Phys. Lett,* **1,** 10, 1962.
F. P. Ziemba and E. Everhart, *Phys. Rev. Lett.* **2,** 299, 1959.

2.15 Reactions to Nuclear Anti-analogue States (*Nature* **261,** 456, 1976)

Reactions to isobaric analogue states have been extensively studied ever since their discovery by Anderson and Wong in 1962, and have yielded much useful information on nuclear structure and on the nucleon optical potential (§ 2.11). More recently, it has proved

possible to detect reactions to anti-analogue states, and analyses of their cross sections are giving interesting results.

The simplest reaction to these states is the (p,n) reaction, that adds a proton and removes a neutron from the ground state of the target nucleus. The final nucleus thus has the same number of nucleons as the target nucleus and essentially the same mass; this is why the final states are called 'isobaric'. At the same time the charge has been increased by one, and the ways of doing this can most easily be described using the isobaric spin formalism, which is exactly similar to the corresponding formalism for ordinary spin. Each nuclear state has an isobaric spin, with three components like a spin vector. The third component T_3 is directly related to the nuclear charge, $T_3 = \frac{1}{2}(N-Z)$, where N and Z are the numbers of neutrons and protons in the nucleus. All the states of a nucleus thus have the same value of T_3, but they can have any total isobaric spin equal to or greater than T_3, since no vector can be shorter than any one of its components.

The ground states of nuclei nearly always have $T = T_3$, so when we increase the charge by one by a (p,n) reaction we reduce T_3 by one, since by convention a neutron has $T_3 = \frac{1}{2}$ and a proton has $T_3 = -\frac{1}{2}$. The final states can thus have a total isobaric spin of T or $T - 1$. The state with isobaric spin T is the isobaric analogue state, and apart from small electromagnetic effects it has exactly the same structure as the target ground state, except of course for the reduced charge. All the nucleons are coupled together in the same way, and we can say that the only difference is that one isobaric spin vector has been flipped so that its third component is $-\frac{1}{2}$ instead of $\frac{1}{2}$. Quantum mechanically the states have a very high overlap, and so reactions from one to the other take place easily, and it is their high cross sections that enable them to be detected even though many other reactions are also taking place.

The anti-analogue state of isobaric spin $T - 1$ is just the opposite; quantum mechanically its structure is nearly orthogonal to that of the ground state of the target. Reactions to this state are thus very difficult, and can only take place at all because of small differences in structure from complete orthogonality. Unlike the analogue state reactions, the anti-analogue state reactions are sensitive to small components of the wavefunctions, and they are thus difficult to describe theoretically as well as being difficult to detect due to their low cross sections.

Early work on anti-analogue state reactions used the (^{3}He,t) reaction, which also has the net effect of adding a proton and removing a neutron. Calculations of the cross section of the reaction on ^{40}Ar by Schaeffer and Bertsch (1972) showed that the direct component can only account for a very small fraction of the observed cross section, but that a reasonable fit can be obtained by assuming that the reaction takes place mainly by a two-step process in which a (^{3}He, α) reaction is rapidly followed by an (α, t) reaction. Similar results were obtained for the (^{3}He,t) reaction on ^{48}Ca.

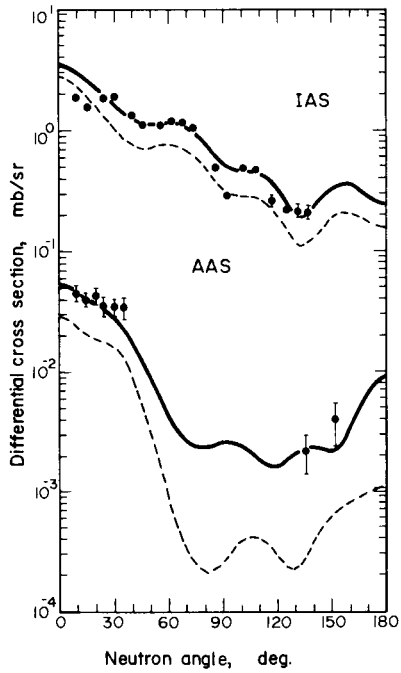

Fig. 41. Differential cross sections of the ^{40}Ar(p,n)^{40}K reaction at 24 MeV to the isobaric analogue and anti-analogue states compared with distorted wave caculations assuming that the reactions take place in one step. The dashed curves show the result of the direct transition only and the solid curves the result of including the knock-on exchange contributions. The isobaric analogue state cross sections were obtained by Bentley and colleagues (1971).

Studies have now been made of the (p,n) reaction to the anti-analogue state of ^{40}Ar by Galonsky and colleagues of Michigan State University (1975). They used 24 MeV protons, and were able to detect the very small cross sections of the anti-analogue state reaction using a large liquid scintillator and a time-of-flight spectrometer. As shown in the figure, these cross sections are only about 1% of the corresponding analogue state ones.

They analysed these data using the distorted wave theory assuming that the reaction takes place on one step, and including both the direct and the knock-on exchange contributions. The dashed curves in Fig. 41 are for the direct process only and the solid curves show the result of including exchange. The parameters of the distorting potentials and of the effective nucleon-nucleon interaction were all taken from previous work.

It is clear from the figure that this calculation gives cross sections in very good agreement with the experimental data, showing that at least in this case it is not necessary to take into account the possibility of two-step reactions in which the incident and outgoing particles are composite, for then the exchange processes are expected to be more likely than the direct.

The relative probabilities of one-step and multi-step processes is a very interesting question, and it is likely that further studies of reactions to anti-analogue state will provide important information. They should also tell us more about the smaller components of the nuclear wavefunctions.

References

J. D. Anderson and C. Wong, *Phys. Rev. Lett.* **8,** 442, 1962.
R. F. Bentley, J. D. Carlson, D. A. Lind, R. B. Perkins and C. D. Zafiratos, *Phys. Rev. Lett.* **27,** 1081, 1971.
A. Galonsky, J. G. Branson, R. R. Doering and D. M. Patterson, *Phys. Rev. Lett.* **35,** 1208, 1975.
R. Schaeffer and G. F. Bertsch, *Phys. Lett.* **38B,** 159, 1972.

2.16 Nuclear Spectroscopy with the (α, ^{2}He) Reaction (*Nature* **264,** 511, 1976)

Nucleon transfer reactions are one of the most powerful ways of

determining the properties of nuclear states, and over the years very many studies have been made of practically every nucleus in the periodic table. The one-nucleon transfer reactions are particularly useful for determining the single-particle properties of nuclei, while reactions transferring more than one nucleon provide information about their collective properties.

For practical reasons not all nucleon transfer reactions are equally easy to carry out. For example, reactions with incoming or outgoing neutrons cannot be studied with the same energy resolution as those involving charged particles. Any addition to the list of reactions available for nuclear spectroscopy is therefore most welcome, and in recent years use has been made of reactions that have unstable outgoing particles.

One of the first of these unstable particles was the nucleus ^{8}Be, which rapidly decays into two alpha particles. The energy of breakup is however very small, only 96 keV, so the two alpha particles are emitted in almost the same direction, and are thus easily detected. Now another such particle, the nucleus ^{2}He, consisting of two protons in a $^{1}S_{0}$, $T = 1$ state, has been shown by a group at Berkeley to be detectable in nuclear reactions. This is important because the (α, ^{2}He) reaction can now be studied, and this provides a convenient way of transferring two neutrons to a nucleus.

In their preliminary studies Jahn *et al.* (1976) show how the ^{2}He nuclei can be detected by a pair of proton counters. Almost as soon as it is emitted from a reaction, the ^{2}He nucleus breaks up into two protons, travelling in almost the same direction, and these can almost simultaneously activate two adjacent proton counters. The number of counts from two unrelated protons is very small.

They have used this detection system to study the (α, ^{2}He) reaction on ^{12}C, ^{13}C, and ^{16}O and find energy spectra very similar to those found for reactions with stable outgoing particles. It is therefore possible to use it to study the structure of the residual nuclei.

Some of their spectra are shown in Fig. 42, and it is notable that very few states are excited, showing that the reaction is very selective. This means that the reaction will only go to states of a particular structure, and this enhances its value as a spectroscopic tool.

Examination of the states excited in the reactions mentioned shows

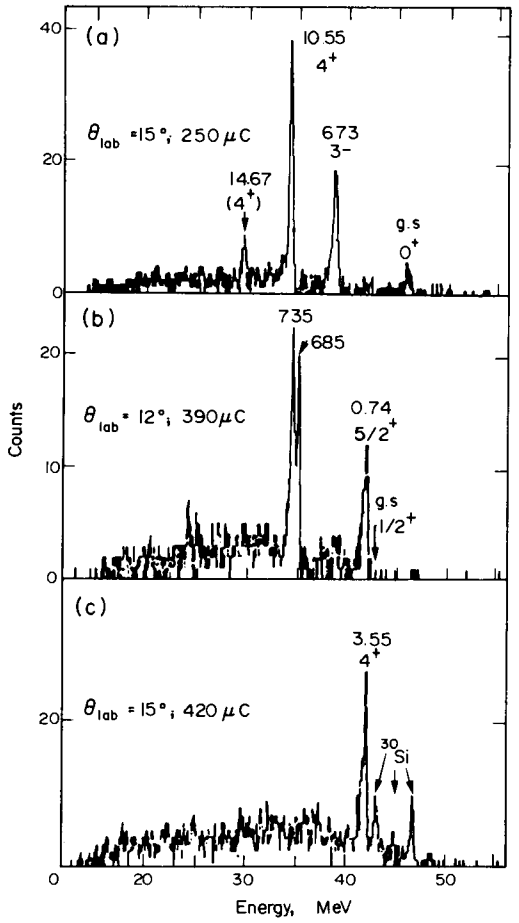

Fig. 42. Energy spectra of ^{2}He nuclei from the (a, ^{2}He) reaction on ^{12}C (a), ^{13}C (b), and ^{16}O (c).

that they are all of high spin. The final nuclei are ^{14}C, ^{15}C and ^{18}O and the states excited are the 3^- at 6.73 MeV and the 4^+ at 10.55 MeV in ^{14}C; the $5/2^+$ at 0.74 MeV in ^{14}C; the $5/2^+$ at 0.74 MeV in ^{15}C: and the 4^+ at 3.55 MeV in ^{18}O.

The preferential excitation of high spin states has already been observed in the (α, d) reaction and these states are favoured because the kinematics of the reaction are such that the neutron–proton pair is easily captured into a relative triplet state about an undisturbed target core. In the same way the observed selectivity in the $(\alpha, {}^2He)$ reaction corresponds to the capture of a neutron–neutron pair into a relative singlet state. At 65 MeV, the energy of the alpha particles used in this experiment, the angular momentum transferred in a surface reaction is about four or five units of $\hbar$, so that states formed by capturing the two neutrons into d orbitals with the configuration $(d_{5/2}{}^2)_{4+}$ should be preferentially excited. The known spins of the states that are selectively excited are in agreement with this simple picture. Similar arguments can be used to predict the states that will be excited in reactions at different energies and on different nuclei.

These results already show the usefulness of the $(\alpha, {}^2He)$ reaction in exciting states of high spin in nuclei. It is likely to be applied to study the structure of many nuclei throughout the periodic table.

References

R. Jahn, G. J. Wozniak, D. P. Stahel and J. Cerny, *Phys. Rev. Lett.* **37**, 812, 1976.
R. Jahn, D. P. Stahel, G. J. Wozniak, R. J. de Meijer and J. Cerny, *Phys. Rev.* **C18**, 9, 1978.
R. J. de Meijer, R. Kamermans, J. van Driel and H. P. Morsch, *Phys. Rev.* **C16**, 2442, 1977.

2.17 The (α, α^*) Reaction

(*Nature* **266**, 121, 1977)

There is now a growing interest in using nuclear reactions with unstable emitted particles in studies of nuclear structure. Among the possible reactions, those leading to the emission of ^8Be are the easiest to use, because the ^8Be decays rapidly into two alpha particles that can be detected in coincidence. Another practicable reaction of this type is the $(\alpha, {}^2He)$ reaction, where the unstable ^2He nucleus is detected by the coincidence of the protons into which it decays (§2.16). Such reactions open up new possibilities for nuclear spectroscopy, so it is

useful to see whether there are any more unstable particles that can be detected in a similar way.

One of the possibilities that has been recently realized is the inelastic scattering of alpha particles with the emission in the excited state at 20.1 MeV. This is an unbound monopole 0^+ state with a width of 0.27 MeV. An alpha particle in this state readily decays into a proton and a triton, and since the energy release is only 0.3 MeV the decay products are emitted in almost the same direction and so can easily be detected by coincidence techniques.

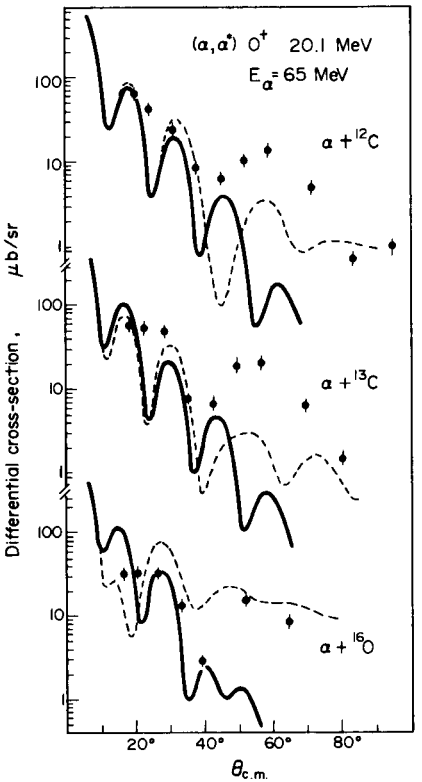

Fig. 43. Differential cross section for the (a, a^*) reaction to the ground states of ^{12}C, ^{13}C and ^{16}O compared with distorted wave calculations using transition densities obtained from the particle-hole (solid curves) and collective (dashed curves) models.

This reaction has recently been observed by Jahn and colleagues (1976). They irradiated targets of ^{12}C, ^{13}C and ^{16}O with 65 MeV alpha particles and looked for protons and tritons emitted in coincidence. They found definite evidence that alpha particles are sometimes emitted in the state of monopole excitation, and in the case of the reaction on ^{12}C their energies corresponded to the reactions that leave the residual ^{12}C nucleus in the ground state, in the 2^+ state at 4.44 MeV and in the 3^- state at 9.64 MeV. The cross-sections for these reactions are about one-thousandth of those of the corresponding reactions with the emission of alpha particles in their ground state.

Distorted wave calculations were made to see if the observed cross sections could be accounted for by existing theories. The transition matrix elements were calculated microscopically using the particle-hole model and also the collective model. The distorted waves were generated by optical potentials fitted to the elastic scattering of 65 MeV alpha particles.

These calculations agree quite well with the absolute values of the experimental cross sections, but not very well with the details of the angular distributions, as shown in Fig. 43. This discrepancy may indicate the importance of higher order effects, in particular the two-step reactions that proceed through an intermediate state.

The detection of this reaction opens up a new area of nuclear reaction and nuclear structure studies, and in particular suggests that it may be useful to look for the $(^3He, a^*)$ and (d, a^*) reactions as well.

Reference

R. Jahn, D. P. Stahel, G. J. Wozniak, J. Cerny and H. P. Morsch, *Phys. Lett.* **65B**, 339, 1976.

2.18 The Fission of Light Nuclei

(*New Scientist* **78,** 669, 1978)

An important step forward in the study of fission of light elements has recently been made by Professor A. E. Litherland's group at Toronto University (Sandorfi, 1978). They were able to detect the fission of magnesium into two carbon nuclei by the inelastic scattering of

electrons from 20 to 30 MeV. Although the cross-sections are exceedingly small, they detected the fission events by the tracks they form in a polycarbonate film called Macrofol. After etching, the tracks are visible under a microscope.

The fission of heavy nuclei like uranium and plutonium is very familiar, but it is not so widely known that quite light nuclei can also undergo fission. This is important for our understanding of how exactly fission takes place. In the case of heavy nuclei there are over 200 nucleons taking part in the process and so it is only possible to use a collective theory such as the liquid drop model that does not take the nucleons into account individually. We can then understand fission up to a point, but it would be much better if we could study it microscopically, considering each nucleon individually. We cannot hope to do this for the heavy nuclei, but the discovery a few years ago that light nuclei such as magnesium can also undergo fission brings a microscopic analysis within the bounds of possibility, since there is a much smaller number of nucleons to take into account.

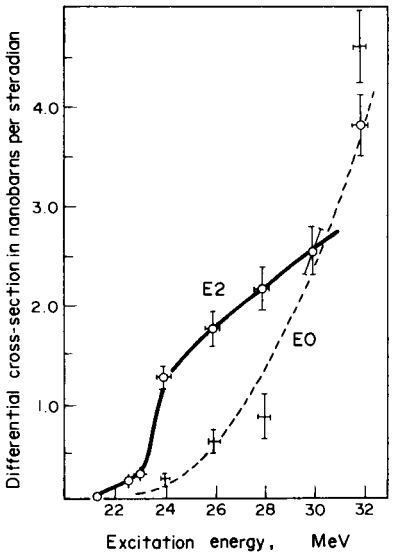

Fig. 44. Differential electrofission cross-sections for magnesium-24.

By studying the increase of cross-section with energy of the electrons, and the relative numbers of fission fragments at angles of 45 and 90 degrees to the electron beam, they were able to distinguish between the electric monopole and electric quadrupole excitations, corresponding to the decay of magnesium 24 with angular momenta 0 and 2 units respectively (see Fig. 44).

They also calculated from these results the cross-section for photofission—fission initiated by gamma rays—and its dependence on energy shows a marked resonance at about 22.7 MeV (see Fig. 45).

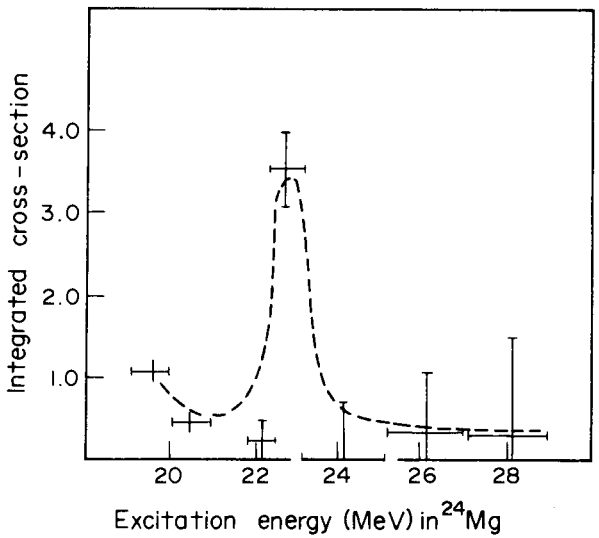

Fig. 45. Photofission cross-section for magnesium-24.

Subsidiary measurements of the angular distribution of the carbon-12 fission fragments showed that this is a 2^+ resonance. The team made further measurements with a gold radiator in front of the target to study the photofission produced by real photons. The results suggest that the fission yield from magnesium excited to around 21 MeV may result from excitations with the giant monopole resonance.

These experiments on the fission of magnesium provide a challenge

to theorists in nuclear physics to do more detailed calculations than hitherto on the different models proposed for fission in order to pick out the most successful one and improve upon it.

The data could then be used to turn these collective models based on fission of heavy nuclei into theories of fission describing the mechanisms involved and the part played by each nucleon.

Reference

A. M. Sandorfi, L. R. Kilius, H. W. Lee and A. E. Litherland, *Phys. Rev. Lett.* **40,** 1248, 1978.

2.19 The Pion Double-charge-exchange Reaction (*New Scientist* **73,** 329, 1977)

The Los Alamos Meson Physics Facility has just provided the first evidence of the long-sought pion double-charge-exchange reaction. In these reactions, a positive pion interacts with a nucleus by a two-step process and a negative pion emerges. The net result is the addition of two charges to the nucleus, or in other words the conversion of two neutrons to two protons. The inverse reaction, with negative pion in and positive pion out, has the opposite effect.

These reactions are interesting because they provide a way of making nuclei with the same structure and same total numbers of nucleons, but different numbers of neutrons and protons, as the ground states of stable nuclei. These are the so-called isobaric analogue states that have added so much to our knowledge of nuclear structure.

The experimental set-up is shown in Fig. 46. The positive pions are produced in the first target, and passed through focusing and bending magnets tuned to admit positive pions. This separates the pions from all the other particles emitted from the production target. The pions then interact with the main target of oxygen, and the emerging particles then pass through a second set of focusing and bending magnets tuned to admit only negative pions. Finally the purified beam of negative pions enters an array of plastic Cerenkov and scintillation counters that enable their energy spectrum to be measured.

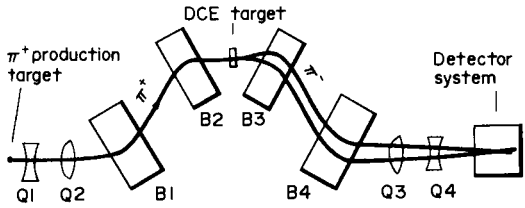

Fig. 46. Schematic layout of experiment.

This energy spectrum has a peak at 130.7 MeV for incident positive pions of 139 MeV. This energy is just what would be expected for the reaction $^{18}O(\pi^+,\pi^-)^{18}Ne$ to the ground state of neon, showing that the double-charge-exchange reaction has taken place.

The differential cross-section of the reaction at 0° was found to be about $1.8\,\mu$b/sr, which is very similar to the best theoretical estimates.

Now that this reaction has been definitely shown to occur, it is likely to be used to study the analogue states of many nuclei.

Reference

T. Marks, M. P. Baker, R. L. Burman, M. D. Cooper, R. H. Heffner, R. J. Holt, D. M. Lee, D. J. Malbrough, B. M. Preedom, R. P. Redwine, J. E. Spencer and B. Zeidman, *Phys. Rev. Lett.* **38**, 149, 1977.

CHAPTER 3

Heavy Ion Reactions

Extensive and detailed accounts of the theory and experiment of heavy ion reactions may be found in the following books:

W. Nörenberg and H. A. Weidenmüller, *Introduction to the Theory of Heavy-Ion Collisions,* Springer-Verlag, 1976.

P. E. Hodgson, *Nuclear Heavy-Ion Reactions,* Oxford, 1978.

3.1 Energetic Nuclear Collisions

(*Nature* **265,** 105, 1977)

When two nuclei collide at high energies there is a very strong interaction and many complicated reactions take place. The nuclei can excite each other and exchange a few nucleons before separating again, or they can fuse together for a short while to form a compound system that decays by emission of nucleons and alpha particles. At higher energies a nuclear shock wave can develop and this surges rapidly through the nucleus and causes the emission of a spray of nuclear fragments.

Some progress has already been made in understanding these reactions using the classical concepts of viscosity and the mechanics of shock waves, but further progress requires a more detailed quantum-mechanical treatment. The motion of the nuclei must be described in terms of the coordinates of their constituent nucleons by wavefunctions satisfying the Schrödinger equation.

Many theories of nuclear structure have now been developed that treat the motion of the constituent nucleons in this way, in particular the Hartree–Fock self-consistent field theory. This gives a series of coupled equations for the nucleon wavefunctions that can be solved in

principle to give the single-particle wave functions and all the properties that can be derived therefrom. This is a very complicated calculation that can only be carried out in practice by making several simplifying approximations.

The problem of understanding a nuclear collision in a similar way is immensely more complicated, essentially because it is dynamic. Although a time-dependent Hartree–Fock theory has been developed, it is difficult to apply it to nuclear collisions.

Faced with such a complicated problem, the best way to proceed is to make a simple model that, it is hoped, contains many of its main features, but is practicable to solve. Comparison between the solutions of the simple problem and the experimental data will then indicate the usefulness of the model, and possibly suggest ways of improving it. At the same time increasing familiarity with the mathematical structure of the simple solution may make it easier to see how the model can be made more realistic without at the same time making it impossible to solve.

This approach has recently been used by Bonche, Koonin and Negele (1976) in a first attempt to make a quantum-mechanical theory of the energetic interactions of heavy ions. To make the calculations tractable they made very drastic assumptions, and yet rather surprisingly the results showed many of the features of the experimental data and thus encourage the development of the theory in more detail.

The first great simplification was to assume that the whole interaction essentially takes place in one dimension. They thus considered the collision of two slabs of nuclear matter having a specified thickness in their direction of motion but extending indefinitely in the directions at right angles. They also assumed that these slabs were completely symmetric in spin and isospin.

The Hartree–Fock theory requires the interaction between two nucleons, and this is known to be very complicated. They therefore constructed a simplified form of the interaction that contains most of the physics and adjusted its parameters to give the best overall agreement with nuclear properties.

In its full generality, the time-dependent Hartree–Fock theory gives a set of coupled non-linear integro-differential equations in three dimensions for the wavefunctions of the nucleons. After making the

above approximations they reduce to a set of coupled linear equations that are readily solved by existing electronic computer techniques.

These equations were solved for a series of different initial conditions. They first of all studied the oscillations of a single slab, and found that these could take place at certain definite frequencies. These oscillations correspond to the collective 'breathing mode' oscillations of nuclei, that is oscillations without change of shape. The frequencies of such oscillations depend on the nuclear compressibility (see Volume 1, § 2.10).

Next they found out how a slab interacts with a potential, and in particular how it is affected by passing through a potential barrier. At a speed $E/A = 10$ MeV and barrier of Gaussian form and height equal to the incident kinetic energy there is hardly any reflection, and the transmitted slab has a different density profile showing that it is in an excited state.

The excitation consists of density ripples moving through the slab and calculations show that 36% of the incident kinetic energy is converted into such excitations. This behaviour is markedly different from that of a single particle encountering a barrier at comparable energies: in that case only half the incident wave is transmitted and half is reflected. This comparison shows the importance of collective effects in the slab interaction: the attractive single-particle potential due to the other nucleons moving through the barrier reduces the effective potential and hence favours transmission over reflection.

As the barrier height is increased, so is the proportion of the slab that is reflected, until when the barrier is twice the incident kinetic energy it reaches 71%. In addition, the transmitted and reflected portions each split up into two pieces, one slowly moving and the other rapidly moving.

These studies are a useful preliminary to the main object of the calculations, namely to calculate the interaction of two nuclei, here represented by two slabs. At low energies ($E/A \sim 0.5$ MeV) the slabs fuse together to form a compound slab of rather uniform density that continues to oscillate without breaking up (see § 3.19, p. 165).

At a somewhat higher energy ($E/A \approx 3.5$ MeV) the compound slab is formed and then almost immediately separates again. Each fragment

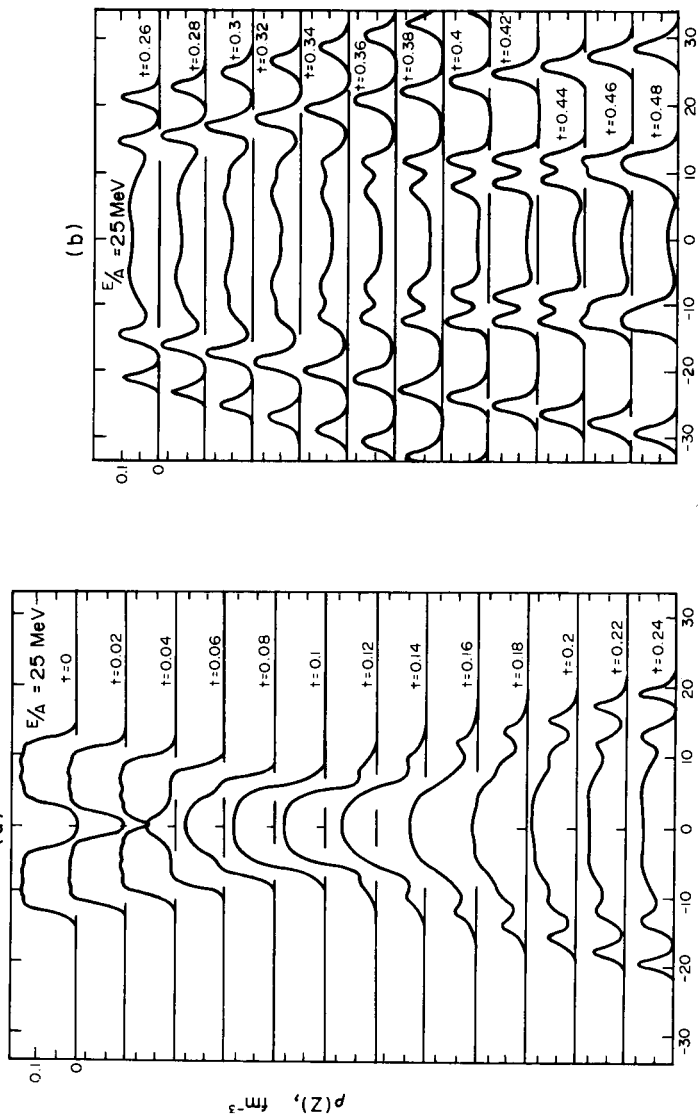

Fig. 47. Density profiles at various times t for the collisions of two slabs at a velocity corresponding to $E/A = 25$ MeV, showing the formation of a shock wave that propagates rapidly outwards, followed by a general fragmentation. (Times in units of 10^{-21} s.)

is oscillating strongly after the interaction, showing that it is highly excited. This process corresponds to the deep inelastic scattering of heavy ions, when two nuclei are strongly excited in a collision but essentially retain their identity, apart perhaps from the exchange of a few nucleons (see § 3.18, p. 160).

At much higher energies ($E/A = 25$ MeV) some quite new phenomena appear. As shown in Fig. 47, a region of very high density is formed, and from this region shock waves propagate outwards in both directions: these are indicated by the waves moving outwards at velocities higher than the incident slabs. When these waves of higher density reach the surface of the slab they separate from it, forming separate fragments that propagate rapidly outwards. Secondary waves follow them, and the region of almost uniform density that is formed for a short time in the central region breaks up from both ends into separate waves that also travel outwards and separate when they reach the surface, until eventually the whole compound system has broken up into fragments. Thus the model shows very well the phenomena of shock waves and fragmentation that take place in very energetic nuclear collisions.

An important advance has recently been made by Cusson, Smith and Maruhn (1976) in the form of a time-dependent Hartree–Fock (TDHF) calculation of the reaction $^{16}O + {}^{16}O$ in three dimensions. The TDHF model they used assumes that the time-dependent wave function is given by a single Slater determinant whose occupied single-particle orbits obey the TDHF Schrödinger equation. For the interaction between the particles they used a simplified form of the Skyrme interaction, and assumed spin and isospin saturation, so that the spatial wave function applies to alpha particles.

Some of their results are shown in Fig. 48, which gives the contours of the densities of the two interacting ions at various times in the plane of the collision, integrated over the direction perpendicular to that plane. The time scale is in units of fm/c, that is about 3×10^{-24} s so the whole interaction takes about 10^{-21} s. These contour plots show that when a collision takes place at an impact parameter equal to about half the radius of the ions the outer regions interact strongly and stick the ions together in a dumb-bell shape which rotates about its centre of mass. As the system rotates, complicated internal motions take place,

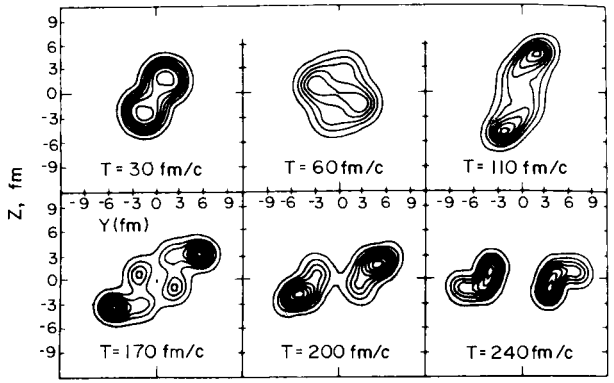

Fig. 48. Contours of the nuclear density for the collision of ^{16}O with ^{16}O at $E/A = 24$ MeV and an impact parameter of 4 fm. The contours are in the scattering plane and the density is integrated over the co-ordinate perpendicular to it.

some parts rotating more rapidly than others. At one stage (T = 170 fm/c) small regions of higher density corresponding to alpha particles form in the region between the main mass concentrations. These are later attracted back and a neck forms between the two ions. The neck narrows and finally breaks, and the particles separate. They are now irregular in shape, indicating that they have been highly excited by the collision.

At no time in this interaction are high densities observed, indicating that the energy is too low for compression and shock wave phenomena to develop.

References

P. Bonche, S. Koonin and J. W. Negele, *Phys. Rev.* **C13**, 1226, 1976.
R. Y. Cusson, R. K. Smith and T. A. Maruhn, *Phys. Rev. Lett.* **36**, 1166, 1976.

3.2 The Dynamics of Nuclear Collisions
(*New Scientist* **73**, 15, 1977)

The processes taking place when two carbon nuclei collide head-on are very graphically illustrated by a series of calculations recently published by Maruhn and Cusson (1976).

These calculations were made by the time-dependent Hartree–Fock method, which involves solving the Schrödinger equation describing the motion of the nuclei at a series of different times, and thus obtaining what are effectively a series of snapshots of the densities of the nuclei throughout the whole interaction process.

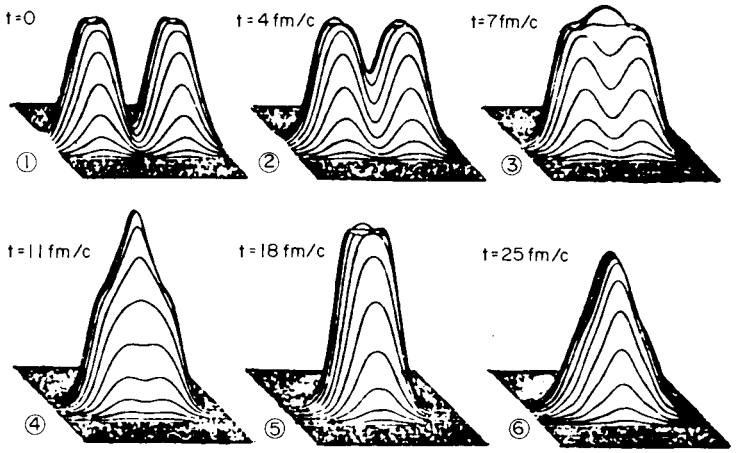

Fig. 49. Perspective three-dimensional plots of the total density versus the coordinates z and p, at $E/A = 64$ MeV/A. The fourth frame, at $t =$ 11 fm/c, shows the highest density observed in this work, $D \approx 0.23$ nucleons/fm^3.

These calculations refer to head-on collisions, and the neutrons and protons are treated separately, and both Coulomb and spin-orbit forces are included. Calculations at 1.6 MeV per nucleon in the centre of mass system showed the brief formation and decay of the resonant molecular state of magnesium 24. At the higher energy of 64 MeV per nucleon shown here the two carbon nuclei combine to form a highly excited state of magnesium 24 which wobbles about for some time and

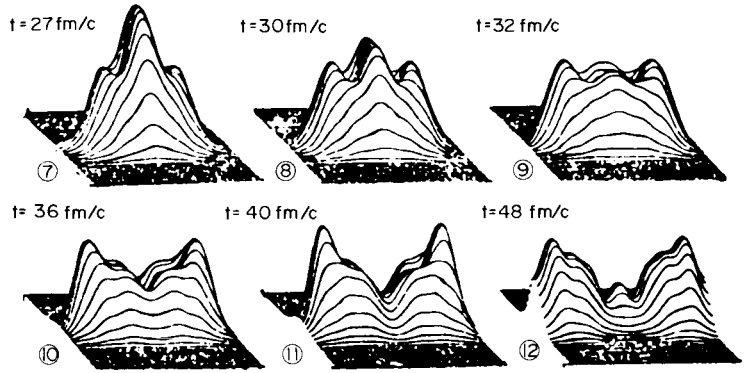

Fig. 50. Same as Fig. 49 but at later time. One observes in the last frame the fragments emerge in a highly excited internal state.

then finally separates into two carbon nuclei again. These have very irregular density profiles in contrast to the smooth ones before the collision, and this shows that the outgoing carbon nuclei are very highly excited. In the collision some of the energy of motion has been converted into internal energy, a process known as inelastic scattering.

In these pictures the time scale is in units of fm/c corresponding to about 3.10^{-24} seconds. The whole interaction therefore takes about 2.10^{-22} seconds (see Figs. 49 and 50).

These pictures provide a very direct way of studying the changes in shape that occur when two nuclei collide at high energies.

Reference

T. A. Maruhn and R. Y. Cusson, *Nucl. Phys.* **A270,** 471, 1976.

3.3 Nuclear Molecules

(*New Scientist* **73,** 218, 1977)

We are all familiar with the way that atoms can combine to form molecules: for example one oxygen and two hydrogen atoms can combine to form a molecule of water. Inside the molecule, the atoms retain most of their internal properties, but in addition they are joined

to the other atoms by molecular (electromagnetic) forces to make the molecule. The molecule itself has properties of its own, as in the case of water, quite different from those of its constituent atoms.

It is interesting to speculate whether the nuclei of atoms can combine in a similar way to form nuclear molecules. The short-range character of the nuclear forces means that the nuclei in such a molecule must be almost touching, for otherwise they would not stay together. Atomic nuclei are 100 000 times smaller than atoms themselves, and we thus arrive at the picture of a nuclear molecule as two tiny nuclei practically touching each other, and held together by the sum total of all the nucleon-nucleon interactions in the region around the point where they are nearest together. Some of the differences and similarities of atomic and nuclear molecules are shown in Fig. 51.

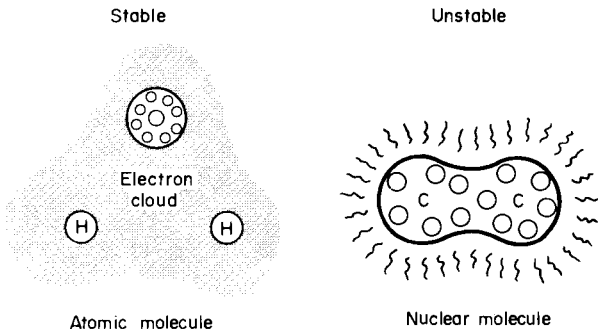

Fig. 51. Atomic molecules, like water (sketched left), consist of clouds of light electrons around a few tiny nuclei. Nuclear molecules would be nuclei just touching one another (right).

The forces holding atomic molecules together are attractive at large distances and repulsive at small distances, so that there is an equilibrium distance corresponding to the most stable configuration. Many molecules are stable and hold together until broken up by an energetic interaction. Nuclear forces however are so strong that even if a nuclear molecule can exist at all it is likely to be on a very short-lived

and precarious knife-edge between flying apart and coalescing to form a compound nucleus. We would not expect to find stable nuclear molecules.

The extreme instability of nuclear molecules means that we can only hope to detect them, if at all, as short-lived intermediate states in reactions between two nuclei. If two nuclei collide head-on, or nearly head-on, they will stick together to form a compound nucleus at low energies, and break each other into fragments at high energies. But if

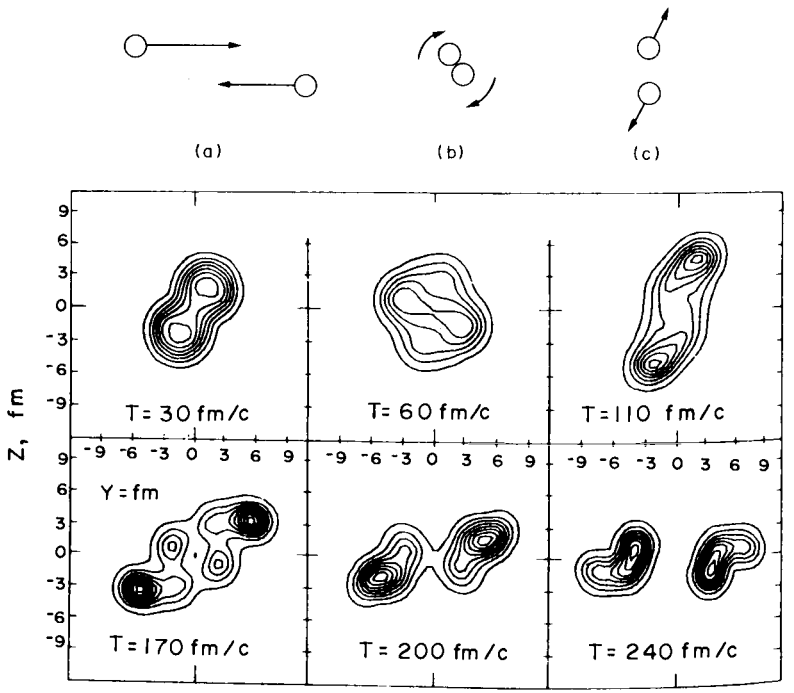

Fig. 52. Nuclear molecules may be formed when two nuclei approach so as to just graze past one another (a). They touch and stick together like two water droplets, spinning rapidly around one another (b), and finally fly apart again (c). In the computer model of such a collision also pictured here a nuclear molecule is formed (top left), spins and oscillates (later pictures), and finally breaks up (bottom right) (Cusson *et al.*, 1976).

the collision is a glancing one, then there is just a chance that they will stick together without seriously losing their shapes, and rotate around each other like a dumb-bell. After a very few rotations they will either fly apart or coalesce, but while they are in the dumb-bell configuration they form a nuclear molecule, as shown in Fig. 52.

We cannot of course see this happening, so if we want it to be more than an interesting speculation we have to see what effect the formation and decay of a nuclear molecule is likely to have on the cross-section of the reaction or, in other words, on the probability that the reaction takes place.

The formation of a nuclear molecule is most likely to be visible in the variation in the interaction rate ("cross-section") of two nuclei with the energy of their collision—the "excitation function, as it is called. When two nuclei just scatter elastically off each other, like two rubber balls, or if they just give each other energy or exchange one or two nucleons, the cross-section varies smoothly with energy. This is characteristic of reactions that take place very rapidly, in the time that it takes for the two nuclei to pass each other. On the other hand when two nuclei coalesce to form a compound system the cross-section varies very rapidly with energy depending on the energies of the allowed states of the combined system.

When the energy of the reaction is such that the compound system can be formed in one of its excited states, the cross-section is high, and

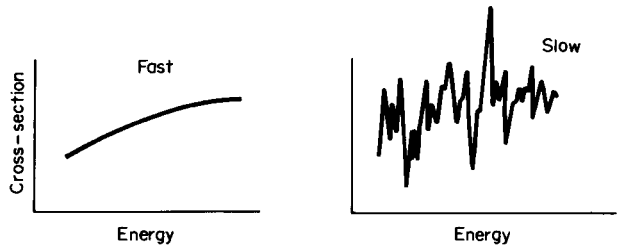

Fig. 53. When one nucleus is fired at another, its probability of hitting it is called the "cross-section" for the reaction. If this quantity varies smoothly with the energy of the incoming nucleus, then Heisenberg's uncertainty principle tells us that the meeting of the nuclei was brief. If there is much variation the meeting was lengthy and complex processes—such as the formation of a nuclear molecule—must have taken place.

when it is such that there is no available state it is zero. At high energies of excitation of the compound system the states are very close together in energy and they are spread over a range of energies so that they overlap. In such cases the cross-section varies in a jagged way with energy, as shown in Fig. 53. This type of reaction takes very much longer, maybe over a million times as long as the reactions that give a smooth excitation function.

This tells us that we can learn something about the time taken by a nuclear reaction by looking at the way its cross-section varies with energy. This is in fact just the Heisenberg uncertainty relation between energy and time: the longer the reaction takes the smaller the energy spread and vice-versa. Thus, as we have seen, a reaction that takes a long time has a jagged excitation function, while a rapid reaction has one that varies smoothly with energy.

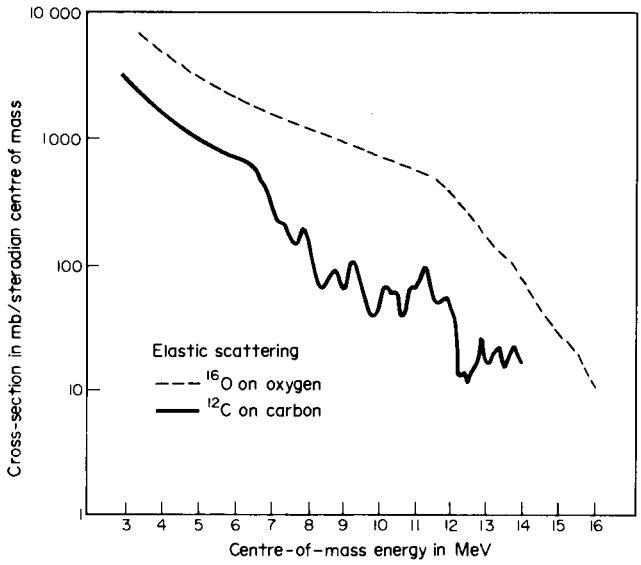

Fig. 54. The variation with incident energy for the cross-section between carbon nuclei (below) and oxygen nuclei (above) showing fast variation for carbon but not for oxygen. This may indicate that two carbons form a nuclear molecule but not two oxygens (Bromley *et al.*, 1960).

Now a nuclear molecule, if it exists, lives for a time longer than it takes for the nuclei to pass each other, but much shorter than that taken for the formation of the compound system. The corresponding excitation function is therefore expected to show jagged peaks but each peak is much broader than those found in the compound system reaction.

In their pioneer study of the elastic scattering of two carbon nuclei, Bromley, Kuehner and Almqvist in 1960 found just this sort of structure, as shown in Fig. 54. They interpreted the peaks in the excitation function as due to short-lived molecular states in which the two carbon nuclei orbit round each other like a dumb-bell.

Of course it is important not to jump to conclusions: just because we find peaks in the excitation function that are similar to the peaks that we might expect if a transient molecule was formed does not prove that the molecule was really present. There may be other reasons for the peaks. We must therefore make more measurements to try to determine the properties of the nuclear molecules, and also develop a theory of the formation and breakup of the molecules and see if its predictions are confirmed by our measurements.

One of the most important properties of a nuclear state after its energy is its angular momentum or spin. This can easily be found from the angular distribution of the two halves of the presumed molecule after it has flown apart. This has now been found for many peaks in excitation functions.

To understand the energies and spins it is necessary to show that they can be calculated from a physically-reasonable force. Now when two nuclei collide the force between them consists of three parts: the purely nuclear force, the electrostatic force, and the centrifugal force that arises from the rotation of one nucleus around the other. Each of these parts of the total force is quite well known and when they are added together they give an interaction energy that has the radial variation shown in Fig. 55. It can be seen that this energy has a minimum value at the point marked by the arrow. This means that the force is attractive at larger distances and repulsive at smaller distances, just like the molecular potential in atoms. A minimum of this type does not always occur; this depends on the relative strengths of the three parts of the potential, and this varies from case to case.

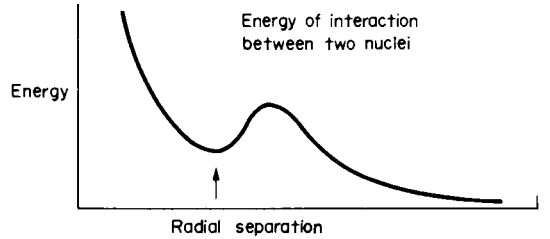

Fig. 55. Combining nuclear, electromagnetic, and centrifugal forces can give this interaction between nuclei.

When a minimum is present, a quantum-mechanical calculation can be made and shows as expected that the excitation function has characteristic peaks like those shown in Fig. 54. The calculation gives the energies and the spins of the states responsible for these peaks, and if these agree with the measured values then this is good evidence for the correctness of our hypothesis of the transient formation of a nuclear molecule. Just such agreement between theory and experiment has indeed been found for some of the peaks in the excitation function for the scattering of two carbon nuclei.

Before accepting this explanation, it is necessary to make as many subsidiary checks as possible. For example, the possibility that the peaks could be due to the near coincidence of a large number of narrow compound nucleus peaks must be excluded; this has been done on statistical grounds. Then we can look at the cross-sections of all the other reactions that take place at the same time as the elastic scattering. This has been done, and as shown in Fig. 56 these show peaks at just the same energies.

Another check is connected with the picture of the molecule as formed in a grazing collision, as shown in Fig. 52. Since we know the radii of the nuclei very well and also their energy, we can easily calculate their angular momentum about each other when in the dumb-bell configuration, and this is just the angular momentum of the state. When this is done, we do indeed find the same value as that determined from the angular distribution of the two nuclei after breakup.

The interpretation of the states as those of a rotating dumb-bell also suggests that the states form a set of states corresponding to different

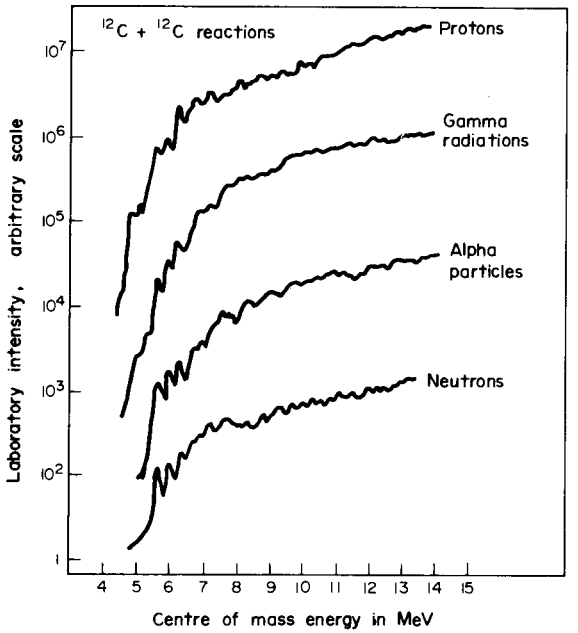

Fig. 56. Cross-section of carbon on carbon for emission of particles also shows evidence of nuclear molecule formation (Almqvist *et al.*, 1960).

rates of rotation—a "rotation band"—just like those found in deformed nuclei. Indeed the compound system in the case of the collision of two carbon nuclei is magnesium-24, which is known to be deformed. As shown in Fig. 57, the low-lying states of this nucleus form a rotational band, easily recognized because the energies are proportional to $J(J + 1)$, where J is the angular momentum of the state (which according to quantum mechanics can take only integer values). Thus if the energy is plotted against $J(J + 1)$, as in the figure, the states of a rotational band fall on a straight line.

On the same figure the molecular states are also plotted, and it is evident that they also fall on a straight line, showing that they form another rotational band at higher energies. Closer study shows that each of the higher states in this band is split into a number of

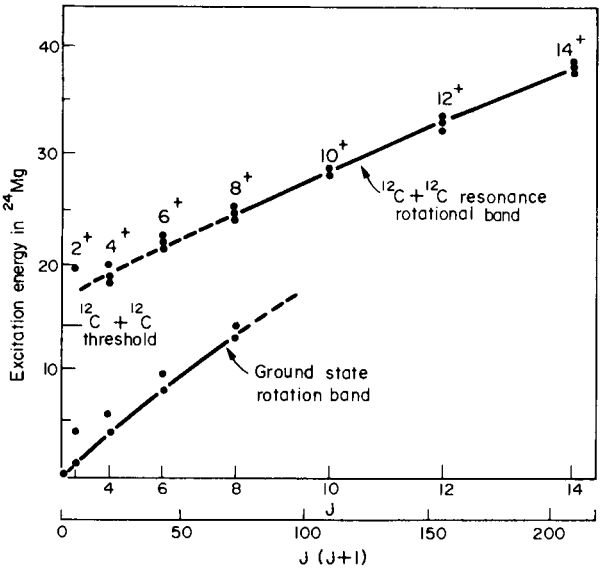

Fig. 57. Energies of the states of magnesium-24 plotted against $J(J + 1)$ where J is the spin, showing the ground state band and the set of states in carbon-12 interactions with carbon-12 which are interpreted as showing the molecular state of the magnesium-24 nucleus. While the ground state of magnesium-24 is nearly spherical, its molecular state will be like a dumb-bell. This illustrates that the nuclear molecule formed from nuclei A and B can be seen as a highly distorted version of the nucleus $A + B$ (Cosman *et al.*, 1975).

components, and this is fully consistent with the transient nature of the molecular states.

Thus on the whole there seems to be good evidence that in some reactions nuclear molecules are formed as transient systems. Many reactions have now been studied, and it is found that the characteristic structure appears in some reactions but not in others. For example it does not appear in the scattering of oxygen by oxygen also shown in Fig. 54. An acceptable theory of nuclear molecules must be able to explain why they are not found in some reactions as well as explaining why they appear when they do. This is obviously connected with the structure of the compound system, in particular with the density of

states at the appropriate excitation energy, and some correlation between these quantities has indeed been found.

The formation of nuclear molecules also seems to be influenced by whether the two nuclei are each composed of a whole number of alpha-particles: when they are, molecules are easily formed. Even the addition of one nucleon seems to destroy the molecules. Thus they are readily formed in the collision of two carbon-12 nuclei, but if one of them is replaced by a carbon-13 nucleus a molecule is no longer formed.

These two conditions explain in a qualitative way most of the cases of the appearance or non-appearance of nuclear molecules, but much detailed work needs to be done before the explanation is put on a firm basis. More detailed theories of the nuclear interaction are proving successful in explaining many of the molecular states that have been observed. The field of study of nuclear molecules will be an interesting one for some years yet, and there may be more surprises in store.

References

E. Almqvist, D. A. Bromley and J. A. Kuehner, *Phys. Rev. Lett.* **4**, 515, 1960.
D. A. Bromley, J. A. Kuehner and E. Almqvist, *Phys. Rev. Lett.* **4**, 365, 1960.
E. R. Cosman, T. M. Cormier, R. Van Bibber, A. Sperduto, G. Young, J. Erskine, L. R. Greenwood and O. Hansen, *Phys. Rev. Lett.* **35**, 265, 1975.
R. Y. Cusson, R. K. Smith and T. A. Maruhn, *Phys. Rev. Lett.* **36**, 1166, 1976.

3.4 Existence of Nuclear Molecules Confirmed

(*New Scientist,* **74,** 458, 1977)

There is already considerable evidence that two colliding ^{12}C nuclei form transient nuclear molecules; they orbit around each other for several periods before either coalescing or flying apart. The energy states of such nuclear molecules form a rotational band, with energies proportional to $J(J + 1)$, where J is the spin of the state, just like those of ordinary molecules (see § 3.3, p. 114).

These resonances have recently been strikingly confirmed by a group working at the State University of New York and at Brookhaven National Laboratory (Cormier *et al.,* 1977). They measured the total cross-section for the mutual inelastic scattering reaction in which both

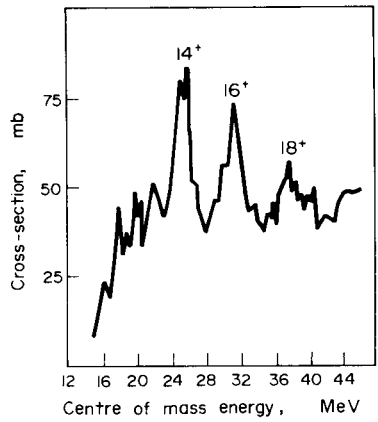

Fig. 58. Cross-section for the reaction exciting both ^{12}C nuclei to their 2^+ states at 4.44 MeV as a function of energy in the centre of mass system.

^{12}C nuclei are excited to the first 2^+ state at 4.44 MeV, and the results are shown in Fig. 58. It is notable that this cross-section shows a series of broad and somewhat ragged peaks, and their mean energies are just what would be expected if they have the spins shown and are members of a rotational band. This is shown in Fig. 59, where these energies are plotted against $J(J+1)$. The assignment of these spins is supported by calculations of the cross-section of the reaction going to each of them, which is just what would be expected for the spins shown.

The raggedness of the peaks is also well understood. Each ragged peak is formed of a large number of sharp resonances corresponding to states of the compound nucleus, which are irregularly spaced in energy. The broad molecular resonances can only be seen through the compound nucleus reactions that pass through these intermediate compound nucleus states; they are called the doorway states on the way to the excitation of the compound nucleus. It is as if we can only look at the molecular resonances through spectacles that will only transmit particles of the energies corresponding to the myriad states of the compound nucleus. If these states were evenly spaced and equally strong, we would see the molecular states as smooth peaks in the cross-section as a function of energy. But because they are irregularly spaced and of a range of strengths, the molecular resonances appear as ragged peaks.

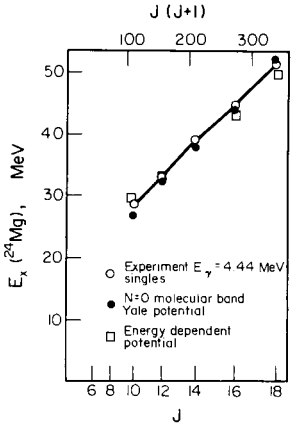

Fig. 59. Excitation energy of the $^{12}C + ^{12}C$ system as a function of $J(J+1)$ showing the linear relation characteristic of a rotational band. The additional points correspond to calculated energies obtained from two particular $^{12}C - ^{12}C$ potentials.

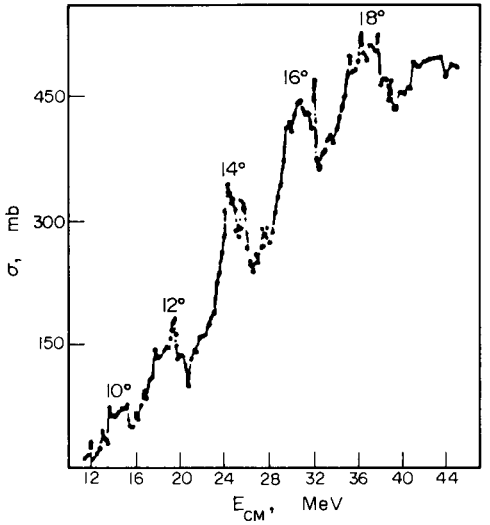

Fig. 60. Total cross-section for the emission of a gamma ray corresponding to the transition from the 2^+ excited state at 4.44 MeV to the ground state. This shows very clearly the sequence of rotational states.

In addition to confirming the energies of several states of the molecular band, this new result provides strong evidence for additional resonances of higher spins and energies than have been observed so far. The whole series of states from the 10^+ state to the 18^+ state is clearly shown in the total cross-section for the emission of the gamma ray corresponding to the transition from the 2^+ state at 4.44 MeV to the ground state (Fig. 60). This provides very clear and direct evidence for the existence of a rotational band.

References

T. M. Cormier, J. Applegate, G. M. Berkowitz, P. Braun-Munzinger, P. M. Cormier, J. W. Harris, C. M. Jachcinski, L. L. Lee, J. Barrette and H. E. Wegner, *Phys. Rev. Lett.* **38**, 940, 1977.

3.5 Surface Waves in Heavy Ion Elastic Scattering
(*New Scientist*, **74**, 779, 1977)

The elastic scattering of heavy ions is generally quite well understood. At low energies they interact mainly through their Coulomb electrostatic fields, and the cross-section follows the Rutherford formula. As the energy increases the ions interact through their nuclear fields and reactions can occur, thus reducing the cross-section below the Rutherford value. The magnitude of the cross-section usually oscillates around an average value due to quantum-mechanical diffraction effects. The whole interaction between the ions through their Coulomb and nuclear fields can be quite well described by an optical model potential.

Since the elastic scattering cross-section falls very rapidly with increasing scattering angle, most measurements so far have been made on the cross-sections in the forward direction only. A group at the State University of New York and at Brookhaven National Laboratory have recently measured the elastic scattering of ^{16}O by ^{28}Si ions at a centre of mass energy of 35 MeV in the backward direction as well, as far as 180°. The results are shown in Fig. 61, and it is apparent that the backward cross-section behaves in a quite unexpected way: it is far greater and more oscillatory than was expected.

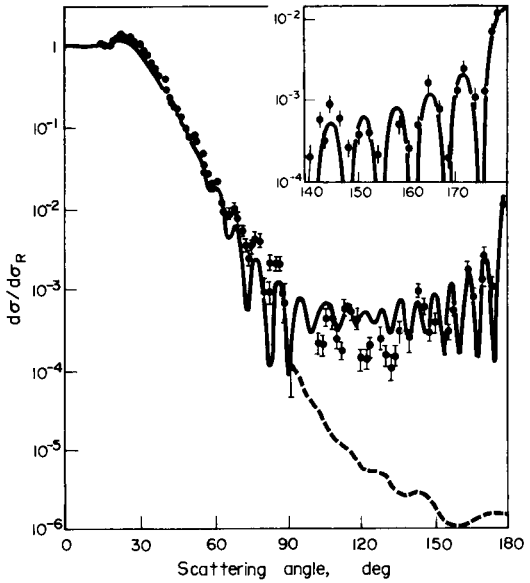

Fig. 61. Elastic scattering cross-section for the interaction of ^{16}O and ^{28}Si nuclei at 35 MeV expressed as a ratio to the Rutherford cross-section. The curves show the results of calculations described in the text.

The clue to the explanation of this behaviour is found in the observation that the cross-section in the backward direction is quite closely proportional to the square of the Legendre polynomial of order 26 (see inset) which corresponds to the relative orbital angular momenta of the two ions when they are just touching. This shows that the backward cross-section is largely due to interactions with impact parameters corresponding to grazing collisions. What is happening is that the ions are slightly sticky and if they make a grazing collision they stick together for a short while and orbit around each other before separating again. This enhances the contribution of the corresponding partial waves, and thus enhances the cross-section. In the wave language we can say that the waves corresponding to one ion run around the surface of the other ion.

A theory of this process can easily be developed by expressing the contribution of the grazing partial wave in a resonant form, and this gives the full curve in the figure; it fits the observations quite well over

the whole angular range. The dotted curve shows the result of an optical model calculation, without such a resonant term, that was fitted to the forward angle data only. While the inclusion of an explicit resonant term shows the physics of the interaction clearly, it is also possible to account for the cross-section with the optical model, at least in principle. It is possible to find potentials that automatically give a resonance in a particular partial wave, and the width of the resonance can be controlled by allowing the potential to depend on the orbital angular momentum quantum number. These are the surface-transparent potentials that allow orbiting to take place.

So far an optical potential that will fit this data has not yet been found, and it remains to be seen whether the resonance or the optical model gives a more natural account of the cross-section as a function of energy.

This work shows that there is still much to be learnt even from such simple interactions as the elastic scattering of two ions.

References

J. Barrette, M. J. LeVine, P. Braun-Munzinger, G. M. Berkowitz, M. Gai, J. W. Harris and C. M. Jachcinski, *Phys. Rev. Lett.* **40**, 445, 1978.

P. Braun-Munzinger and J. Barrette, Symposium on Heavy Ion Elastic Scattering, Rochester 1977.

P. Braun-Munzinger, G. M. Berkowitz, T. M. Cormier, C. M. Jachcinski, J. W. Harris, J. Barrette and M. J. LeVine, *Phys. Rev. Lett.* **38**, 944, 1977.

3.6 Strong Absorption in $^{40}Ca-^{40}Ca$ Elastic Scattering (*Nature* **259**, 13, 1976)

Many studies of the elastic scattering of heavy ions have now been made, and it is usually found that the differential cross section has a diffraction structure that varies smoothly with the incident energy and is well described by the optical model.

A notable exception to this behaviour was found some years ago by Bromley *et al.* (1967, 1968): the cross section for $^{16}O-^{16}O$ elastic scattering shows a very irregular behaviour as a function of incident energy. This is in marked contrast to the corresponding data for $^{18}O-^{18}O$, which varies smoothly with energy as expected.

This early work, together with subsequent studies, showed that this notable difference in behaviour is determined by a balance between the strong absorption of the lower partial waves and the weaker absorption of the higher partial waves. For heavy ion collisions many features of classical behaviour remain, so that partial waves correspond to the interactions at different radial distances: the lower to interactions inside the nucleus and the outer to interactions in the nuclear surface and beyond. The scattering is thus determined by the absorbing part of the optical potential, and it was found that the observed behaviour could well be reproduced by allowing the strength of the absorption to depend on the orbital angular momentum quantum number L, being strong for small L and weak for large L.

More physically, it was shown that the absorption is mainly due to the direct reactions strongly coupled to the entrance channel. When there are many of these, the nuclear surface is nearly opaque and one observes the small structureless cross section strongly decreasing with energy—behaviour typical of strong absorption. This is the case for $^{18}O-^{18}O$, which has two neutrons outside the stable ^{18}O core that can be excited and transferred in many ways, leading to many possible reaction channels.

The situation is quite different for $^{16}O-^{16}O$ which is stable and difficult to excite and so absorbs weakly. Each partial wave makes its own particular contribution, giving the strongly-marked fluctuations in the cross section as a function of energy.

This explanation accounts for all the data in the oxygen region, but it is clearly desirable to confirm it by measurements on other nuclei. It is increasingly difficult to make measurements on heavier nuclei because the strong Coulomb repulsion must be overcome before the nuclear interactions can take place, and this requires high incident energies.

The next lightest nucleus after ^{16}O that has a very stable doubly-closed shell structure is ^{40}Ca, and so it is desirable to make measurements of $^{40}Ca-^{40}Ca$ scattering. This has recently been done by Doubre *et al.* (1975) at Orsay in France, and some of their results are shown in Fig. 62.

It is notable that, contrary to expectation, the cross sections fall smoothly with increasing energy, so characteristic of strong absorption. An optical model calculation with an absorption increasing with

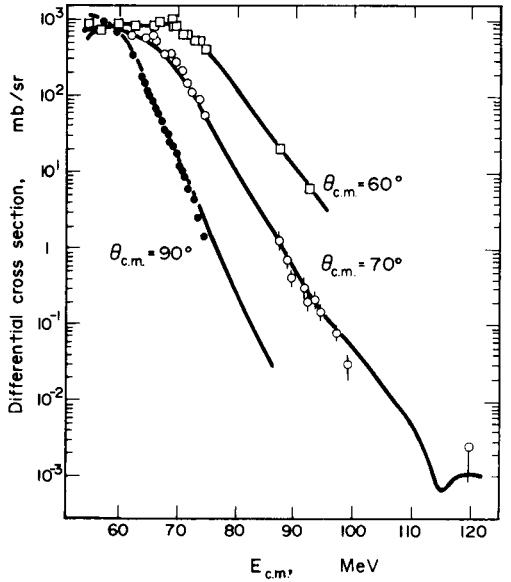

Fig. 62. Differential cross section for $^{40}Ca-^{40}Ca$ elastic scattering at three angles as a function of energy and compared with optical model calculations.

energy agrees well with the experimental data. The physical explanation of this result is not clear. The explanation used in the oxygen region fails for calcium, and it may be that the density of states in the appropriate region of excitation is sufficiently high in the calcium case for the required absorption to occur. More measurements are in progress to provide data for a more comprehensive study of these effects.

Comment

Further measurements of this interaction have been made by Doubre *et al.* (1977) and they find that the differential cross-sections at seven energies from 64.8 to 120 MeV can be well fitted by the same optical potential. The absence of structure in the excitation function is ascribed to the large mass and charge of the colliding nuclei.

References

H. Doubre, J. C. Roynette, J. C. Jacmart, N. Poffé, M. Riou, E. Plagnol and P. de Saintignon, *Phys. Rev. Lett.* **35**, 508, 1975.
H. Doubre, J. C. Jacmart, E. Plagnol, N. Poffé, M. Riou and J. C. Roynette, *Phys. Rev.* **C15**, 693, 1977.
R. H. Siemssen, J. V. Maher, A. Weidinger and D. A. Bromley, *Phys. Rev. Lett.* **19**, 369, 1967; **20**, 175, 1968.

3.7 Negative Deflection Angles in Heavy Ion Scattering (*Nature* **271**, 408, 1978)

When two nuclei interact at energies high enough to overcome their mutual electrostatic repulsion their quantum-mechanical wavelengths are usually small compared with their own radii, so that it is possible for many purposes to consider them as classical particles moving along well-defined orbits. If we think of the scattering angle as a function of the impact parameter we find several curious effects, in particular that several impact parameters can give the same scattering angle. It has now proved possible to distinguish these orbits experimentally.

The orbits can be visualized by considering the interaction for various impact parameters, or distances of closest approach in the absence of all interactions. For large impact parameters the projectile feels only the long-range repulsive Coulomb (or electrostatic) field and is deflected through a small positive angle. As the impact parameter is decreased the nuclei come closer together so the Coulomb interaction is larger and the repulsion and thus the deflection angle are greater. Thus initially the deflection angle increases as the impact parameter decreases.

As the impact parameter is still further decreased the nuclei approach close enough for their short-range attractive nuclear fields to interact. These oppose the repulsive Coulomb force and thus reduce the scattering angle. Eventually as the impact parameter is reduced still further there comes a point when the Coulomb and nuclear fields exactly balance and the particle is not scattered at all. At still smaller impact parameters the scattering angle becomes negative, and the corresponding orbits wind round the back of the target nucleus as shown in the inset to Fig. 63.

Although there is a clear physical difference between the orbits

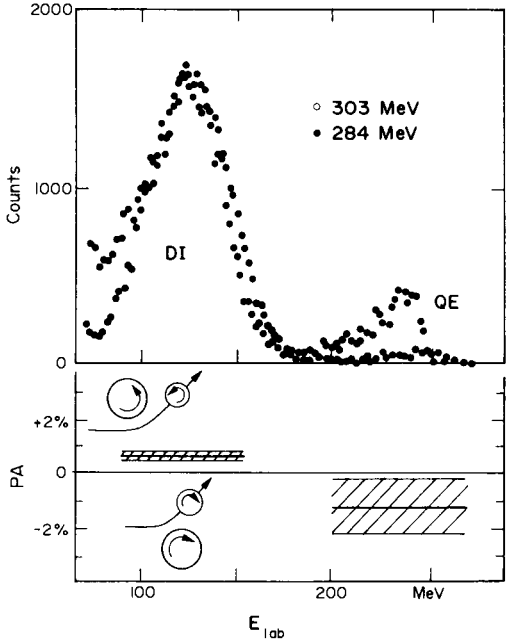

Fig. 63. The upper half of this figure shows the coincident energy spectra of emerging particles with charges between 11 and 21 from the interaction of 284 and 303 MeV argon nuclei with natural silver. The deep inelastic and quasi-elastic groups are clearly distinguished. The lower part of the figure shows the corresponding polarizations, and the inset shows how these follow from the classical orbit picture of the interaction.

corresponding to positive and negative scattering angles, they cannot be distinguished experimentally just by studying the differential cross sections, since equal numbers of particles are incident on both sides of the target nuclei. Thus until recently it was not possible to confirm these negative deflection angles experimentally, although they are theoretically very plausible.

It has now been shown by Trautmann and colleagues (1977) that it is possible to do this by measuring the polarization of the residual nuclei, which depends on whether the scattering was to positive or negative angles. This is because in these interactions some of the orbital angular momentum of the projectile is given to the target nucleus, so that it is left spinning. If now we consider two orbits that both give emergent

particles in the same direction, but one corresponding to positive and the other to negative scattering angle, we find that they leave the residual nucleus spinning in opposite directions, as shown in the inset to the figure. This may easily be seen physically by using the concept of tangential friction; the interactions that take place as the nuclei brush past each other transfer energy and this is felt by the projectile as a tangential force tending to set it into rotation; the same force also sets the target nucleus into rotation.

The particles that have traversed the two types of orbit can be distinguished by the amount of energy they have lost in the interaction. Those scattered through positive deflection angles have been strongly repelled by the Coulomb field and weakly attracted by the nuclear field. Since the loss of energy and the transfer of particles takes place mainly through the nuclear field, such particles will on the average lose rather little energy. On the other hand those particles that are scattered through negative deflection angles have been acted on by a relatively weak Coulomb field but a very strong nuclear field, and so will have lost on the average much more energy. This is illustrated by the figure, which shows the energy spectrum of the particles emitted at 35° from the interaction of 284 and 303 MeV argon nuclei with a target of natural silver. There are two distinct peaks, the one at higher energies corresponding to the particles that have lost rather little energy in quasi-elastic interactions, and the one at lower energies that have lost much more energy in deep inelastic interactions.

It is possible therefore to identify the particles that have been scattered through positive and negative deflection angles so all that remains is to show that they have indeed left the residual nuclei spinning in opposite directions. This was done by measuring the circular polarization of the de-excitation gamma rays corresponding to the two groups. In the initial stages of the de-excitation process charged and neutral particles are emitted, and this will in general reduce the value but not change the sign of the nuclear polarization. Thus the circular polarization of the gamma rays emitted in the last stages of the de-excitation process, which has the same sign as the nuclear polarization, tells us about the direction of spin of the residual nucleus immediately after the interaction.

The results of the measurements of the circular polarizations of the

gamma rays in coincidence with the two groups of particles are shown in the figure. Those corresponding to the negative deflection angles have a small positive polarization, whereas those corresponding to positive deflection angles have a small negative polarization, which is just what we expect from the theory of the process. This agreement with the theory of the orbits responsible for the positive and negative scattering angles and the energy losses of the particles in the two groups confirms the overall correctness of the picture. This is a remarkable illustration of the value of classical arguments in understanding the details of interactions between nuclei at high energies.

Reference

W. Trautmann, J. De Boer, W. Dünnweber, G. Graw, R. Kopp, C. Lauterbach, H. Puchta and U. Lynen, *Phys. Rev. Lett.* **39**, 1062, 1977.

3.8 Spin Dependence of Heavy Ion Transfer Reactions (*Nature* **268**, 18, 1977)

There have been many studies of reactions between heavy ions in which one or more nucleons are transferred, and it is usually found that the cross section can be accounted for quite well by the distorted wave theory. In some cases it is found that the cross sections are more sensitive to particular aspects of nuclear structure than the corresponding reactions with light projectiles, and this makes them useful tools in nuclear spectroscopy.

An example of this is the spin-dependent effects in some transfer reactions. If a particle is transferred from a $(l_2 j_2)$ state in the projectile to a $(l_1 j_1)$ state in the residual nucleus the angular momentum selection rules allow several values of the transferred angular momentum L, and these depend on whether the angular momentum given to the residual nucleus is $j_1 = l_1 + \frac{1}{2}$ or $j_1 = l_1 - \frac{1}{2}$. In the particular case when $l_2 = 0$, then $L = l_1$ and it is possible to study the dependence of the cross section on j_1 for a given value of L.

Such a study has recently been carried out by a group at the University of Minnesota for the ^{28}Si(^{19}F,^{16}O)^{31}P reaction at 60 MeV (Kubono *et al.*, 1977). In this reaction three nucleons are

transferred, but it is a good approximation to consider these as a triton-like cluster and thus retain the simplicity of a one-nucleon transfer reaction. This is likely to be quite a good approximation since 92% of the ^{19}F wavefunction can be expressed as a cluster of three particles in a relative 1s state moving with angular momentum $l_2 = 0$ with respect to the ^{16}O core. The experimental cross sections for the $L = 2$ transfers to the lowest $\frac{3}{2}^+$ and $\frac{5}{2}^+$ states in ^{31}P are shown in Fig. 64; these differ markedly and show how the reaction can depend on j as

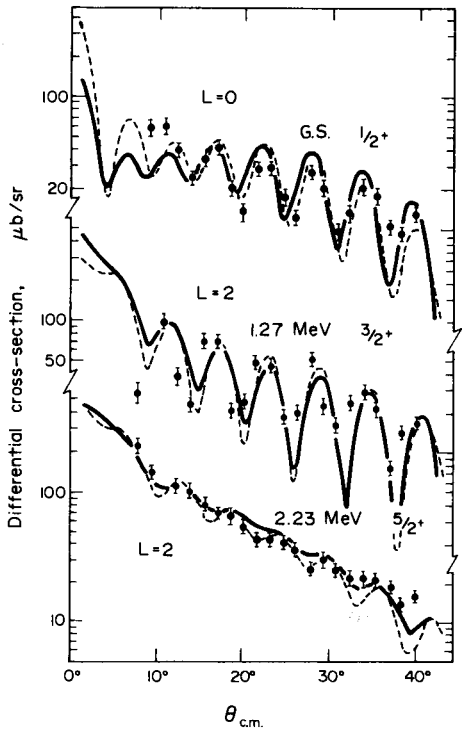

Fig. 64. Differential cross section for the reaction $^{28}Si(^{19}F,^{16}O)^{31}P$ at 60 MeV to three states in ^{31}P compared with normalised distorted wave calculations including a spin-orbit potential in the incident and exit channels. The dashed curves show the effect of including inelastic excitations.

well as on L. The cross section for the $L = 0$ reaction to the $\frac{1}{2}^+$ ground state is also shown.

The first distorted wave calculations, made with a finite range interaction and taking recoil into account, did not give a satisfactory fit to the data, and there was no appreciable improvement when inelastic excitation of the projectile was included by making a full coupled-channels calculation. The satisfactory fit shown in the figure was obtained when spin-orbit potentials were included in the distorting potentials in the incident and exit channels. Once again the fit was very little affected by the inclusion of inelastic excitations.

This work shows that the pronounced j-dependent effects in three nucleon transfer reactions can be accounted for using the distorted wave theory provided spin-orbit potentials are included in the distorting potentials. It also provides striking confirmation of the validity of the cluster transfer approximation and shows that in this case inelastic excitations are relatively unimportant.

Further studies of similar reactions will be needed to confirm that the essential physics of the reaction has indeed been well understood, and if this is the case then the reaction, and others like it, should prove to be a powerful spectroscopic tool for determining the spins of the final states in the residual nuclei.

Comments by Professor P. J. Ellis

Elastic scattering data have now been taken for the exit channel $^{16}O + {}^{31}P$ and it is not fitted by the optical potentials used in the analysis. The effect of using potentials that do fit the data is being investigated.

The original calculations with spin-orbit forces were carried out in the no-recoil approximation. It now appears from the work of C. F. Maguire that this approximation is less accurate in the presence of spin-orbit potentials than in their absence. In particular, the cross-section of the 2.23 MeV $5/2^+$ state shows significant oscillations in the full-recoil calculation. This point is also being studied.

Although we have found that spin-orbit potentials of similar magnitude are useful in obtaining the correct phasing for angular distributions in the $^{40}Ca(^{13}C,{}^{14}N)^{39}K$ reaction (Bayman *et al.*, 1978) folding models using the two-body spin-orbit component of the

nucleon-nucleon interaction yield much smaller magnitudes than we require (Moffa, 1977; Petrovich *et al.*, 1978). Thus the origin of the spin-orbit potentials is still unclear.

References

B. F. Bayman, A. Dudek-Ellis and P. J. Ellis, *Nucl. Phys.* **A301,** 141, 1978.
S. Kubono, D. Dehnard, D. A. Lewis, T. K. Li, J. L. Artz, D. J. Weber, P. J. Ellis and A. Dudek-Ellis, *Phys. Rev. Lett.* **38,** 817, 1977.
P. J. Moffa, *Phys. Rev.* **C16,** 1431, 1977.
F. Petrovich, D. Stanley, L. A. Parks and P. Nagel, *Phys. Rev.* **C17,** 1642, 1978.

3.9 Recoil and Transfer
(*Nature* **243,** 13, 1973)

Very many investigations have established the one-nucleon transfer reaction as a powerful way of investigating the single-particle character of nuclear states. Most of this work has used incident particles consisting of rather few nucleons, in particular the familiar (d,p) and (d,n) reactions, and also reactions initiated by tritons, helions and alpha particles.

In recent years, however, heavy ions have come into their own now that they can be accelerated to energies sufficiently high to surmount the Coulomb barrier of the nucleus and interact with the nuclear field. These reactions have several features that make it useful to study their properties in detail. In particular, they often show semi-classical characteristics that simplify the analysis of the cross-sections, and also the heavy ions bring in high angular momenta that make it possible to excite states of high spin. Furthermore, these reactions often show marked selectivity in that they tend preferentially to populate states of a particularly simple structure.

The distorted wave Born approximation (DWBA) formalism has been used with great success to analyse the (d,p) and similar reactions; it has yielded important information on nuclear structure, particularly the spectroscopic factors. This theory has naturally also been applied to one-nucleon transfer reactions between heavy ions and it has been found to give excellent results in some cases but not in others.

A particular notable discrepancy is found for reactions between light

nuclei. These have cross-sections that fall off steadily with increasing angle, whereas the DWBA predicts angular distributions showing a marked oscillatory structure. The reason for this is that in conventional DWBA calculations the nuclear recoil is neglected, and this is justified if the mass of the incident particle is much less than that of the target nucleus. In the case of reactions between heavy ions these masses are comparable and recoil can no longer be ignored.

Examination of the angular momentum conservation relations in

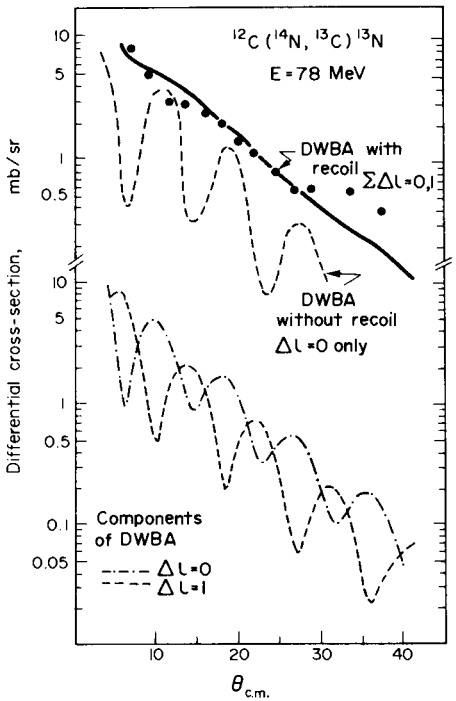

Fig. 65. Differential cross-section for a one-nucleon heavy ion transfer reaction compared with DWBA calculations. The upper dashed curve shows the DWBA calculations without recoil ($\Delta J = 0$ only) and the two lower curves the DWBA calculations with recoil ($\Delta J = 0$ and 1). The sum of these two lower curves is the full curve, which agree well with the experimental data.

the reactions shows that if recoil is neglected the change Δl in the orbital angular momentum of the transferred particle must be zero, whereas if recoil is taken into account Δl may be 0 or 1.

The inclusion of recoil effects makes the calculations much more complicated, but it still remains within the capacity of fast computers. A program including recoil effects has recently been written and DeVries and Kubo (1973) have used it to investigate the importance of these effects. They find, as shown in Fig. 65, that the $\Delta l = 0$ and $\Delta l = 1$ contributions to the reaction amplitude both oscillate as a function of reaction angle, but that the oscillations are out of phase so that their sum varies smoothly with angle, just like the experimental data. This shows very clearly that recoil effects must be included in DWBA calculations of nucleon transfer between heavy ions of comparable mass.

The calculations also give the product of the two spectroscopic factors for the transition, and this is close to the theoretical value of Cohen and Kurath. Thus the DWBA theory is able to give a good account of both the angular distribution and the absolute magnitude of the cross-section for single-nucleon transfer between heavy ions. It now seems likely, subject to further tests, that these reactions can be used with some confidence to determine unknown spectroscopic factors and will thus become an important tool for the determination of nuclear structure.

Reference

R. DeVries and K. I. Kubo, *Phys. Rev. Lett.* **30,** 325, 1973.

3.10 Heavy Ion Transfer Reactions (*Nature* **246,** 334, 1973)

Many studies of nucleon transfer reactions between heavy ions have shown typically bell-shaped angular distributions centred at angles around 30°. These distributions can easily be understood using a classical model of the interaction. The lighter of the two ions approaches the heavier along a Coulomb hyperbolic orbit and the reaction in which a nucleon is transferred from one ion to the other is most likely when this orbit just grazes the surface of the heavier ion.

For larger impact parameters the lighter ion passes beyond the nuclear field of the heavier ion and no nuclear reaction can take place. For smaller impact parameters the ions interact strongly and many complicated reactions take place, so that the probability of the simple transfer reaction is again reduced. Thus there is a maximum in the cross section at the angle corresponding to the deflection characteristic of a grazing collision, and it falls for smaller and for larger angles giving the observed bell-shaped curve.

Quantum mechanical analyses of such reactions can be made using the distorted wave theory and taking into account finite range and recoil effects. These are generally in agreement with the data but in some cases they have shown rapid oscillations superposed on the overall bell-shaped curve. It thus becomes interesting to see if these rapid oscillations can be detected experimentally and also if they can be understood theoretically. This has recently been done by a group at Brookhaven National Laboratory (Chasman, Kahana and Schneider, 1973).

They measured the differential cross section for the proton-transfer reaction $^{48}Ca(^{14}N,^{13}C)^{49}Sc$ to the ground and 3.08 MeV states of ^{49}Sc at an incident energy of the nitrogen ions of 50 MeV. Preliminary data showed the expected bell-shaped curve at 30° but with an additional peak at about 10°. The first distorted wave calculations gave a smooth bell-shaped curve without the forward peak but it was found that if the absorbing part of the optical potential describing the motion of the incident particle is slightly reduced, the forward peak appears and in addition oscillations of higher angular frequency (about 6°) appear on the bell-shaped curve.

Further measurements were therefore made to see if these oscillations are real, and the points on Fig. 66 show that this is indeed the case. The distorted wave calculations reproduce these complicated oscillations remarkably accurately, confirming the reliability of the calculations.

The physical origin of these small-angle oscillations is still not understood. Diffraction theory suggests that they must be associated with a distance of the order of the diameter of the target nucleus, so the obvious explanation is that they are due to interference between the projectile paths on opposite sides of the target nucleus. This is

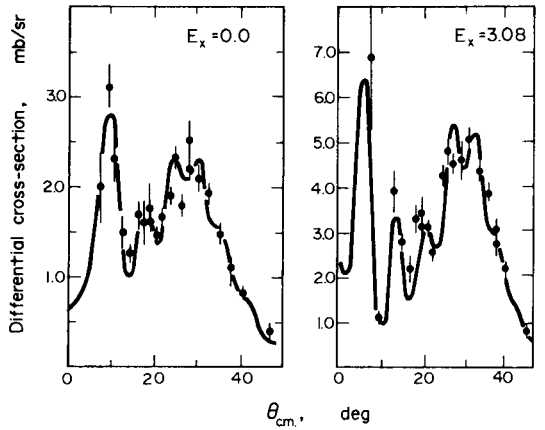

Fig. 66. Differential cross sections for the proton transfer reaction $^{48}Ca(^{14}N,^{13}C)^{49}Sc$ to the ground and 3.08 MeV states of ^{49}Sc at an incident nitrogen energy of 50 MeV, compared with distorted wave calculations which include recoil.

confirmed by calculations starting with the quantum mechanical expression for the cross section and using approximate analytical forms for the partial wave amplitudes and phases. It is then possible to obtain an expression very similar to those of classical diffraction models consisting of two terms, corresponding to interactions on opposite sides of the nucleus. The form of the cross section is then determined by the relative magnitudes of these terms, which varies with the incident energy and the interaction potential.

At low energies the classical scattering angle corresponding to grazing collisions is large, the two terms do not interfere and the classical bell-shaped cross section results. At higher energies the scattering angle is less and the small-angle oscillations appear superimposed on the classical cross section. The onset of these oscillations depends on the absorbing potential. The lower this potential the lower the energy for which the incident particle feels the real nuclear potential and so the lower the energy at which the oscillations appear.

The distorted wave calculations also allow the absolute magnitude of the transfer cross section to be related to the spectroscopic factor for

the single-particle transition. The values extracted from the experimental results are found to be in excellent agreement with the nuclear structure calculations of Cohen and Kurath.

This work shows that nuclear transfer between heavy ions is very well understood theoretically, so that it is now a powerful method of obtaining information on nuclear structure.

Reference

C. Chasman, S. Kahana and M. J. Schneider, *Phys. Rev. Lett.* **31**, 1074, 1973.

3.11 Two-nucleon Transfer between Heavy Ions (*Nature* **251**, 188, 1974)

The theoretical analysis of reactions between heavy ions in which two nucleons are transferred from the projectile to the target has now been developed to a high degree of sophistication. The basic distorted wave theory was formulated many years ago and successfully applied to analyse (d,p) reactions. But in the case of heavy ion reactions many of the approximations that are made for (d,p) reactions are no longer valid, in particular the use of a zero-range interaction and the neglect of recoil. Inclusion of these effects is very complicated and greatly increases the computation time. Furthermore it has become increasingly clear that in many transfer reactions involving collective nuclei the contributions from two-step processes that take place through the pre-excitation of the target nucleus or by post-excitation of the residual nucleus must also be included. Lastly in heavy ion reactions there are substantial contributions from a large range of incident orbital angular momenta.

All these factors have combined to make the whole calculation prohibitively long, even on the fastest computer, if it is carried out in the usual way. Recently, however, Low and Tamura (1974) have developed new techniques for evaluating the multidimensional integrals that occur in these calculations, and these have so strikingly reduced the computing time that these calculations are now practicable.

These new computing techniques have been applied by Tamura,

Low and Udagawa (1974) to calculate the cross section for the two nucleon transfer reaction $^{76}Ge(^{16}O,^{14}C)^{78}Se$ to the ground and first excited (2^+) state of the final nucleus. Comparison with the measurements of Lemaire, Mermaz, Sztark and Cunsolo shows that the distorted wave calculations are inadequate, even when finite range effects are taken into account (see dotted line in figure). The cross section for the reaction to the ground state shows too much oscillation and is too high at small angles, while that of the reaction to the 2^+ state at 0.613 MeV is far too small.

They then took into account the inelastic excitation in the exit channel. The residual nucleus ^{78}Se is easily excited into low-lying collective states, so it is possible for the two transferred nucleons to be first added to the target to give ^{78}Se in its ground state, and then for the outgoing ^{14}C nucleus to interact again and excite the ^{78}Se nucleus to the 2^+ state. This two-step contribution to the reaction adds to the direct contribution when the two nucleons are transferred so as to produce the ^{78}Se nucleus immediately in its 2^+ state. There is also a small effect on the cross section of the reaction to the ground state, for this similarly has a two-step component that goes first to the 2^+ state, which is then de-excited by inelastic scattering in the exit channel.

This complicated calculation can be carried out without any adjustment of parameters. The wave function of the two transferred protons to be added to the target was obtained using the standard Bardeen–Cooper–Schreiffer method with the Random Phase Approximation. The single-particle energies were taken from previous work and the strength of the pairing interaction was determined by fitting the experimental separation energy. The separation of the two protons from the ^{16}O was calculated using the fractional parentage coefficients of Cohen and Kurath.

The results of this calculation, taking the two-step processes in the exit channel into account, are shown by the full line in Fig. 67. The agreement is excellent, indicating that the essential physics of the process is now well understood. In particular, it is clear why the inclusion of the two-step processes produces such a dramatic improvement. Since the ^{76}Ge and ^{78}Se nuclei are both superconducting, the transition from the ground state of the target to the ground state of the final nucleus is much stronger than the transition to the first

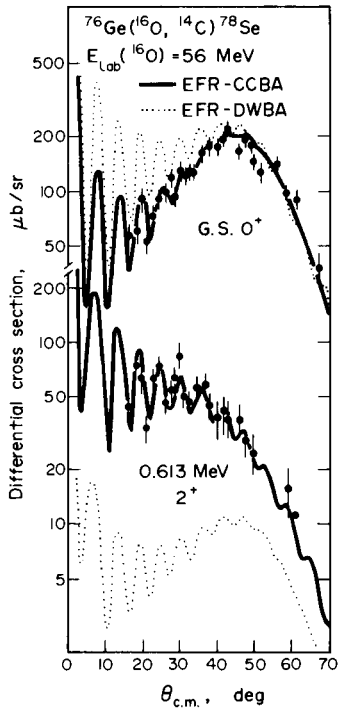

Fig. 67. Differential cross section for the two-proton transfer reaction ^{76}Ge(^{16}O,^{14}C)^{78}Se to the ground and 2^+ excited state of ^{78}Se compared with exact finite range calculations. The dotted line shows the one-step distorted wave calculation (EFR-DWBA) and the full line shows the coupled channels calculation (EFR-CCBA) that takes into account the contributions of two-step processes in the exit channel.

excited state. Thus inclusion of the two-step process greatly enhances the 2^+ cross section but has a much smaller, though still important, effect on the reaction to the ground state.

There are still more effects that could be taken into account, in particular the inelastic effects in the entrance channel. In the calculation of the form factor of the transferred protons only the most important term, corresponding to 1s relative motion of the two protons, was taken into account, and a fuller calculation could investigate the contribution of the higher order terms. Nevertheless

the success of the present calculations suggests that the most important effects have already been included, and that these improvements will not substantially affect the detailed understanding of this reaction that has now been achieved.

Reference

K. Low and T. Tamura, *Phys. Lett.* **48B**, 285, 1974.
T. Tamura, K. Low and T. Udagawa, *Phys. Lett.* **51B**, 116, 1974.

3.12 Two-step Transfer Reactions between Heavy Ions (*Nature* **255**, 250, 1975)

Last year some measurements were made of the differential cross section of the $^{48}Ca(^{16}O,^{15}C)^{49}Ti$ reaction at 56 MeV by the Argonne group (Kovar *et al.*, 1974). This is a strange reaction: at first glance it looks like a one-nucleon transfer reaction, but closer examination shows that the transferred 'nucleon' must carry two charges. The only possible mechanism is thus a series of nucleon transfer reactions equivalent to a transfer of two protons minus one neutron. This might be expected to be very unlikely, but in fact it is found that the cross section of the reaction to the ground state of ^{49}Ti is comparable to that of normal one-nucleon transfer reactions.

In recent years there has been much interest in multistep contributions to nuclear reactions. These are recognised to be of two types: first those that can proceed through the excitation of the target or the residual nucleus by inelastic scattering (§ 3.11) and second those proceeding by a series of particle transfer processes. Calculations have been made in a variety of ways for both processes, and in many cases it has been found that the inclusion of multistep contributions greatly improves the agreement between theory and experiment.

In most of the reactions studied so far both these processes could conceivably contribute, and it is sometimes not clear which is the dominant one, except in reactions involving highly collective nuclei which are very easily excited by inelastic scattering, so that the first process dominates. The special feature of the $(^{16}O,^{15}C)$ reaction is that it must proceed by successive particle transfer, and so it furnishes an excellent case to test the multiple particle transfer theories.

These calculations are exceptionally complicated because in heavy ion reactions it is not sufficiently accurate to make the zero-range and no-recoil approximations that greatly simplify the calculations for light ion reactions.

The Texas group of Tamura, Udagawa and Low have however found ways of carrying out the full calculation for heavy ions without loss of accuracy and sufficiently economically for them to be done in a practicable time on a fast computer. They have written computer programs to do both types of multistep calculation for heavy ions, and have now applied one of them to the $^{48}Ca(^{16}O,^{15}C)^{49}Ti$ reaction (Udagawa *et al.*, 1975).

They considered two possible reaction mechanisms, one-neutron pickup followed by two-proton transfer and *vice versa*, and added their amplitudes to obtain the total cross section. Written out in full, the two reaction mechanisms are $^{48}Ca(^{16}O,^{17}O)^{47}Ca(^{17}O,^{15}C)^{49}Ti$ and $^{48}Ca(^{16}O,^{14}C)^{50}Ti(^{14}C,^{15}C)^{49}Ti$. The intermediate nuclei ^{47}Ca and ^{50}Ti were assumed to be in their ground states and in the first reaction the ^{17}O nucleus could be either in its $5/2^+$ ground state or its first $1/2^+$ excited state, leading respectively to the $1/2^+$ ground state and $5/2^+$ excited state at 0.747 MeV in the final nucleus ^{49}Ti, both of which were observed. In the second reaction the ^{14}C nucleus remained in its ground state.

As the experimental cross sections are structureless and of low accuracy it is not possible to make a good test of the calculations solely by the fit to the angular distribution. It is necessary to try to reproduce the absolute magnitude of the cross section, and this is particularly important because one of the exceptional features of this reaction is the high value of the cross section to the ground state of ^{49}Ti.

To obtain an absolute cross section all the parameters of the calculation must be fixed beforehand by reference to other reactions. This was done in the present case by fitting available data for the one-neutron transfer reaction $^{48}Ca(^{16}O,^{17}O)^{47}Ca$ and the two-proton transfer reaction $^{48}Ca(^{16}O,^{14}C)^{50}Ti$ which are the same or similar to those involved in the postulated mechanisms for the $^{48}Ca(^{16}O,^{15}C)^{49}Ti$ reaction.

The results of these calculations are shown in Fig. 68, and it is apparent that the absolute magnitudes are correctly given, and that the

shapes of the calculated angular distributions are consistent with the experimental results. It is particularly gratifying to find that the relatively high cross section of the reaction to the ground state of ^{49}Ti is correctly given. The relative magnitudes of the two reactions are attributable to complicated interferences between the contributing processes.

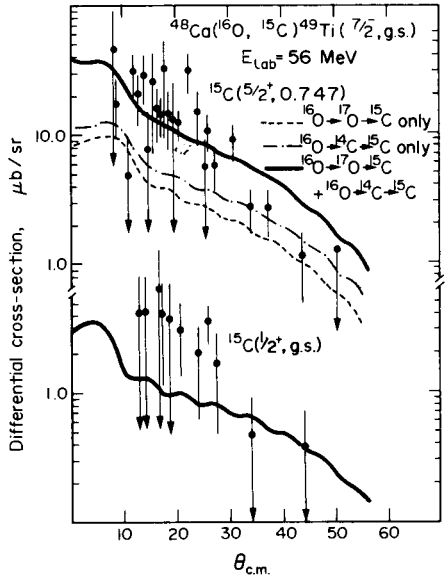

Fig. 68. Differential cross section for the ^{48}Ca(^{16}O,^{15}C)^{49}Ti reaction to the ground and first excited states of ^{49}Ti compared with exact coupled reaction channel calculations. The contributions of the two postulated reaction mechanisms are shown separately and added together.

More precise data are needed before we can learn more about the details of this reaction, and other possible contributing processes must be considered, but this pioneer calculation of a multistep article transfer process shows that these reactions are now amenable to quantitative calculations, and it is likely that many more such calculations will be made in the future.

References

D. G. Kovar, W. Henning, B. Zeidman, Y. Eisen and H. T. Fortune, *Phys. Rev. Lett.* **33**, 1161, 1974.
T. Udagawa, T. Tamura and K. S. Low, *Phys. Rev. Lett.* **34**, 30, 1975.

3.13 Coulomb–nuclear Interference
(*Nature* **247**, 6, 1974)

An interesting example of interference between Coulomb and nuclear scattering amplitudes has recently been found in the inelastic scattering of heavy ions by nuclei. This interference can be understood classically in a qualitative way, and can also be calculated accurately using the distorted wave theory.

This interference is made possible by the particular character of the field between heavy ions which allows incident particles with different classical impact parameters to be scattered through the same angle. To see how this comes about, consider the behaviour of the scattering angle as the impact parameter is steadily reduced.

For large impact parameters the projectile interacts only with the repulsive Coulomb field of the target, and is deflected through a small angle that steadily increases as the impact parameter is reduced. When the distance of closest approach becomes comparable to the sum of the radii of the projectile and target, the nuclear force begins to attract the projectile, thus reducing the scattering angle. At still smaller impact parameters the projectile is repelled by the centrifugal force, thus increasing the scattering angle again. The resulting variation of scattering angle is shown in Fig. 69 for 60 MeV ^{16}O ions on ^{58}Ni.

In such cases there are three values of the impact parameter corresponding to each scattering angle between the critical scattering angles $\theta(R_1)$ and $\theta(R_2)$. The chief contribution to the scattering comes from angles around the critical angles, so a semi-classical theory can be made by adding the corresponding amplitudes, with appropriate phase and attenuation factors. The turning point corresponding to the larger impact parameter refers to the orbit further away from the nucleus where the projectile is moving mainly in the Coulomb field, whereas the other turning point refers to the orbit nearer the nucleus where the projectile is under the influence of both the Coulomb and nuclear

fields. These amplitudes interfere, and because they vary with angle in a different way the interference is sometimes destructive and sometimes constructive.

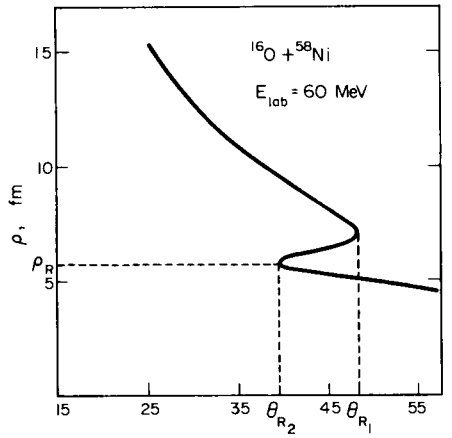

Fig. 69. Variation of the scattering angle θ with the impact parameter ρ for 60 MeV ^{16}O ions on ^{58}Ni (Malfliet, Landowne and Rostokin, 1973).

These effects appear in elastic scattering around the region of the critical angles, but are much more prominent in inelastic scattering. For small angles the cross section for the excitation of the lowest $J^\pi = 2^+$ state of the target is almost entirely due to Coulomb excitation, while for large angles it is mostly due to nuclear excitation. In the intermediate regions around the critical angles the interference effects are strongly marked as shown in Fig. 70.

The whole process can be described quantitatively by the distorted wave theory, using the appropriate vibrational model for the 2^+ state. The results of such calculations are also given in Fig. 70 and show that the interference effects are accurately given by the theory. Detailed fitting in the interference region gives improved values of the parameters of the distorting potential and of the nuclear dynamical deformation parameter.

This interference phenomenon is a good example of the way interactions between heavy ions can be understood semi-classically

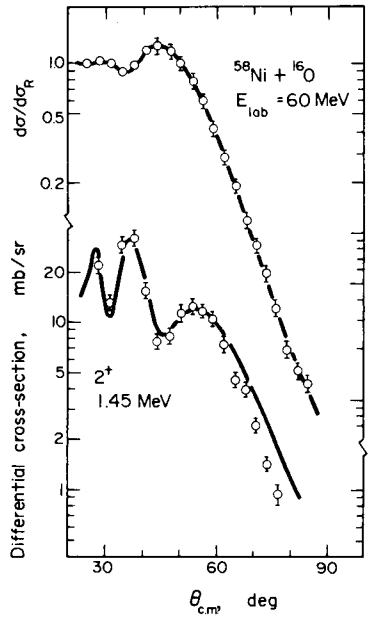

Fig. 70. Differential cross sections for the elastic and inelastic scattering of 60 MeV ^{16}O ions by ^{58}Ni showing the interference effects in the region of the critical angles. The curves are obtained using the distorted wave theory (Christensen, 1973).

and then analysed by the distorted wave theory to give additional information of nuclear structure.

References

P. R. Christensen, I. Chernov, E. E. Gross, R. Stokstad and F. Videbaek, *Nucl. Phys.* **A207,** 433, 1973.

R. A. Malfliet, S. Landowne and V. Rostokin, *Phys. Lett.* **44B,** 238, 1973.

3.14 Interference in Heavy Ion Inelastic Scattering (*Nature* **248,** 735, 1974)

One of the most interesting features of heavy ion interactions is the interference effects between the different processes that can take place

when the interacting ions differ by only a few nucleons. For example, if ^{16}O is scattered by ^{17}O the neutron transfer reaction from ^{17}O to the ground state of ^{16}O gives the same emerging particles as the simple elastic scattering and so is indistinguishable from it. The corresponding amplitudes interfere quantum mechanically and if they are of comparable magnitude this is evident in the observed elastic scattering cross sections.

Interference phenomena are sensitive to the relative amplitudes and phases of the contributing process so they can provide a detailed check of the models used to calculate them, in this case of the distorted wave theory of the interaction and the optical potentials used, as well as of

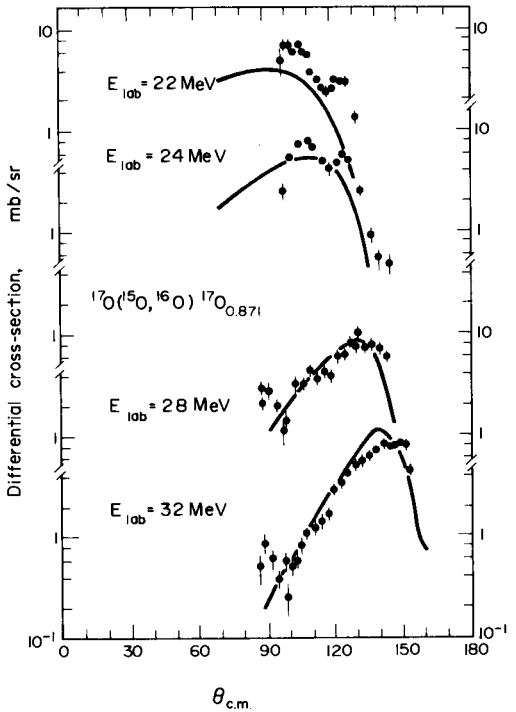

Fig. 71. Differential cross sections for the inelastic scattering of ^{16}O by ^{17}O compared with distorted wave calculations of the one-neutron transfer process.

the spectroscopic factors used to obtain the transfer amplitude. Many studies of elastic scattering of similar ions are being made with these aims in mind.

A group at the Max Planck Institute for Nuclear Physics in Heidelberg (Gelbke, Baur, Bock, Braun-Munzinger, Grochulski, Harney and Stock, 1974) has recently obtained evidence for the occurrence of similar interference phenomena in the inelastic scattering of similar heavy ions. They bombarded ^{16}O with ^{17}O ions with energies ranging from 22 to 32 MeV and measured the cross section for the reaction leaving a ^{17}O ion in its $\frac{1}{2}+$ state at 0.871 MeV.

This process can take place in at least two ways. First, the energy of

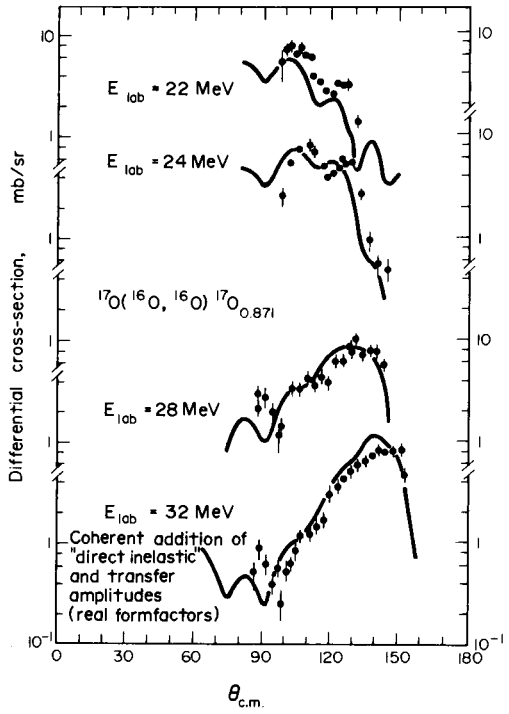

Fig. 72. Differential cross sections for the inelastic scattering of ^{16}O by ^{17}O compared with distorted wave calculations of the coherent addition of the direct inelastic and inelastic transfer process.

the interaction can simply promote the odd neutron in ^{17}O from its ground state orbit to the one corresponding to the 0.871 MeV state; this is the normal inelastic scattering mechanism. But an experimentally indistinguishable result is obtained if the odd neutron in the incident ^{17}O ion is transferred to the orbit in the target ^{16}O that leaves the resulting ^{17}O nucleus in its 0.851 MeV state. This process gives a cross section that is peaked in the backward direction whereas the former process gives one peaked in the forward direction. At the energies of this experiment both amplitudes have broad angular peaks and similar absolute magnitudes, so significant interference effects can occur.

These cross sections were calculated using the distorted wave theory and the results obtained for the dominant transfer inelastic process above are shown in Fig. 71. The overall behaviour of the cross sections is given quite well but close examination shows fine structure in the data that is not reproduced theoretically. Additional calculations were then made including the contribution from the direct inelastic scattering process, and the results (Fig. 72) show that the fine structure is at least qualitatively reproduced. A perfect fit is not to be expected because higher order processes are not taken into account explicitly in this work. Some implicit account was taken of them by multiplying the direct inelastic scattering amplitude by a factor of 1.81 and this gives a much improved fit.

This work provides convincing evidence for the presence of interference effects in the inelastic scattering of heavy ions and is likely to develop into a useful spectroscopic tool.

Reference

C. K. Gelbke, G. Baur, R. Bock, P. Braun-Munzinger, W. Grochulski, H. L. Harney and R. Stock, *Nucl. Phys.* **A219**, 253, 1974.

3.15 Multiple Transfer Processes in Heavy Ion Reactions (*Nature* **252**, 12, 1974)

Experimental studies of the inelastic scattering of heavy ions have revealed a pronounced oscillatory structure in the angular distributions, and this has been explained as an interference effect between the

direct inelastic scattering and one-step transfer inelastic scattering. Such effects are particularly strong when the interacting ions differ only by the transferred nucleon, for example in the reaction $^{17}O(^{16}O, ^{16}O')^{17}O^*$; so that by the transfer process they effectively exchange their identities (§3.14). Though calculations with this model give a good qualitative account of the data, there remain significant discrepancies, and now Baur and Wolter (1974) have shown that these result from the contribution of double transfer processes. Such processes are familiar in the atomic scattering of ions, where electrons are transferred back and forth many times, and some evidence for them has been found in nuclear processes such as the scattering of alpha particles by ^{7}Li (§2.14).

Baur and Wolter studied the inelastic scattering reaction $^{17}O(^{16}O, ^{16}O')^{17}O^*$ to the $\frac{1}{2}^+$ state of ^{17}O at 0.871 MeV at several incident energies. They set up a system of coupled wave equations that enabled them to calculate the cross sections of the direct inelastic scattering together with the contributions due to the single and double transfer processes.

The contributions of these processes are compared in Fig. 73 with experimental cross section for an incident energy of 22 MeV. The direct inelastic process alone gives a smooth angular distribution with its main strength in the backward hemisphere. The one-step transfer alone also gives a smooth distribution but has a much higher cross section and is broadly peaked around 100°. These two processes together interfere to give an oscillatory distribution that agrees qualitatively with the experimental data, but shows a significant phase difference. The two-step transfer alone gives a smooth distribution very similar to the direct inelastic process, but with a higher overall cross section, and when it is combined with the direct inelastic and the one-step transfer it gives a distribution that agrees very well with the experimental data. The inclusion of the two-step process has thus essentially accounted for the phase difference in the previous comparison without this process.

The full calculation with the one- and two-step transfer processes as well as the direct inelastic scattering was repeated for some other energies and they were seen to give a very good overall account of the change of the cross section with energy. It is likely that the small

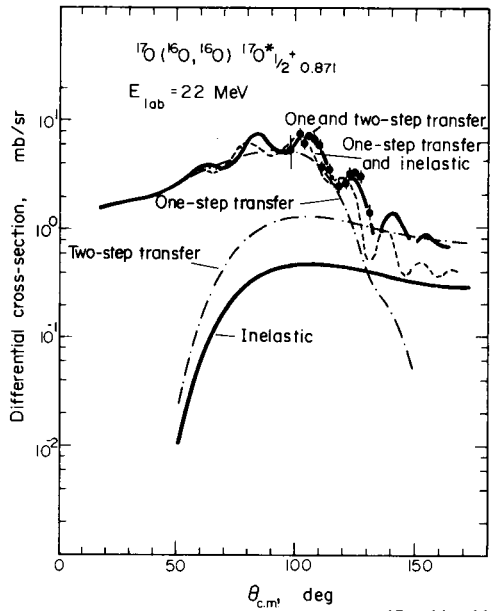

Fig. 73. Differential cross section for the $^{17}O(^{16}O,^{16}O')^{17}O^*$ ($\frac{1}{2}^+$, 0.871 MeV) reaction at 22 MeV compared with coupled channel calculations of the direct inelastic, one-step transfer and two-step transfer processes, both individually and combined together.

discrepancies that remain can be accounted for by higher order transfer processes. The calculations also give the cross sections for elastic scattering, and these agree well with the experimental data.

Comment by Professor G. Baur

The real difficulty in the more accurate treatment of this reaction lies in the microscopic evaluation of the 'direct inelastic' amplitude. This would require, apart from good wavefunctions for the states in ^{17}O, a reliable knowledge of the effective projectile-nucleon (in this case ^{16}O-nucleon) interaction. Perhaps also the $d_{3/2}$ unbound single-particle state plays a role as an intermediate state. Further calculations have been made by Imanishi *et al.* (1977).

References

G. Baur and H. H. Wolter, *Phys. Lett.* **51B,** 205, 1974.
B. Imanishi, O. Tanimura and H. Ohnishi, *Proceedings of the International Conference on Nuclear Structure* (Tokyo, 1977), 588.

3.16 High Spin States of Nuclei
(*Nature* **247,** 255, 1974)

Reactions between heavy ions are proving valuable tools for the investigation of high spin states of nuclei at high excitation energies. Heavy ions readily produce such states because they bring energy to the compound nucleus without high velocities; for example, 100 MeV can be brought in by a ^{10}B nucleus or by a single nucleon but the velocity of the nucleon would be much higher than that of the ion and so there would be a greater likelihood of direct reactions or of disintegration of the target nucleus. Furthermore, if the collision takes place non-centrally the compound nucleus is given a large angular momentum, so there is an enhanced probability of exciting high spin states.

This selectivity of heavy ion reactions is important because at moderately high excitation energies there is often a high density of nuclear states. Only a very few of these have high spins and a heavy ion measurement at relatively low resolution is able to pick them out easily whereas a less selective reaction would require much higher resolution to show them with the same degree of clarity.

The spin of a particular state may be obtained by comparing the angular distribution of the reaction leading to it with the predictions of the statistical theory of nuclear reactions due to Hauser and Feshbach. This theory predicts that the angular distribution is symmetric about 90° in the centre-of-mass system and gives cross sections that depend quite critically in shape and magnitude on the assumed spin of the final state. The identification of the reaction mechanism may be further checked by studying the characteristic fluctuations in intensity of the emerging particles as a function of incident energy.

This method of studying high spin states has recently been used by Gomez del Campo, Ford, Robinson, Stelson, McGrory and Thornton (1973) to determine the energies and spins of rotational states in ^{22}Na by the $^{10}B(^{16}O,\alpha)^{22}Na$ reaction.

The angular distributions of the alpha particles emitted at energies corresponding to several states of ^{22}Na were found to be very well fitted by the Hauser–Feshbach statistical model calculations, confirming both the assigned spins and the assumed character of the reaction.

These high spin states in ^{22}Na are members of rotational bands and the dependence of their energies on $J(J+1)$ is shown in Fig. 74. It is clear that the bands can be followed to high spin values, and that there are systematic deviations from the $J(J+1)$ proportionality. Further confirmation of the spin assignments is provided by the energies given by shell-model calculation, and these are also included in the figure.

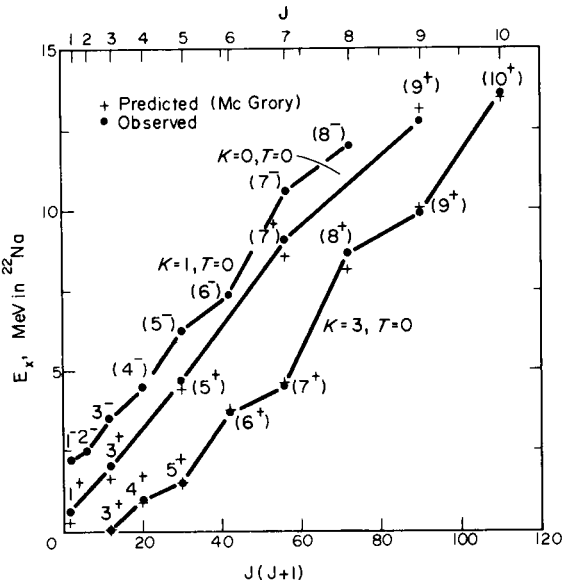

Fig. 74. Excitation energies of states in three rotational bands in ^{22}Na as a function of $J(J+1)$. The dots refer to the measured energies and the crosses to shell model calculations.

This example shows the advantages of heavy ion reactions for studying high spin states, and it is likely that this method will be extensively used in the future.

References

J. Gomez del Campo, J. L. C. Ford, R. L. Robinson, P. H. Stelson and S. T. Thornton, *Phys. Lett.* **46B**, 180, 1973.
W. Hauser and H. Feshbach, *Phys. Rev.* **87**, 366, 1952.

3.17 Nuclear States of High Spin
(*Nature* **257**, 181, 1975)

One of the most powerful ways of determining the spins of nuclear states is by one-nucleon transfer reactions: the angular distribution of the emitted particles is characteristic of the angular momentum transfer, and this usually suffices, sometimes in association with other data, to fix the spin of the final state in the residual nucleus.

This method works best for low spins, corresponding to angular momentum transfers of 0, 1 and 2. For higher spins the angular distribution is not so characteristic, and the reaction may be forbidden by the spin selection rules.

Among the methods applicable to high spin states the (^{7}Li,p) reaction is proving useful, and a recent paper by Bishop and Fortune (1975) provides a good illustration of this.

At low energies on light nuclei the (^{7}Li,p) reaction proceeds predominantly through the compound nucleus. The ^{7}Li is captured by the target nucleus to form a compound system which then can decay by proton emission. It is then found that the total cross section for the reaction is closely proportional to $(2J + 1)$, where J is the spin of the final nuclear state. This relation has been tested for a large number of states, and can be used with some confidence to determine unknown spins.

Bishop and Fortune studied the reaction ^{14}N(^{7}Li,p)^{20}F, and their results for some positive and negative parity states of ^{20}F with known spins are shown in Fig. 75. The cross sections are closely proportional to $(2J + 1)$ and the ratio of the total cross section to $(2J + 1)$ is 5.05 ± 0.08 for the positive parity states and 6.74 ± 0.20 for the negative parity states. The proportionality is so closely followed that it is possible to use the total cross sections for the (^{7}Li,p) reaction to determine the spins of some other states. The identification can be strengthened by seeing how well the state fits into the rotational band structure of the low-lying states of ^{20}F.

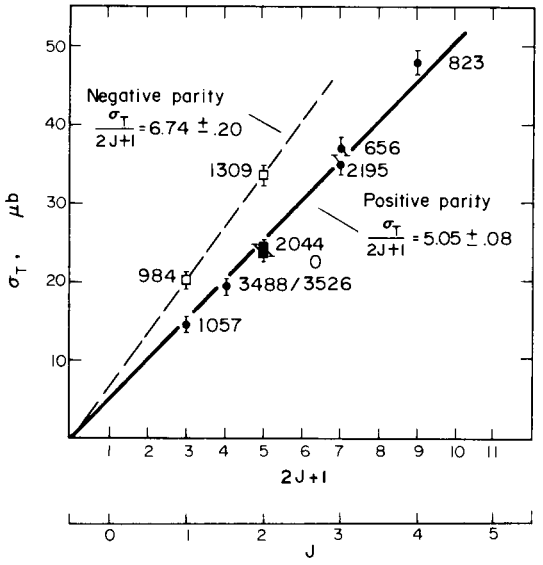

Fig. 75. Total cross sections for the $^{14}N(^7Li,p)^{20}F$ reaction to a number of positive and negative parity states of ^{20}F plotted as a function of $(2J + 1)$.

The method used is simply to calculate the spin from the expression $\frac{1}{2}[(\sigma_T/5.05) - 1]$ for positive parity states and $\frac{1}{2}[(\sigma_T/6.74) - 1]$ for negative parity states and to compare these spin values with those of the possible states that fit into the band structure.

For the state at 2.87 MeV for example, the calculated spins are 3.5 for a positive parity state and 2.5 for negative parity. For the known band structure the assignment 3^- is considered the most likely. In a similar way one of two states at 2.97 MeV is probably identified as 4^-. Probable spin assignments are made to several other states as well.

This work shows the usefulness of the (^{7}Li,p) reaction in determining the spins of nuclear states, when used in conjunction with other techniques.

Reference

J. N. Bishop and H. T. Fortune, *Phys. Rev. Lett.* **34**, 1350, 1975.

3.18 Nuclear Friction

(*Nature* **256,** 261, 1975)

Many complicated interactions take place when two nuclei collide at high energies, so that it is impracticable to develop a detailed quantum-mechanical theory. Instead, it has been found possible to understand some of the more important qualitative features of these interactions by making use of classical concepts such as orbit theory, friction and the behaviour of drops of liquid.

Among the more notable features of the energetic collisions of heavy ions is the rather distinct division between interactions in which a few nucleons are transferred from one ion to the other, with little loss of energy, and the so-called 'strongly damped' collisions in which the ions lose a substantial fraction of their energy. For each type of interaction, particular scattering angles are favoured, depending on the energy of the interaction.

In some cases the strongly damped inelastic collisions have energy losses as high as 200 MeV even though the final nuclei are very similar to the initial ones. This suggests that the nuclei can become highly excited in the interaction without substantially losing their identities or their original trajectories. After the interaction it is found that the ions have significantly less energy than they would have gained from Coulomb repulsion alone if they had started from a position of rest with their surfaces just touching.

In addition to these direct reactions, it is always possible for the two ions to coalesce or fuse together to form a compound nucleus, and the cross section for this is substantially less than the total cross section.

Beck and Gross (1973) have proposed that these phenomena may be understood if we think of the nuclei as experiencing strong frictional forces as they move in each other's field. These frictional forces convert kinetic energy into internal excitation energy, and thus reduce their relative angular momenta. In some cases the loss of angular momentum is so great that the nuclei cannot separate again, and they fuse together. In other cases they succeed in separating but only after strong mutual excitation has taken place.

This theory has recently been extended by Bondorf, Huizenga, Sobel and Sperber (1975), who give a more detailed account of the processes

that occur when one ion collides with another at high energy. The mutual interaction of the two ions may be described by a potential with three terms; first, the repulsive electrostatic or Coulomb potential, equal to $Z_1 Z_2 e^2/r$ outside the ions and rather less inside, where Z_1 and Z_2 are the charges on the ions and r their distance apart. Second, there is the strongly attractive nuclear potential that essentially acts only within the volume occupied by the ions themselves and falls off exponentially outside. Third, there is the centrifugal potential $l(l+1)/r^2$ that accounts for the increasing difficulty for ions with high relative angular momenta l to approach each other; it is therefore repulsive.

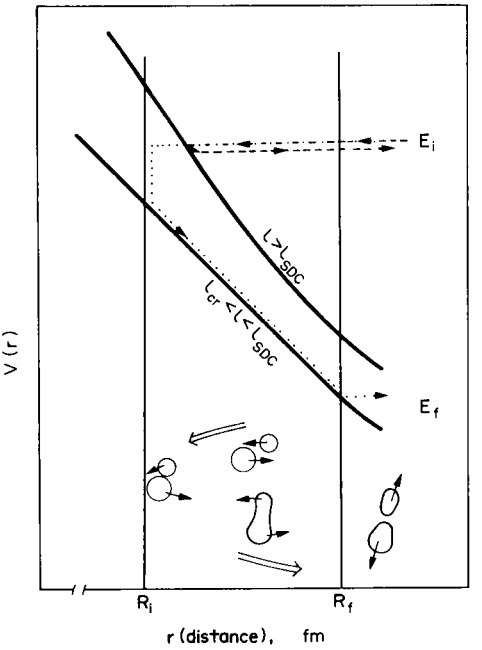

Fig. 76. Schematic representation of the energy for strongly damped collisions. For $l > l_{SDC}$, the ions fail to reach the separation R_1 at which they interact strongly, and therefore elastic scattering or few-nucleon transfer occurs. For $l_{cr} < l < l_{SDC}$ they reach R_1 and the radial and rotational kinetic energies are suddenly dissipated. The ions stick together for a short while, then a neck develops due to the repulsive Coulomb force, retarded by radial friction. The sketches in the lower part of the figure indicate the shape of the system as the strongly damped collision develops.

At high energies l is large and the centrifugal potential dominates, so the total potential depends on l and r in the way shown for two values of l in Fig. 76. The potential is more strongly repulsive for higher l and falls off rapidly as r increases.

This potential describes the forces acting on one ion due to the other, and classically speaking determines their orbits during the interaction. As soon as the ions touch each other additional energy-dissipating forces come into play, and these are usually represented by an absorbing potential. Quantum-mechanically this can be included by allowing the potential to become complex, as an imaginary potential has the effect of absorbing an incident wave, just as the refraction and absorption of a light wave can be described by attributing to the medium a complex refractive index.

We are now in a position to describe what happens to one ion that encounters another ion with orbital angular momentum l. If l is high the potential prevents the ions from touching and the ion is elastically scattered or possibly the ions excite each other through their Coulomb fields. As l is progressively reduced the ions come closer together and begin to interact through their nuclear fields as well. Nuclear inelastic scattering can take place, and also the transfer of a few nucleons from one ion to the other. All these processes involve rather little energy, as the ions separate again with nearly the same energies as they had before the interaction. These processes are represented by the dashed line on the figure.

At slightly lower values of l the ions interact very strongly: this happens quite suddenly because the nuclear densities rise very rapidly in the region of the nuclear surface. There is thus a critical l_{SDC} (strongly damped collision) below which the ions interact strongly. They stick together and nearly all their radial kinetic energy and angular momentum is suddenly dissipated. If R_{i} is the radial distance at which the nuclei initially touch, then such ions follow the path shown by the dotted line in the figure. After a sudden loss of energy that brings the angular momentum down to a value l the joint system continues to rotate like a dumb-bell and further energy is lost in mutual excitation. These processes are extremely complicated at the nucleon level but may be described in a very general way using the classical concept of friction.

At this point we make use of a familiar observation from the behaviour of colliding drops of liquid, namely that what happens when they approach each other is not the same as what happens when they separate. As they come together, they remain spherical and join together only when their separation is the sum of their radii. But when they separate a neck forms between them and gradually narrows as they separate, finally breaking only when the drops are separated by a distance substantially greater than the sum of their radii when spherical.

We assume that the same thing happens for colliding nuclei. As they begin to separate, a neck forms between them and energy is continually lost. They finally separate only when their distance apart is R_f which is subtantially greater than R_i.

For even smaller l values, so much energy is dissipated by frictional forces that the nuclei stick together permanently and a compound nucleus is formed. The highest l value for which this occurs is the critical l_c for fusion of the two nuclei.

The cross sections for these processes can be expressed in terms of the angular momenta using the expression for the angular momentum

$$l\hbar = mvR = k\hbar R$$

So that the cross-section

$$\sigma = \pi R^2 = \frac{\pi l^2}{k^2} = \pi \lambda\!\!\!^{-2} l^2$$

Thus the total cross section for strongly damped collisions

$$\sigma_{SDC} = \pi \lambda\!\!\!^{-2}(l_{SDC}^2 - l_{cr}^2)$$

and the cross section for compound nucleus formation

$$\sigma_{CN} = \pi \lambda\!\!\!^{-2}/l_{cr}^2$$

This simple picture of the interaction of heavy ions at high energies explains in a qualitative way some of the features that have already been mentioned.

First, it is clear that for $l > l_{SDC}$, the energy loss is quite small, while for $l < l_{SDC}$, it is very large. This explains the prominent gap in the energy spectrum of the outgoing particles. Second, the formation of a neck means that the ions are separated by more than the sum of their

radii when they part, and so will have less repulsive Coulomb energy, again in accord with measurements. Finally, the cross section for the formation of a compound nucleus is much less than the geometrical cross section.

As an indication of the value of l involved in a typical reaction, Bondorf and colleagues consider the collision of 600 MeV ^{84}Kr with ^{209}Bi and find $l_{SDC} = 250$ and $l_{cr} \approx 75$; showing how large a number of partial waves participate in these reactions. They developed a formalism connecting these parameters of the interaction with the classical angles of emission of the particles at the critical angular momenta, and included a coefficient of friction k by assuming that the frictional force is proportional to the velocity of the ion. From the angles of the observed peaks in the cross-section they deduced values of k and found that it varies with l. In this way they were able to account in a qualitative way for the characteristic angles of emission of the particles losing little energy and of those losing most of their energy.

These ideas have also been worked out by Gross and Kalinowski (1974) using the Newtonian equations of motion with frictional forces. They calculated the interaction potential experienced by the lighter of the two colliding nuclei by averaging the nucleon-nucleus optical potential over the density distribution of the heavier, and assumed a predominantly radial form for the friction tensor. With this simple model they were able to account for a large number of experimental fusion cross sections, and their energy variation.

This model will have to be tested for many reactions over a range of energies but already the results are sufficiently encouraging to show the value of applying the classical concept of friction to nuclear reactions. As in the corresponding macroscopic situation, we use the idea of friction to take account in a simple way of very complicated processes which we do not attempt to describe in detail, and to build them into a more comprehensive picture of the whole interaction.

References

R. Beck and D. H. E. Gross, *Phys. Lett.* **47B**, 143, 1973.

J. P. Bondorf, J. R. Huizenga, M. I. Sobel and D. Sperber, *Phys. Rev.* **C11**, 1265, 1975.

D. H. E. Gross and H. Kalinowski, *Proceedings of the International Conference on Nuclear Physics*, Munich, August 27–September 1, 1973 (North-Holland, American Elsevier, 1973) I, 394; *Phys. Lett.* **48B**, 302, 1974.

D. H. E. Gross, H. Kalinowski and J. N. De, *Lecture Notes in Physics* **33** (Springer) 194, 1975.

3.19 Nuclear Fusion
(*Nature* **261,** 193, 1976)

When two nuclei collide, there is a certain probability, depending on the energy and on the nuclei, that they will fuse to form a compound nucleus, which subsequently decays by the emission of neutrons, charged particles and gamma rays. In recent years there have been many studies of the cross section for nuclear fusion, and some features of the process are now understood (§3.18).

The probability that two nuclei fuse depends on the impact parameter, the shortest distance between their initial directions of motion. If the collision is a glancing one (large impact parameter), a few nucleons may be transferred from one nucleus to the other, or knocked out entirely, but the nuclei will go essentially unchanged. If the collision is more or less head-on (small impact parameter), the nuclei will interact strongly and are likely to fuse.

The probability of fusion also depends on the energy of the collision: at low energies the nuclei are kept apart by the electrostatic repulsion and no reactions can occur. As the energy increases, so does the fusion probability, until at very high energies it begins to decrease because the nuclei are more likely to be shattered by the violence of the impact.

These collisions are far too complicated to be treated in detail by quantum mechanics, but substantial progress has been made towards understanding the fusion cross section by using classical ideas. If R is the impact parameter, then the angular momentum of the lighter ion about the heavier is

$$L\hbar = mvR = k\hbar R$$

If all collisions with impact parameters less than R lead to fusion, then the total fusion cross section

$$\sigma_j = \pi R^2 = \pi^2 L^2/k^2$$

As the energy increases, the peripheral collisions bring in more angular momentum than the compound nucleus can accept, so fusion

can only occur for angular momenta less than some limiting value $L_F < L$ and then

$$\sigma_F = \pi^2 L_F^2 / k^2$$

Very many experimental studies of the fusion of nuclei have now been made, and it is found that the fusion cross sections behave in a systematic way. In particular, measurements have been made of the fusion cross section for several different pairs of nuclei giving the same compound nucleus at the same energy, and also of the same reaction at a series of energies. These have shown that fusion is not a static phenomenon; it depends on the dynamics of the interaction process.

A careful analysis of a wide range of fusion cross sections by Galin and colleagues (1974) led to the remarkably simple conclusion that all the data could be accounted for by assuming that fusion takes place as soon as the interacting nuclei come closer than a distance 1.1 $(A_1^{1/3} + A_2^{1/3})$ fm where A_1 and A_2 are the atomic weights of the two ions. A similar analysis of data on other nuclei was made by Gutbrod and colleagues (1973) and they came to a similar conclusion, but with the difference that the distance that fitted their data was 1.4 $(A_1^{1/3} + A_2^{1/3})$ fm. These two results are significantly different and it is important that they be reconciled.

A theory that does this has been developed by Glas and Mosel (1975). It provides a simple model of the fusion process by assuming that the potential in the region of interest has a parabolic form with depth $V_B + \hbar^2 L(L+1)/2\mathcal{I}_B$ where L is the orbital angular momentum and $\mathcal{I}_B$ the nuclear moment of inertia. This enables the fusion cross section to be calculated analytically, and the formula obtained fits all the experimental values. At low and high energies, it gives to a good approximation the values found by Gutbrod *et al.* and Galin *et al.*, and thus unifies them coherently.

The reason for the change of slope is connected with the upper limit to the relative angular momentum of the two nuclei for which fusion can occur. This upper limit is set in two ways, and since both limits must be obeyed it is the lower of the two that actually determines the fusion cross section. The first limit is set by the nuclear radius R; the angular momentum cannot exceed mvR, where m and v are the mass and

velocity of the lighter of the two ions. In practice glancing collisions do not lead to fusion so the limit is somewhat less than this and allowance must also be made for the reduction of the velocity of the incident nucleus by the Coulomb repulsion.

The other limit is set by the maximum angular momentum that can be given to the nucleus without causing it to fly apart. This is fixed by the internal structure of the nucleus and can be estimated by the liquid drop model. At low energies this limit is not important, and the fusion cross section is limited by the nuclear radius. As the energy increases, the angular momentum mvR increases until it reaches the critical value set by the limit of nuclear stability, and thereafter the fusion cross section is limited by the latter criterion.

These two limits correspond to the two different formulae for the separation between the nuclei for fusion to take place, and the transition region to the value of the angular momentum for which the two limits are approximately the same.

The theory of Glas and Mosel thus very neatly accounts for the variation with energy and with interacting nuclei of all the fusion cross sections available when they completed their work. Since then, however, further results have become available that cannot be accounted for by their theory, at least in its original form. The reason seems to be quite well understood in one case, but not in the other.

The first set of anomalous results was obtained by Gauvin and collaborators (1974). In the collision of two quite heavy nuclei, ^{74}Ge and ^{84}Kr, fusion takes place at a higher energy than is expected from the results for the collision of ^{40}A with ^{118}Sn, which leads to the same compound nucleus. This energy shift is as high as 15 MeV and was totally unexpected and quite outside the uncertainties of the experiment.

A possible explanation of this anomaly is that there is a lower as well as an upper limit to the impact parameter for fusion. It is then easy to adjust the lower limit to give the observed threshold shift, but then one wants to understand why fusion cannot take place for low impact parameters and how this varies with energy and from one nucleus to another.

A way of doing this has recently been suggested by Natowitz and

Namboodiri (1975), making use of the analogy with the collision of two liquid drops. This has been studied by Adam and colleagues (1968), and they did indeed find that at some energies there is a lower as well as an upper limit to the impact parameter for the fusion of the two drops.

Some of their results are shown in Fig. 77, which gives the impact parameters (expressed as fractions of the drop diameter D) for fusion as a function of the impact velocity in m s^{-1}. This diagram is easily understood: fusion takes place for low velocities and impact parameters but if either or both are large the drops either brush past each other or shatter.

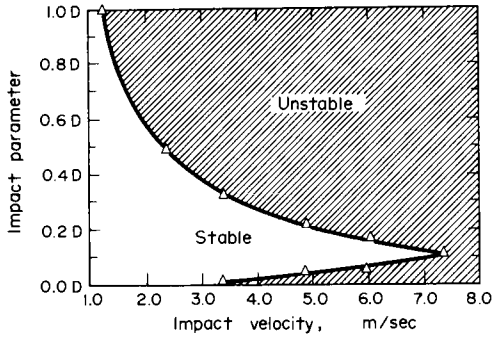

Fig. 77. Diagram showing the ranges of impact parameters and impact velocities leading to the fusion of two equal drops of water (unshaded). The impact parameters are expressed as fractions of the drop diameter $D = 300\,\mu$m. The lower limit to fusion at 3.4 m s^{-1} has a counterpart in nuclear collisions.

The most interesting region occurs for low impact parameters and impact velocities greater than 3.4 m s^{-1}: even though the impact parameter is small fusion cannot take place, and this is just the effect that we want to explain in the collisions of heavy nuclei.

This effect can be understood by considering the collision in more detail. When fusion takes place, the kinetic energy of the colliding drops is transformed into the rotational and vibrational energy of the combined system. Now the kinetic energy can only go into rotational energy if the impact parameter is greater than zero, and the higher the

impact parameter the more rotational energy can be given to the compound system.

For the extreme case of a head-on collision (zero impact parameter) the incident energy can be entirely transformed into vibrational energy for low impact velocities, but at the critical velocity of 3.4 m s^{-1} this is no longer possible. This corresponds to the maximum energy that can go into vibrations of the compound system without breaking it up.

If now the impact parameter is increased, some of the energy can go into rotational energy, so fusion can again take place. Thus for impact velocities above the critical value there is a lower limit to the impact parameter for fusion; below this impact parameter the system cannot be given enough rotational energy to absorb the energy remaining from the incident kinetic energy after as much as possible has been put into vibrations. At still higher impact parameters the rotational energy is so large that the two nuclei cannot stick together and fusion again cannot take place. There is thus a limited range of impact parameters for which fusion can occur.

As the energy increases, so does the rotational energy for a particular impact parameter, so that the lower limit to the impact parameter for fusion rises and the upper limit falls. Eventually at 7.4 m s^{-1} they coincide, and for higher velocities fusion cannot take place at all.

The lower limit to the impact parameter for nuclear fusion can thus easily be understood by considering the behaviour of liquid drops. One important difference is the charge on the nuclei which prevents fusion at smaller impact velocities. For light nuclei the fusion threshold is below the critical impact velocity and so all impact parameters are allowed. The earlier experiments were all in this region and it was here that the systematic behaviour already mentioned was established.

For heavier nuclei, however, the fusion threshold is above the critical impact velocity and so only a limited range of impact parameters leads to fusion. There is thus an energy shift in the curve of fusion cross section as a function of energy compared with the curve that would have been obtained if the lower impact parameters also led to fusion. This higher fusion threshold is just what is observed experimentally for collisions between heavy nuclei.

The second set of data that cannot be understood by the theory of

Glas and Mosel is the fusion cross sections of the interaction $^{12}C + {}^{16}O$ from 13 to 27 MeV measured by Sperr and colleagues (1976). As shown in Fig. 78, the experimental fusion cross sections oscillate

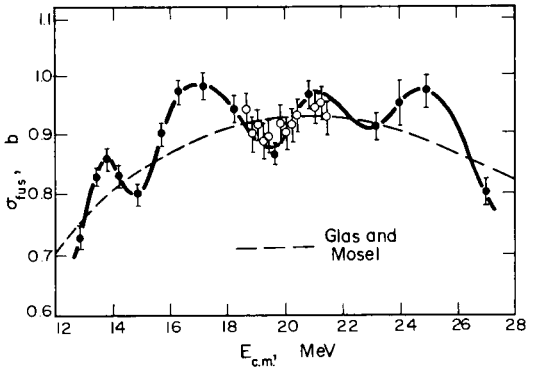

Fig. 78. Fusion cross section for the interaction of ^{12}C and ^{16}O showing the unexplained oscillatory structure superposed on the dependence given by the theory of Glas and Mosel.

around the mean value given by the theory of Glas and Mosel, and it is not at all clear how this behaviour can be explained. One possible explanation, that it is due to the effect of successive partial waves as they come in turn to dominate the reaction, is ruled out because it gives oscillations that have too small a period and too small an amplitude.

Other explanations are that it is due to the effect of resonances in other channels, or to a resonant transfer process (§2.14). According to this explanation, a nucleon can be transferred back and forth between the two approaching nuclei, and this could produce a periodic modulation of the fusion cross sections. This mechanism gives a very characteristic variation of the fusion cross section with energy, and this is approximately in accord with the experimental data.

Comment by Professor Natowitz

The model of Glas and Mosel, like the very similar Bass model, is a critical distance model and therefore quite analogous to the Galin approach. The shift in 'critical distance' from an interaction distance at

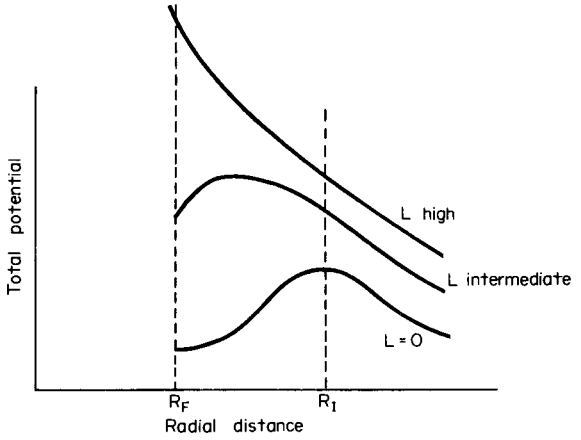
Total potential
L high
L intermediate
L = 0
R_F
R_I
Radial distance

Fig. 79.

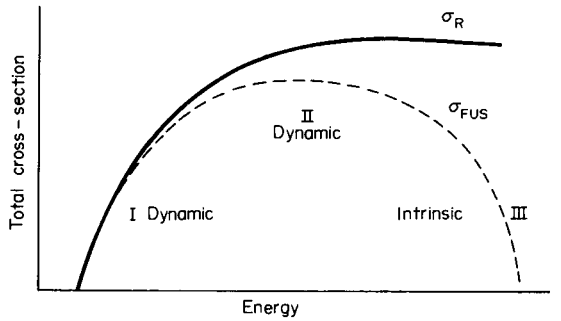
Total cross-section
σ_R
σ_{FUS}
II
Dynamic
I Dynamic
Intrinsic
III
Energy

Fig. 80.

low energy to a smaller fusion distance at high energy results when the centrifugal barrier becomes large so that the nuclei must attain closer contact to feel an attractive potential (Fig. 79).

Eventually the angular momentum is so high that even at R_F the system does not fuse. This would correspond to the liquid drop model or structural limit. Thus one expects the behaviour shown in Fig. 80. The regions I and II are dynamic limits and correspond to the two slopes in the Glas–Mosel model. The third region or intrinsic limit has not yet been definitively identified in fusion work. Since the approach to this region requires higher energies and/or higher masses, the onset of the third region tends to be masked by the occurrence of other processes which make it difficult to determine the fusion cross-section without ambiguity.

The very interesting phenomenon of lower L limits is still widely discussed. Recent Hartree–Fock calculations by Bonche *et al.* (1978) suggest the possibility of such limits in nuclear systems. We are in fact still pursuing this question at the moment and have some preliminary results which correspond quite well to the existence of such a limit.

References

J. R. Adam, N. R. Lindblad and C. D. Hendricks, *J. Appl. Phys.* **39,** 5173, 1968.
R. Bass, *Phys. Lett.* **B47,** 139, 1973; *Nucl. Phys.* **A231,** 45, 1974.
P. Bonche, B. Grammaticos and S. Koonin, *Phys. Rev.* **C17,** 1700, 1978.
J. Galin, D. Guerreau, M. Lefort and X. Tarrago, *Phys. Rev.* **C9,** 1018, 1974.
D. Glas and U. Mosel, *Nucl. Phys.* **A237,** 429, 1975.
H. Gauvin, Y. Le Beyec, M. Lefort and R. L. Hahn, *Phys. Rev.* **C10,** 722, 1974.
H. H. Gutbrod, W. G. Winn and M. Blann, *Nucl. Phys.* **A213,** 267, 1973.
J. B. Natowitz and M. N. Namboodiri, *Phys. Rev.* **C12,** 1678, 1975.
P. Sperr, S. Vigdor, Y. Eisen, W. Henning, D. G. Kovar, T. R. Ophel and B. Zeidman, *Phys. Rev. Lett.* **36,** 405, 1976.

3.20 Fission of Medium Weight Nuclei
(*Nature* **262,** 176, 1976)

The fission of heavy nuclei such as uranium and plutonium is a well known phenomenon of practical importance. In special circumstances lighter nuclei can also undergo fission, and evidence for the fission of nuclei of mass around 80 has recently been found by Braun-Munzinger and colleagues (1976).

The experiment giving evidence of such fission is the interaction of 140 MeV ^{32}S ions with ^{50}Ti. This type of interaction has been studied for many years in order to determine the characteristics of heavy ion reactions, but the particular feature of the new experiment is an array of electronic counters that facilitates determination of the masses and energies of two of the products of the reaction. For each interaction it is possible to measure the (E_1) and mass (A_1) of one of the reaction products by a time-of-flight telescope set at 35° to the incident beam and then the energy and energy loss in an ionization chamber of a second particle emitted on the opposite side of the beam at the same time as the first, together with its angles of emission in and normal to the scattering plane.

Some of the results are shown in the figure in which each point represents a particle of energy E_1 and mass A_1 detected by the time-of-flight telescope. The top part shows all particles and the lower part only those emitted in coincidence with a second particle entering the ionization chamber.

In these plots, the vertical lines around $A = 32$ correspond to the incident ^{32}S ions that have undergone peripheral elastic or quasielastic interactions with the loss or gain of a few nucleons. These interactions have been extensively studied and are now quite well understood. The broad band of points extending from $A \approx 32$ to $A \approx 50$ corresponds mostly to particles coming from the fission of the compound nucleus with $A < 82$ into two fragments of similar mass.

This identification is made by calculating the kinetic energies for the electrostatic repulsion of two charged spheres separated by $\{r_0(A_1^{1/3} + A_2^{1/3}) + 2\}$ fm for $r_0 + 1.0$ and 1.4; with the lighter fragments following the stability valley. The results of this calculation are shown by the solid lines in Fig. 81, and they follow the experimental distribution very well.

Confirmation of this comes from the identification and kinematic correlations of the coincident particles. The ionization chamber measurements of the second particle give its charge Z_2, and assuming its mass is $A_2 + 2Z_2 + 1$, the total mass of the fissioning nucleus is $A_1 + A_2$. For all values of Z_2 between 12 and 16 the average value of $A_1 + A_2$ is between 78.2 and 79.2 compared with the known total $A = 82$. This indicates that on the average about three nucleons are

lost in the reaction. The mass distribution of the fission products is uniform from $A \approx 35$ to $A \approx 55$.

Additional studies of the energy distributions of the secondary particles also confirmed that fission had taken place. The correlation between A_1 and the angle of emission of the second particle showed that several nucleons are evaporated during the reaction, but it was not possible to distinguish between nucleons emitted before or after the fission process.

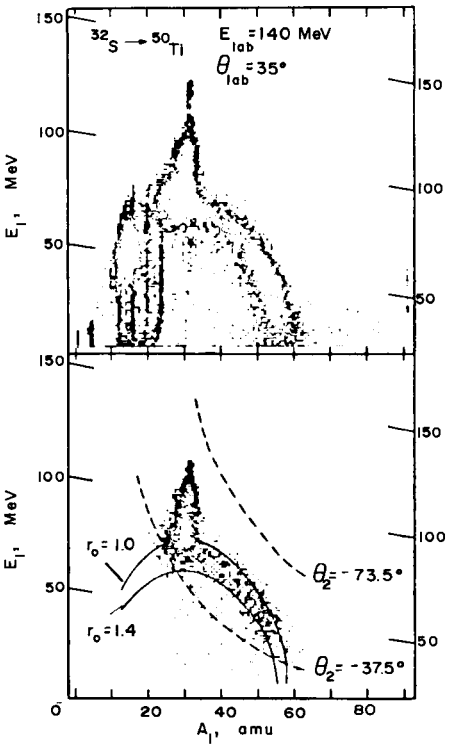

Fig. 81. Plot of the energy and mass number of particles emitted from the interaction of 140 MeV ^{32}S with ^{50}Ti. The top diagram shows all particles and the lower one only those emitted in coincidence with a second particle entering an ionization chamber. The solid lines are calculated for the electrostatic repulsion of two spheres and the dashed lines are the kinematic constraints due to the detector geometry.

This experiment gives the first definite evidence for fission in this mass region and provides a way of studying the fission dynamics of highly excited nuclei with large angular momenta.

Reference

P. Braun-Munzinger, C. K. Gelbke, J. Barrette, B. Zeidman, M. J. LeVine, A. Gamp, H. L. Harney and Th. Walcher, *Phys. Rev. Lett.* **36,** 849, 1976.

3.21 Pion Production in Heavy-ion Collisions (*Nature* **268,** 586, 1977)

A recent measurement of the frequency of pion emission from the collision of heavy ions has given results that disagree with the predictions of the independent particle model of the nucleus and support the pion condensation model of high-density nuclear states.

The frequency of pion production in free nucleon-nucleon collisions is well known, so if nuclei behave just like groups of independent nucleons it is easy to calculate the expected rate of pion production in collisions between two nuclei at high energies. This model might be expected to be valid at energies high enough for the wave-lengths of the interacting nucleons to be rather less than the mean separation of the nucleons in the nucleus. If this is so, the nuclei behave for most purposes as if they are groups of independent nucleons, and the expected rate of pion production is given by the total number of possible nucleon-nucleon interactions, making allowance for multiple scattering and shadowing effects. Significant deviations from the expected number of pions would indicate the presence of strong interactions between the nucleons in the interacting nuclei.

The experimental determination of the pion production rate was made by McNulty *et al.* (1977). They exposed a stack of G5 nuclear emulsion to a beam of 280 MeV per nucleon neon nuclei at the Princeton accelerator. Examination of the developed emulsion under the microscope showed the tracks of these neon nuclei, and 189 tracks were found of nuclei that had collided with a nucleus in the emulsion. Many pion tracks were observed originating in these collision events, and careful subsidiary measurements established that pion tracks could be distinguished from those of protons and alpha particles. The

results for the rate of pion production as a function of the energy of the neon nuclei, and also for the pion energy spectrum, are shown in the figures.

A calculation of the rate of pion production expected from the independent particle model has recently been made by Bertsch. He found that the fraction of collisions from which pions emerge should increase from about 1 in 3,000 at the threshold energy of about 54 MeV to about 1 in 27 at energies of 250 MeV per nucleon. This is in complete disagreement with the results shown in Fig. 82, which show that about 70% of collisions at energies between 100 and 280 MeV per nucleon show pion emission.

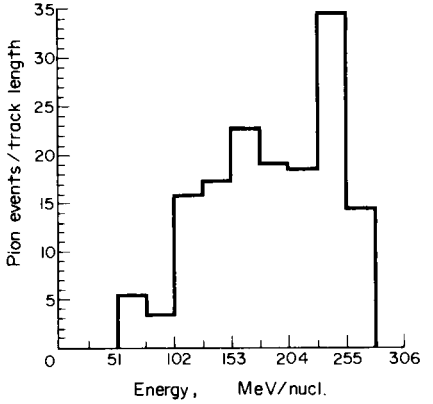

Fig. 82 Pion production as function of neon energy.

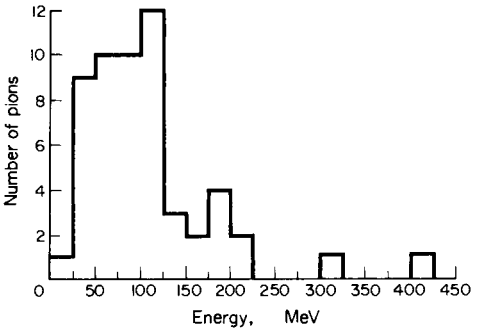

Fig. 83. Pion energy spectrum.

Some other calculations of pion production in heavy-ion collisions have been made by Kitazoe *et al.* (1975) using the hydrodynamic model to include the collective effects on the formation of high-density states in nuclear matter in high energy heavy-ion collisions. In such collisions it is possible for nuclear matter to be compressed momentarily to very high densities, and this could have a considerable effect on the rate of pion production. The high densities are associated with high temperatures, and these can result in pion condensation in just the same way as a gas is ionized with the liberation of electrons when its temperature and pressure are raised. The probability of pion formation can be calculated from statistical theory assuming thermodynamic equilibrium between the pion and nucleon components. In a later paper they reformulated the theory relativistically and evaluated the rate of pion production quantum mechanically.

In particular they calculated the effect of the condensation of zero-momentum pions, and found that this might be appreciable at incident energies of 120 to 440 MeV per nucleon, reaching a peak at an incident energy of about 220 MeV per nucleon. They estimate that as many pions as 0.4 per nucleon may be produced and allowing for those that do not escape from the nucleus gives a result in agreement with the experimental results.

These calculations are still in an early stage, but it is notable that they give results similar to those found experimentally, while those based on the independent particle model are far too low. This indicates that some new process is taking place in energetic collisions between heavy ions, and this should be a strong stimulus to further experimental and theoretical work.

References

G. F. Bertsch, *Phys. Rev.* **C15,** 713, 1977.
Y. Kitazoe and M. Sano, *Lett. Nuovo. Cimento,* **14,** 400, 407, 1975.
Y. Kitazoe, M. Sano and H. Tok, *Lett. Nuovo Cimento,* **13,** 139, 1975.
P. J. McNulty, G. E. Farrell, R. C. Filz, W. Schimmerling and K. G. Vosburgh, *Phys. Rev. Lett.* **38,** 1519, 1977.

Some months later, a paper was published claiming that these results are erroneous (*Nature* **273,** 102, 1978)

Last year McNulty *et al.* (1977) measured the frequency of pion emission from the interactions of 280 MeV per nucleon neon nuclei with nuclei in G5 nuclear emulsion and found that it was very much higher than the rate calculated by Bertsch from the independent particle model. This suggested that collective effects, perhaps associated with pion condensation, greatly enhance the frequency of pion production.

It has now been found by Lindstrom *et al.* at Berkeley (1978) that these measurements are probably in error, due to the misidentification of proton tracks as pion tracks. It is not easy to distinguish between the tracks of relativistic protons and pions in nuclear emulsions, because both have ionization close to the minimum value. McNulty *et al.* used multiple scattering measurements to do this, and Lindstrom *et al.* conclude that these must have been in error.

In their work, Lindstrom *et al.* examined a similar stack of emulsion exposed to neon nuclei of about the same energy, and looked for pions coming to rest in the emulsion. This is a much more definite measurement because the tracks of pions and protons can easily be distinguished near the ends of their ranges. In an area of emulsion that should, if the previously reported production rate were accurate, contain the tracks of about 50 stopping pions they did not find any. This shows that the rate of pion production is less than 0.06 of that found by McNulty *et al.*, and is thus not inconsistent with the predictions of the independent particle model.

Reference

P. J. Lindstrom, H. J. Crawford, D. E. Greiner, R. Hagstrom and H. H. Heckman, *Phys. Rev. Lett.* **40,** 93, 1978.

3.22 High-energy Nucleus-nucleus Collisions (*Nature* **268,** 690, 1977)

Very many complicated processes can take place when two heavy nuclei collide at high energies, and these can be studied in a global way

by measuring the mass distribution of the reaction products. A sufficient proportion of these products is radioactive, so this can be done by a radiochemical analysis of the target after irradiation. Such analyses give only the total cross sections for the production of the various fragment nuclei, and thus complement the detailed studies of individual reactions to particular final nuclear states.

Among the cross sections that can be determined by this method are those for fusion, when the two nuclei fuse together to form a compound nucleus, and quasi-fission, in which several tens of nucleons are transferred from one nucleus to another by a deep inelastic collision. Previous studies of the interaction of ^{40}Ar with ^{238}U and of ^{84}Kr with ^{238}U show that in the former case 55% of the total reaction cross section may be ascribed to fusion and 9% to quasi-fission while in the latter there is only 4% fusion and 38% quasi-fission. These results suggest that as the mass of the projectile increases the probability of fusion falls rapidly. This is of great practical importance for those who are trying to make superheavy nuclei by the collisions of heavy nuclei since it shows that the heavier the interacting nuclei the less likely they are to stick together, implying that heavy-ion experiments designed to produce superheavy nuclei are considerably less feasible than has been previously supposed.

As it is very important to verify this conclusion and confirm that this trend is indeed a universal one, a further measurement of the reaction products from the interaction of ^{56}Fe with ^{238}U has recently been made by Reus and collaborators from the Universities of Marburg and Manchester (1977). They find that 14% of the total reaction cross section is due to fusion, and 26% to quasi-fission, in line with the previous results.

The experiment was made by bombarding a target of ^{238}U with 538 MeV ^{56}Fe ions from the Manchester Linear Accelerator. After irradiation, the target was analysed radiochemically and the cross sections for the production of 173 nuclides were determined. The results are shown in Fig. 84 as a function of atomic mass, and show a number of distinct peaks which can be attributed to particular processes. Thus component A is assigned to fusion reactions (followed subsequently by fission) because the form of the mass yield curve in this region is consistent with that of a broad Gaussian distribution

peaking at a mass value of 137±2, which is the estimated most probable mass for fusion–fission products in this interaction.

The component B has a shape and location indicating that it is due to low energy asymmetric fission following the quasi-elastic transfer of a few nucleons from one nucleus to the other. Component D is obtained by subtracting A and B from the total mass–yield curve, and its maximum corresponds to the mass number to be expected from the

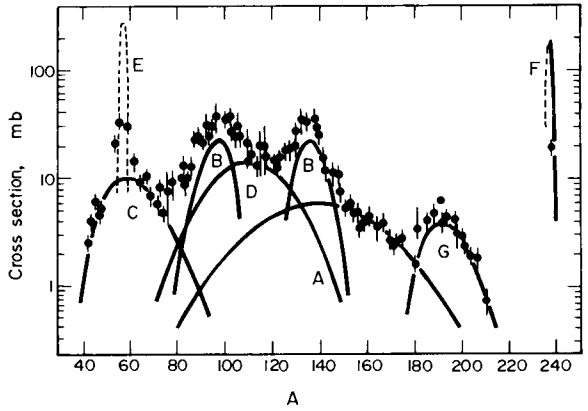

Fig. 84. Mass yield curve for the fragments from the interaction of 538 MeV ^{56}Fe with ^{238}U, analysed into components corresponding to various reaction mechanisms as described in the text.

symmetric fission of nuclei formed by the deep inelastic transfer of several tens of nuclei between target and projectile, and so it is assigned to fission following quasi-fission, or sequential fission. Component G corresponds to those nuclei that are formed by deep inelastic transfer from target to projectile and survive sequential fission, and component C is the light quasi-fission partner. Finally the two sharp peaks at either end of the distribution, components E and F, are due to quasi-elastic transfer. They are not very well determined because many of the nuclides in these mass regions have half lives that are unsuitable for radio-chemical assay. As a check on the whole analysis, the total cross section calculated for this interaction agrees with the sum of all the individual cross sections.

Integration of the cross section corresponding to each component enables the relative importance of the various processes to be found.

The type of interaction that is likely to lead to the formation of superheavy nuclei is fusion of the interacting nuclei to form a compound system. This is of course expected to be rather unstable, so it soon breaks up, probably by fission. The important thing is that the compound system lives long enough for its properties to be studied, and this is not the case for any of the other processes identified in this analysis.

This experiment, together with the two previous ones already mentioned, gives fusion cross sections of 620, 190 and 55 mb for the interactions of Ar, Fe and Kr with uranium, showing that the higher the mass of the projectile the lower the fusion cross section. Experiments designed to produce superheavy nuclei will thus have to rely on reactions initiated by projectiles much lighter than the target, and this severely reduces the range of nuclei that might be produced.

Reference

U. Reus, A. M. Habbestad Wätzig, R. A. Esterlund, P. Patzelt and I. S. Grant, *Phys. Rev. Lett.* **39,** 171, 1977.

3.23 Colliding Nuclei Make a Nuclear Fireball
(*New Scientist* **72,** 385, 1976)

When two atomic nuclei collide at very high energies they are both shattered, and fragments fly out in all directions. It is a very complicated process, impossible to calculate in detail, but now it seems possible to understand the energies and angular distributions of the emitted protons by using the concept of a 'nuclear fireball' (Westfall *et al.*, 1976).

The basic idea is illustrated in Fig. 85. When two nuclei collide, they remove cylindrical slices from each other. After the collision there are three pieces: the undisturbed parts of the two nuclei with the slices missing and the nucleons from both nuclei in the overlapping region. The undisturbed slices are not in their equilibrium shapes so they wobble about for a while and emit a few particles until they come to rest.

The nucleons in the overlap region, where the nuclei have interacted violently, are in a state of intense excitation. It is assumed that they

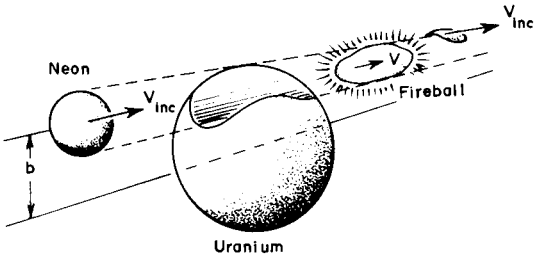

Fig. 85.

together form a fireball that moves forward with rather less than the velocity of the incoming nucleus. The actual velocity of the fireball depends on how many of its nucleons come from the incident particle and how many from the stationary target nucleus, and can easily be calculated from the conservation of momentum. The number of nucleons in the fireball depends on the sizes of the colliding nuclei and on whether the collision is grazing or head-on: the more nearly head-on it is, the more nucleons in the fireball.

The calculation of the disintegration of the fireball assumes that it is hot, with a temperature fixed by the available energy per nucleon. At about 300 to 400 MeV per nucleon the emitted particles have the same energy distribution as the molecules of an ordinary gas (the Maxwell–Boltzmann distribution). At higher energies the distribution is somewhat modified. The fireball emits particles equally in all directions, but as it is moving forward very rapidly the net result is that most of the particles are seen to be moving forward in the direction of the incoming nucleus.

The results of these calculations for the collision of ^{20}Ne and ^{4}He nuclei with uranium at an energy of 400 MeV per nucleon agree very well with the experimental energy and angular distributions of the protons emitted from the collision.

At higher energies the fireball model is not so successful, probably because the nucleons from the two nuclei that are in the overlapping interaction region cannot stick together so easily to form a fireball; they probably tend to fly apart before statistical equilibrium can be established, so that the concept of a decaying fireball is no longer applicable.

At lower energies the model also fails, because the effect of the collision tends to spread further through the compound system, so that the distinction between the inert and the fireball region can no longer be made.

Nevertheless, the model is very successful over a wide range of energies showing the usefulness of thermodynamic concepts in relativistic heavy ion collisions.

Reference

G. D. Westfall, J. Gosset, P. J. Johansen, A. M. Poskanzer, W. G. Meyer, H. H. Gutbrod, A. Sandoval and R. Stock, *Phys. Rev. Lett.* **37**, 1202, 1976.

3.24 Fireball Theory under Test at Bevalac
(*New Scientist* **75**, 471, 1976)

When two atomic nuclei collide at very high energies they are both broken up, and pieces fly out in all directions. So many particles are involved that it is impossible to make a detailed theory, but it is nevertheless possible to understand some of the overall features such as the energy, mass and angular distribution of the fragments on the basis of quite simple models.

One of these models, which certainly explains some of the observations, is the fireball model (see § 3.23, p. 181). According to this model, two nuclei that collide at high energies remove cylindrical slices from each other. The two pieces left behind wobble about for some time and emit a few particles until they return to an equilibirium shape. The parts of the two nuclei that interact together form a very highly excited fireball that moves rapidly forward with a velocity that can be calculated from the conservation of momentum.

This fireball emits very energetic fragments in all directions, but as it is itself moving forward rapidly, more of these particles appear to a stationary observer to be moving forward in the direction of the bombarding nucleus.

Application of statistical theory to the process of de-excitation of the fireball enables the energy distribution of the fragments to be calculated, and this can be compared with the experimental data. Predictions for protons agreed very well with the experimental data.

Now J. Stevenson and colleagues (1977) of the University of California at Berkeley have made some detailed measurements that do not agree with the fireball model. They used the Lawrence Berkeley Laboratory Bevalac to bombard gold with 20 GeV argon nuclei and uranium with 8 GeV neon nuclei, and they measured the energy and angular distributions of a series of fragments from lithium to fluorine.

Analysis of these distributions showed that they are consistent with the fragments having been emitted equally in all directions from a source moving in the direction of the beam with a velocity about 0.08 of that of light. The energy distributions are consistent with either an exponential or a Maxwellian distribution with respect to the source.

Some of these results agree with the fireball model and some do not. Thus the average temperature of the source, obtained from studies of all the fragments, is about 52 MeV (equivalent to about 5×10^{11} K), and assuming that the source is a fireball gives an estimated temperature of 49 MeV, in very good agreement. However the fireball model also gives an estimated velocity of the fireball of 0.27 of the velocity of light, much higher than the observed value of 0.08 c.

Another possible model is the extreme assumption that the two colliding nuclei simply explode on impact. This gives a calculated velocity of the source of 0.08, in excellent agreement with the measured value, but a temperature of only 14 MeV, which is much too low. Thus it seems that neither the fireball model nor the explosion model can explain the new data.

More detailed analysis shows that the new work confirms the previous result that the fireball model gives a good account of the angular and energy distributions of the emitted protons, but also shows that the model becomes rapidly worse in explaining the behaviour of the heavier fragments.

It is thus likely that it will be necessary to develop a more sophisticated model to acount for all the new measurements. It may be necessary to take account of various collective and non-thermal processes, such as compression waves, multiple scattering by clusters of nucleons in the nucleus, and perhaps the emission of clusters from the nucleus. This is certainly a challenging problem, and its solution should give further insight into the properties of nuclei at very high excitation energies.

Reference

J. Stevenson, P. B. Price and K. Frankel, *Phys. Rev. Lett.* **38,** 1125, 1977.

3.25 Knockout Precedes Fireball in Nuclear Collisions
(*New Scientist* **76,** 220, 1977)

A new theory of the mechanism of very high energy collisions between two heavy nuclei proposes that, at least in the initial stages of the collision, the individual nucleons are effectively free.

The new nuclear theory may complement existing models which were beginning to run into difficulties. So far two theories have been suggested to account for the observations, the fireball theory and the explosion theory (see §§ 3.22 and 3.23). According to the fireball theory the regions of the nuclei that interpenetrate during the collision form a very highly excited fireball that subsequently decays by emitting fast particles. The other regions of the two nuclei that are left behind are much less highly excited and decay by emitting much less energetic particles. On the explosion theory, on the other hand, both nuclei are shattered into fragments on the first impact.

Detailed comparison between the predictions of these two theories and the experimental data show that the fireball theory gives the correct temperature for the excited compound system but a forward velocity that is much too high, while the explosion theory gives the correct velocity but too low a temperature.

Now Steven Koonin of the Niels Bohr Institute in Copenhagen has made a new suggestion that accounts very well for part of the data, and is very reasonable on physical grounds. He has examined the initial stages of the interaction, and calculates the energy and angular distribution of the first protons knocked out.

To do this Koonin makes use of the known momentum distribution of the nucleon-nucleon collisions. At high energies the nuclei can be considered for this calculation as consisting of independent nucleons, so that the free nucleon-nucleon cross-section can be used. Koonin made allowance, however, for the overall binding of the nucleons in the nuclei.

Koonin applied the results of these calculations to the collision of

^{20}Ne with uranium at 250 MeV per nucleon. The results are compared with the experimental proton spectra in Fig. 86. The calculated curves have been scaled to make the best fit to the data, but the scale factors are in general accord with what would be expected from the model.

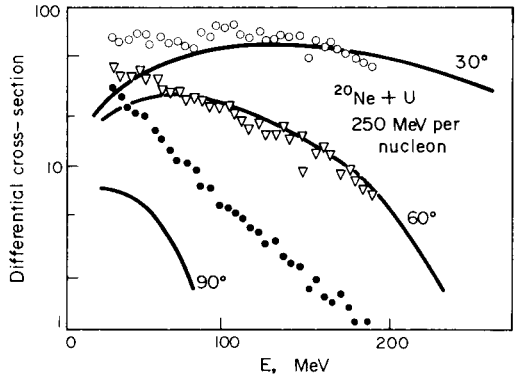

Fig. 86. Treating the nucleons as free fits forward scattering data.

The model agrees very well with the data for the more energetic particles emitted in the forward direction: the particles that are naturally expected to come from direct inter-nucleon 'knock-on' collisions. The calculations do not agree with the data for the less energetic and backward particles, but this again is to be expected, because the knocked-on particles come only from the initial stages of the interaction while the slower and more evenly emitted particles come from the subsequent decay of the remaining fragments. These comparisons with the experimental data show that the knock-on theory provides a good description of the initial stages of the interaction between two nuclei. It is possible that the fireball theory or the explosion theory would help to understand the subsequent stages, but further work needs to be done to see how their conclusions would be affected by taking account of the knock-out processes in the initial stages of the interaction.

Reference

S. E. Koonin, *Phys. Rev. Lett.* **39**, 680, 1977.

3.26 Nucleon Coalescence
(*Nature* **265,** 210, 1977)

Recent experiments on the interaction of relativistic heavy ions with silver and uranium have provided evidence that the emitted nucleons tend to stick together to form composite particles, so that the numbers of high energy ^{3}He and ^{4}He particles are two or three orders of magnitude greater than those found for proton-induced reactions at comparable velocities. It was found that more ^{3}He were emitted than ^{4}He, and this made it doubtful whether both their emissions could be explained by the same process.

To study this matter in more detail, Gutbrod and colleagues (1976) have measured the energy spectra at several angles of the protons, deuterons, tritons, helions (^{3}He) and alpha particles (^{4}He) emitted when uranium is bombarded with 250, 400 and 2,100 MeV per nucleon ^{20}Ne ions and with 400 MeV per nucleon alpha particles, and some typical results are shown in the figure.

To try to account for these distributions, they developed a theory that had already been used by Butler and Pearson to explain the observation of high energy deuterons emitted from nuclei bombarded with energetic protons. This theory assumes that among the cascade of nucleons emitted from such reactions there will be some neutron-proton pairs with rather low relative momenta. The nucleons of each pair can interact with each other and with the surrounding nuclear field to form a deuteron, the nuclear field serving to absorb excess energy and momenta. This model enables the energy spectra of the deuterons to be calculated from that of the cascade nucleons.

The theory was modified to calculate the spectra of the lighter particles emitted from relativistic heavy ion collisions, and the results are compared in Fig. 87 with the experimental data. It is seen that the overall features are accounted for very well.

An important parameter of the theory is the greatest relative momentum between the neutron and the proton for which they can coalesce. This momentum was adjusted for each of the reactions investigated so as to give the best overall fit to the experimental data, and it was found that the best values were around 130 MeV/c in each case. This constancy checks the validity of the theory.

It still remains to understand the details of the mechanism of nucleon coalescence, but it is certainly encouraging that a relatively simple theory can account so well for so much experimental data relating to very complicated reactions.

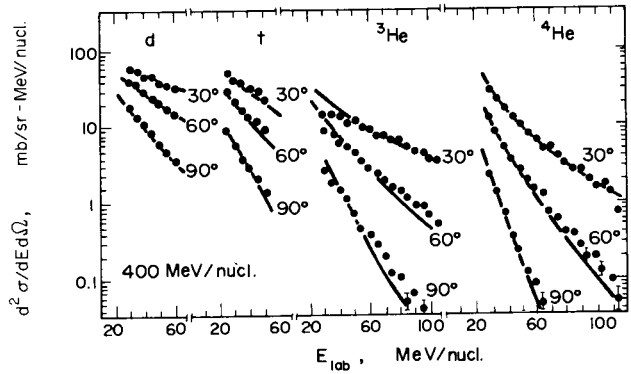

Fig. 87 Experimental energy spectra of the deuterons (d), tritons (t), helions (^{3}He) and alpha particles (^{4}He) emitted from uranium irradiated by ^{20}Ne ions at 400 MeV per nucleon.

Reference

H. H. Gutbrod, A. Sandoval, P. J. Johansen, A. M. Poskanzer, J. Gosset, W. G. Meyer, G. D. Westfall and R. Stock, *Phys. Rev. Lett.* **37**, 667, 1976.

3.27 Nuclear Shock Waves
(*Nature* **258,** 570, 1975)

The concepts of classical physics can often be used to gain a useful insight into nuclear phenomena, especially when relatively large numbers of high energy nucleons are involved. An example of this is provided by what happens when two nuclei collide at high energy. In the region where they first interact the density rises suddenly, and if the relative velocity of the nuclei is greater than the rate of propagation of this density disturbance through the nucleus a nuclear shock wave develops.

The rate of propagation of the shock wave is the velocity of sound in nuclear matter and this can be estimated from the known nuclear compressibility (see Vol. 1, § 2.10) to be that corresponding to an energy of about 10 MeV per nucleon for the colliding nuclei. Such energies can be attained by many heavy ion accelerators so it is possible in principle to produce nuclear shock wave phenomena.

The development of such shock waves has been calculated by Scheib, Mueller and Greiner (1974), and they find for $^{16}O-^{16}O$ collisions that even for centre-of-mass energies of 100 MeV densities almost twice normal appear. For energies of 1,000 MeV, densities fives times normal occur, and in each case a shock wave is expected.

The shock wave itself is essentially a sharp discontinuity in the nuclear pressure, density and velocity, and it is essential for its application to nuclei that the thickness of the shockwave front, or region of rapidly varying properties, is small compared with the nucleus itself. The thickness is approximately the same as the mean free path of the nucleons in the nucleus, and as this is rather less than 1 fm, whereas nuclei typically have diameters of a few fm, this condition is expected to be satisfied.

The shockwave phenomena occurring when two spheres of matter collide have already been worked out for stars, and have been applied to nuclei by Wong and Welton (1974). For simplicity they considered the collision of two slabs of nuclear matter in one dimension and used the Brueckner equation of state to calculate the density and energy of the nuclear matter in the shock wave as a function of the Mach number, the ratio of the velocity of the shock wave to that of the nuclear sound. They found that the shock wave propagates along the collision axis and that dissociation occurs at a Mach number of about two. Thus we expect to find showers of nucleons emitted in the forward and backward directions.

If one of the colliding nuclei is much lighter than the other, the shock wave front is conical, with the semi-angle of the cone given by the ratio of the shock-wave and particle velocities, just like the electromagnetic wavefront in the Čerenkov effect. Figure 88 shows a schematic illustration of the development of such a shock wave when an ^{16}O ion collides with ^{238}U at energies of more than 10 MeV per nucleon. Such waves are emitted at a definite angle that can be related precisely to the

energy of the incident particle. If such an effect were observed in nuclei it could provide evidence of nuclear shock waves.

An attempt to detect nuclear shock waves in energetic heavy ion interactions has been made by the Berkeley group (Crawford *et al.*, 1975) by bombarding gold nuclei with 25 GeV ^{12}C ions. At such high

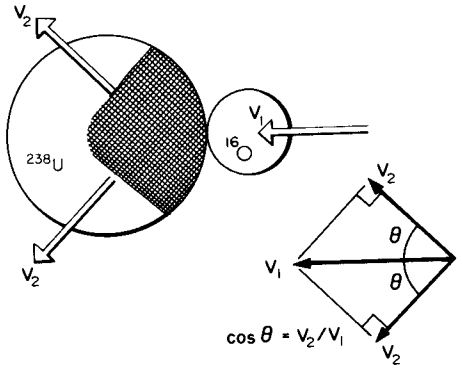

Fig. 88. Schematic illustration of the development of a shock wave front after the collision of an ^{16}O ion with a ^{238}U nucleus.

energies, corresponding to velocities about a fifth of that of light, one might expect a nuclear shock wave to develop. They measured the angular distribution of fragments with charges from 5 to 9 and energies up to 1,000 MeV emitted from the nuclear disintegrations and looked for the peak around 50° that would be the definitive sign of a nuclear shock wave. The data did indeed show a slight maximum at this angle, but it was not statistically significant and cannot be interpreted as evidence for a shock wave.

Another attempt to detect nuclear shock waves has been made recently by Remsberg and Perry at Brookhaven National Laboratory (1975). They irradiated gold and uranium with 28 GeV protons and looked at the energy spectra of the emitted fragments with charges between 6 and 12. As shown in Fig. 89, the spectra of some of the heavier fragments show a broad peak around 70°; for lighter fragments the peak shifts to smaller angles and becomes less distinct. These peaks occur at about the angles predicted for a nuclear shock wave, and may indicate the initiation of some kind of collective motion directly

associated with the cascade of particles initiated by the incoming proton. More precise data would however be needed to establish the presence of a nuclear shock wave.

Another possible phenomenon that could occur in a nuclear shock wave is the production of what are called ultradense nuclei. These are stable, abnormally dense nuclei in which the energy of compression is

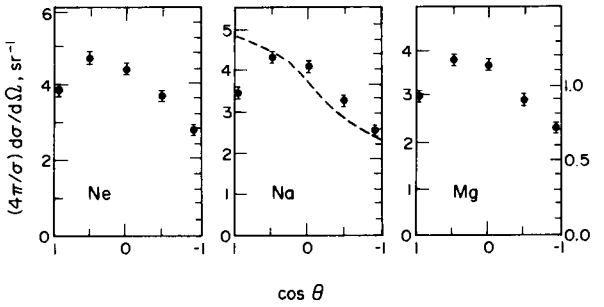

Fig. 89. Angular distribution of fragments from uranium irradiated by 28 GeV protons. The dashed curve refers to carbon emitted from uranium bombarded by 5.5 GeV protons, which shows no peaking.

compensated for by pion condensation. Such nuclei are at present purely theoretical conjectures, based on our present understanding of pion and nucleon forces. It is further conjectured that such nuclei might be formed in a nuclear shock wave, where the nuclear density may be raised two or more times above its normal value. This might be just enough to cause the nuclei or perhaps fragments emitted from the energetic interactions to condense to the ultradense state.

A search for ultradense nuclei has recently been carried out by another group at Berkeley (Price and Stevenson, 1975). They bombarded lead with relativistic argon ions having 1.1–1.6 GeV per nucleon, and looked for emitted particles of Z greater than 20 that might be interpreted as ultradense nuclei. No evidence for such particles was found.

There is thus no definite evidence at present either for nuclear shock waves or for ultradense nuclei, but they both provide a stimulus for more theoretical and experimental work, and show the continuing usefulness of classical ideas even in nuclear physics at high energies.

References

D. A. Bromley, *Proceedings of the International Conference on Reactions between Complex Nuclei,* Nashville, 1974 (North-Holland, Amsterdam) II, 603, 1974.
H. J. Crawford, P. B. Price, J. Stevenson and L. W. Wilson, *Phys. Rev. Lett.* **34,** 329, 1975.
P. B. Price and J. Stevenson, *Phys. Rev. Lett.* **34,** 409, 1975.
L. P. Remsberg and D. G. Perry, *Phys. Rev. Lett.* **35,** 361, 1975.
C. Y. Wong and T. A. Welton, *Phys. Lett.* **49B,** 243, 1974.

3.28 Nuclear Transparency

(*New Scientist,* **73,** 516, 1977)

A group at Milan has recently provided evidence suggesting that nuclei are much more transparent to high energy nucleons (protons and neutrons) than was previously thought. This has important implications for many nuclear reaction calculations; for example it will make the development of shock waves in nuclei in high energy collisions much less likely.

For some years E. Gadioli and colleagues have been studying what happens when an energetic nucleon interacts with a nucleus. First of all the incoming nucleon interacts with a few nucleons on the nuclear surface, giving them some of its energy. This forms a local hot spot on the surface. Some of the nucleons from the spot penetrate further into the nucleus sharing their energy among the other nucleons; ultimately they excite the nucleus as a whole. Other nucleons from the hot spot escape almost at once if they are moving away from the bulk of the nucleus. Later on, the excited nucleus decays by emitting particles and gamma rays in a way that can be easily calculated.

The direct emission of the nucleons from the hot spot is called "precompound emission" because it takes place before the formation of the excited compound nucleus, the relatively long-lived state in which statistical equilibrium is established. These particles have on the average much more energy than those subsequently emitted from the decay of the compound nucleus. A model of the precompound emission called the 'exciton model' has been developed, and this makes it possible to calculate the nucleon energies and angular distribution.

One of the parameters of this theory is the mean free path of the

incident nucleons in the nucleus, or the average distance that a nucleon can go without making a collision. Gadioli found that the agreement between the theory and experiment is greatly improved if this is taken to be about 16.7 fm (about 16 proton diameters) for 20 to 100 MeV nucleons, instead of the much smaller value of 4.2 fm accepted until now.

The larger value of the mean free path also gives much better agreement with the experimental values of the total cross-sections for the reaction of high energy nucleons with nuclei, and with data on the de-excitation of nuclei following the capture of negative pions. It is important to make further tests of the new value of the mean free path by using it in the calculation of other reaction rates. If it is confirmed the existence of shock waves in nuclei will become unlikely—because a condition for the existence of such shock waves is that the mean free path of the nucleons is rather small compared with the size of the nucleus. The new mean free path is, on the contrary, about equal to the diameter of a heavy nucleus (Gadioli *et al.*, 1976).

Comment by Professor Blann

The above article points out one interesting conclusion from the pre-equilibrium work of a group from Milan. Dr. Hodgson has noted that there is a disagreement over the interpretation involved, and solicited comments on this from the two principal parties to the disagreement.

There are two principal formulations for precompound decay: the Hybrid model[1,2] and the Exciton model.[3,4] They differ principally in that one approach considers the emission rate of a 'hot nucleon' to be determined by the ratio of the emission to total transition rate of that nucleon, whereas the second[4,5] considers the emission rate of that nucleon in competition with its own internal transitions plus those of spectators. Both models can reproduce similar spectra. The difference is that the formulation which includes spectator transitions requires the 'spreading rate' to be decreased by a factor of four over that given by estimated N–N collision rates theory[1,2,6] (or by the optical potential) in order to reproduce experimental results.

The disagreement between the two groups concerns the answer to

the question 'Does the factor of four arise because the mean free path of nucleons in nuclear matter is really four times that given by N–N scattering or by the optical model, or is it a consequence of the model formulation?' My own point of view is the second possibility. This is based first on a mathematical model comparison of the Milan formulation and the Hybrid model with an independent approach,[8] secondly due to what I consider to be unacceptable consequences if one accepts the conclusion of 16 f mean free paths.[9,10] Specifically it was shown that present models—such as the intranuclear cascade model—cease to reproduce cross sections in agreement with experimental results if a long mean free path is used.[10] I believe that the optical model would find similar difficulties in reproducing reaction cross sections. Finally I concluded [7–11] that all arguments given by the Milan group in support of their conclusion[5,12] were based on the assumption of its correctness; they seem model dependent, and this issue has been debated by both sides in the literature.[5,8–13]

There is an important point which I wish to emphasize: while I disagree strongly with the Milan group on this point of interpretation of one parameter in their model, and if in time my point of view should prevail, it would in no way alter the importance of the vast contributions made by this group to the understanding of precompound phenomena. It is a side issue in that context, but an important issue in the broader context of reaction models.

References

1. M. Blann, *Phys. Rev. Lett.* **27,** 337; 700E, 1971.
2. M. Blann, *Phys. Rev. Lett.* **28,** 757, 1972.
3. M. Blann and A. Mignerey, *Nucl. Phys.* **A186,** 245, 1972.
4. E. Gadioli, E. Gadioli-Erba and P. G. Sona, *Nucl. Phys.* **A217,** 589, 1973.
5. E. Gadioli, E. Gadioli-Erba, G. Tagliaferri and J. J. Hogan, *Phys. Lett.* **65B,** 311, 1976.
6. K. Kikuchi and M. Kawai, 'Nuclear Matter and Nuclear Reactions,' North-Holland, Amsterdam, 1968.
7. M. Blann, *Nucl. Phys.* **A213,** 570, 1973.
8. M. Blann, *Ann. Rev. Nucl. Sci.* **25,** 123, 1975.
9. M. Blann, *Phys. Lett.* **67B,** 145, 1977.
10. J. Ginocchio and M. Blann, *Phys. Lett.* **68B,** 405, 1977.
11. M. Blann, *Phys. Rev.* **C17,** 1871, 1978.
12. E. Gadioli, E. Gadioli-Erba and G. Tagliaferri, *Phys. Rev.* **C14,** 573, 1976.
13. E. Gadioli, E. Gadioli-Erba and G. Tagliaferri, *Phys. Rev.* **C17,** 2238, 1978.

Comment by E. Gadioli, E. Gadioli-Erba, G. Tagliaferri and J. J. Hogan

The analysis, based on the Exciton model, of a great amount of excitation functions and emitted particle spectra, in nuclear reactions induced by protons of energy up to 150 MeV, indicated that the simplest way to correctly reproduce both the partition of the emitted particle yield among the pre-equilibrium and the evaporation phases and the absolute value of the absorption cross-sections was to assume that the mean free path (m f p) of a nucleon in the nucleus is substantially longer than the one estimated by means of a calculation based on a Fermi gas description for the nucleus and free nucleon-nucleon cross sections (Gadioli *et al.*, 1976, 1977). This last value of the m f p roughly corresponds to the one usually quoted for this important nuclear parameter. The use of a long nucleon m f p also improves the results one obtains by means of different models, namely the Harp–Miller–Berne master equation approach (Miller, 1973) and the intranuclear cascade model (see the discussion of the results obtained with the VEGAS code, in the STEP version (Hogan *et al.*, 1978)). A further confirmation that the above assumption is not unreasonable is afforded by the comparison between the phenomenological values of the volume integrals of the particle-particle collision probability in nuclear matter and the absorbing part of the optical model potential (Gadioli *et al.*, 1978). At present we cannot explain with certainty why the nucleon m f p in nuclear matter should be so long.

This occurrence could be due (i) to the fact that within the nucleus the residual two body interaction which mixes the independent particle model states is weaker than the free nucleon-nucleon interaction, and (or) (ii) to a reduced density of the nucleons which can effectively interact with an excited one (e.g., the analysis of (p,α) reactions seems to indicate a non-negligible probability of preformation of α clusters within the nucleus). The interaction of the excited nucleon with such a structure could be hindered by the combined effect of the kinematics and Pauli principle thus increasing the nucleon m f p).

References

M. Blann, *Phys. Lett.* **67B,** 145, 1977.
E. Gadioli, E. Gadioli-Erba, G. Tagliaferri and J. J. Hogan, *Phys. Lett.* **65B,** 311, 1976; *Phys. Rev.* **C16,** 1404, 1977.
E. Gadioli, E. Gadioli-Erba and G. Tagliaferri, *Phys. Rev.* **C17,** 1294, 1978.
J. Ginocchio and M. Blann, *Phys. Lett.* **68B,** 405, 1977.
J. J. Hogan, K. I. Burns, E. Gadioli, E. Gadioli-Erba and G. Tagliaferri, *Nuovo Cim. Lett.* **23,** 89, 1978.
J. M. Miller, *Proceedings of the International Conference on Nuclear Physics,* Munich, 1973, edited by J. de Boer and H. J. Mang (North-Holland, Amsterdam/American Elsevier, New York, 1973), vol. II.

3.29 Nuclear Shock Waves Unlikely
(*New Scientist,* **73,** 516, 1977)

Conjectures that when two nuclei collide at very high energies a nuclear shock wave may develop—just like the shock wave that occurs when an aircraft flies at more than the speed of sound—have been weakened by a new experiment from Sweden. The results support other work which shows that the mean free path of energetic nucleons in nuclei is greater than was previously thought and too great to sustain shock waves (see § 3.28, p. 192).

The new experiments depend on one of the most striking features of the shock waves: the formation of a conical wave front. The conical waves are very distinctive because their angle of emission is determined only by the ratio of the velocity of the wave in the medium to the velocity of the incoming particle (it is the inverse cosine of that ratio). Thus the angle of emission of the shock wave can easily be calculated, and its variation with the energy of the particle can be compared with that found experimentally.

If shock waves occur in high energy nuclear collisions, we might expect the conical wave to eject particles at just this characteristic angle to the incident beam. If we can find such a peak in the angular distribution, then we would have good evidence for nuclear shock waves. We could confirm the results by seeing how the angle of emission varies with the incident energy.

A group in Lund, Sweden (1977), has therefore made a series of careful experiments to see if they can find this evidence for nuclear shock waves. The group bombarded nuclear emulsions with oxygen

ions of 0.25 and 2.1 GeV per nucleon, and looked for the energetic collisions taking place with the silver and bromine nuclei in the emulsion. Such events are easy to identify as they appear as a large number of tracks of particles originating from a single point. Then the group measured the angular distribution of the tracks corresponding to particles of various types. It turned out that particles were emitted almost equally in all directions at the higher energy, and with some tendency to favour forward emission for the lower energy. There was no sign of any sharp peak due to particles emitted at a particular angle that might show a nuclear shock wave. This cannot be said to actually disprove the existence of nuclear shock waves, since there are many reasons why the sharp peak may be broadened, perhaps beyond recognition. The observed angular distributions can indeed be accounted for by some form of hydrodynamical theory including shock waves, but they can just as easily be explained by nucleon cascade calculations that do not require the presence of shock waves. And there is no sign of the very characteristic peaking at a particular angle that would establish the presence of shock waves beyond reasonable doubt.

Reference

B. Jakobsson, R. Kullberg and I. Otterlund, *Nucl. Phys.* **A276,** 523, 1977.

Name Index

Subject Index